AD-762 440

INTERACTIONS AMONG THE VARIOUS PHENOMENA INVOLVED IN THE DESIGN OF DYNAMIC AND ROTARY MACHINERY AND THEIR EFFECTS IN RELIABILITY. VOLUME I: BASIC REPORT OF REDUCED RESULTS AND UTILIZATION THEREOF

Dimitri Kececioglu, et al

Arizona University

Prepared for:

Office of Naval Research

31 August 1972

DISTRIBUTED BY:

NTIS

National Technical Information Service
U. S. DEPARTMENT OF COMMERCE
5285 Port Royal Road, Springfield Va. 22151

This Document Contains
Missing Page/s That Are
Unavailable In The
Original Document

OR are
Blank pgs.
that have
Been Removed

AD 762440

FIFTH TECHNICAL REPORT

VOL. 1.

INTERACTIONS AMONG THE VARIOUS PHENOMENA INVOLVED IN THE DESIGN OF DYNAMIC AND ROTARY MACHINERY AND THEIR EFFECTS ON RELIABILITY

OFFICE OF NAVAL RESEARCH
CONTRACT N00014-67-A-0209-0002

AUGUST 31, 1972

D D C

Reproduced by
NATIONAL TECHNICAL
INFORMATION SERVICE
U S Department of Commerce
Springfield VA 22151

ENGINEERING EXPERIMENT STATION
COLLEGE OF ENGINEERING
THE UNIVERSITY OF ARIZONA
TUCSON, ARIZONA

214

Fifth Technical Report

1 September 1971 - 31 August 1972

INTERACTIONS AMONG THE VARIOUS PHENOMENA INVOLVED IN THE DESIGN OF DYNAMIC AND ROTARY MACHINERY AND THEIR EFFECTS IN RELIABILITY

VOLUME I - BASIC REPORT OF REDUCED RESULTS AND UTILIZATION THEREOF

by

Dr. Dimitri Kececioglu
Professor and Principal Investigator

and

Louie B. Chester
Chester F. Nolf, Jr.
Joe D. Stultz
Anu Vaze

Aerospace and Mechanical Engineering Department

Engineering Experiment Station
College of Engineering
The University of Arizona
Tucson, Arizona 85721

DDC

for

Office of Naval Research
Arlington, Va.

Contract N00014-67-A-0209-0002

DISTRIBUTION STATEMENT A
Approved for public release;
Distribution Unlimited

31 August 1972

Reproduction in whole or in part
is permitted for any purpose of
the United States Government.

ACKNOWLEDGEMENTS

This report was prepared by those whose names appear on the previous page.

The technical program was administered by M. Keith Ellingsworth, Power Program Code 473, Office of Naval Research, Department of the Navy, Arlington, Virginia. The contract was administered by Mr. Floyd Lance, Administrative Contracting Officier, Office of Naval Research Branch Office, Space Sciences Building, The University of Arizona, Tucson, Arizona.

Grateful acknowledgement is made to Steve Cressey, James Blair, Steve Hall, Gary King and Mike Nelson, University of Arizona students for their contributions to this research; and to secretaries Miss Joann Main and Mrs. Mary Cselenyak for typing this report.

ABSTRACT

The Fifth Technical Report is a continuation of and an addition to the First (Progress), Second, Third, and Fourth Technical Reports to the Office of Naval Research, dated April 30, 1968, July 15, 1968, and August 31, 1971 respectively.

The realization that in mechanical components stress, strength, and the factors that modify them are by nature distributed has pointed to the need for design methods that incorporate the unique powers of the thoeries of probability and statistics. Furthermore, since with any designed product of a mechanical nature a finite probability of failure is associated, this suggests that another probability, Reliability, must be the logical measure of design adequacy of such products.

As the design of reliable and optimized components and systems of dynamic and rotary machinery is becoming a matter of increasing concern, methods by which a specified level of reliability can, in an priori manner, be designed into a component assume great importance. So also does the existence of supporting design data in distributional form.

The Fifth Technical Report describes the continued experimental research on material behavior under fatigue testing. To assure the accuracy and validity of results, the calibration of the two Wiedemann Reversed Bending Fatigue Reliability Research Machines and the four Wire Fatigue Reliability Research Machines was reaccomplished. Descriptions and results of the calibration are presented. Cycles-to-

failure testing was accomplished on fine wire, 0.040 inch diameter, made of AISI 4130, 1038, 1018 and 4340 steel. The Wiedemann Machines were used to perform cycles-to-failure testing of AISI 4130 steel grooved rod, 0.0937 inch base diameter. Also, endurance strength, staircase tests were accomplished on AISI 1038 steel grooved rods of 0.2700 inch base diameter. These endurance strength results were used in a notch sensitivity analysis described herein. Axial fatigue testing was done on AISI 1018 steel grooved rods to generate a Goodman strength diagram. Comparison of the experimental diagram with two theoretical diagrams is described. The results of all testing were analyzed to determine the distributional parameters. The analysis techniques which fit the normal, $\log_e$ normal and Weibull distributions to the data are summarized and the computer programs are included in the Appendices. Individual test results are listed in the data section and the results of the analysis of distributions are shown in histograms overscribed with the frequency distribution curves. Interpretation of the tests results, conclusions drawn therefrom, and recommendations which identify areas where further research is needed, are included.

TABLE OF CONTENTS

		Page
	TABLE OF CONTENTS	v
	ACKNOWLEDGEMENTS	ii
	ABSTRACT	iii
	LIST OF FIGURES	ix
	LIST OF TABLES	xxi
1.0	INTRODUCTION	1
	1.1 PRIOR RESEARCH	1
	1.2 OBJECTIVES FOR THIS REPORT	3
	1.2.1 WIRE RESEARCH MACHINES	3
	1.2.2 WIEDEMANN RESEARCH MACHINES	4
	1.2.3 AXIAL FATIGUE RESEARCH MACHINE	5
2.0	EXPERIMENTAL RESEARCH PROGRAM AND DATA	7
	2.1 WIRE RESEARCH MACHINE	7
	2.1.1 CALIBRATION OF THE WIRE FATIGUE RESEARCH MACHINES	7
	2.1.2 RESEARCH PROGRAM AND DATA	29
	2.2 WIEDEMANN RESEARCH MACHINES	36
	2.2.1 CALIBRATION OF THE WIEDEMANN FATIGUE RESEARCH MACHINES	36
	2.2.1.1 WIEDEMANN (MODIFIED)	36
	2.2.1.2 WIEDEMANN (UNMODIFIED)	53
	2.2.2 RESEARCH PROGRAM AND DATA	69
	2.3 AXIAL FATIGUE RELIABILITY RESEARCH MACHINE	72
	2.3.1 AXIAL FATIGUE TESTING TO GENERATE GOODMAN DIAGRAMS	72

TABLE OF CONTENTS (Continued) Page

2.3.1.1 DETERMINATION OF ENDURANCE STRENGTH DISTRIBUTION AT THE STRESS RATIO $r_s = \infty$ 74

2.3.1.2 DETERMINATION OF STRENGTH DISTRIBUTION AT STRESS RATIO OTHER THAN ∞ 76

2.3.1.3 PLOTTING AND REDUCTION OF STAIRCASE DATA 80

2.3.2 RESEARCH PROGRAM AND DATA 80

3.0 DATA REDUCTION AND RESULTS 83

3.1 CYCLES-TO-FAILURE DATA 83

3.1.1 PROGRAM CYTOFR 83

3.1.2 PROGRAM WEIBULL 86

3.1.3 SUBROUTINE GRAPH 89

3.2 WIRE RESEARCH MACHINES 90

3.2.1 TENSILE DISTRIBUTIONAL PROPERTIES 90

3.2.2 CYCLES-TO-FAILURE DISTRIBUTIONAL PROPERTIES . . . 90

3.2.3 STAIRCASE TEST AND DISTRIBUTIONAL PROPERTIES . . 102

3.3 WIEDEMANN RESEARCH MACHINES 111

3.3.1 TENSILE DISTRIBUTIONAL PROPERTIES 111

3.3.2 CYCLES-TO-FAILURE DISTRIBUTIONAL PROPERTIES . . . 111

3.3.3 STAIRCASE TEST AND DISTRIBUTIONAL PROPERTIES . . . 111

3.3.4 METHODOLOGY FOR CONSTRUCTING S-N DIAGRAMS EMPIRICALLY FROM STATIC ULTIMATE AND ENDURANCE STRENGTH DATA FOR GROOVED AND UNGROOVED SPECIMENS 118

3.3.5 NOTCH SENSITIVITY 137

3.3.5.1 ASPECTS OF NOTCH SENSITIVITY IN FATIGUE 137

TABLE OF CONTENTS (Continued) Page

3.3.5.2 COMPARISON OF THEORETICAL AND ONR EXPERIMENTAL NOTCH SENSITIVITY RESULTS 154

3.3.5.3 RESULTS DRAWN FROM NOTCH SENSITIVITY TESTING 162

3.4 AXIAL FATIGUE RESEARCH MACHINE 162

3.4.1 TENSILE DISTRIBUTIONAL PROPERTIES 162

3.4.2 DISTRIBUTIONAL GOODMAN DIAGRAMS FOR AISI 1018 STEEL 163

3.4.2.1 DETERMINATION OF THE STRENGTH PARAMETERS AT SPECIFIC STRESS RATIOS 163

3.4.2.2 CONVERSION OF STAIRCASE TEST RESULTS INTO DISTRIBUTIONAL GOODMAN DIAGRAMS 163

3.4.2.3 COMPARISON OF EXPERIMENTAL FATIGUE TEST RESULTS WITH ESTABLISHED FAILURE THEORIES 164

3.4.2.4 METHODOLOGY FOR FINDING THE BEST-FIT CURVE THROUGH THE EXPERIMENTAL DATA POINTS 167

4.0 OVERALL CONCLUSIONS 173

4.1 WIRE FATIGUE RESEARCH MACHINE TESTS 173

4.2 WIEDEMANN MACHINE REVERSED BENDING FATIGUE TESTS OF STEELS ROD SPECIMENS 175

4.3 AXIAL MACHINE COMBINED ALTERNATING AND MEAN STRESS TESTS 177

5.0 RECOMMENDATIONS 179

6.0 REFERENCES 183

VOLUME II - RESEARCH DATA

TABLE OF CONTENTS

		Page
7.0	APPENDICES	185
	APPENDIX A PROGRAM WIEDEMANN (MODIFIED)	186
	APPENDIX B PROGRAM WIEDEMANN (UNMODIFIED)	188
	APPENDIX C PROGRAM CYTOFR (UPDATED)	190
	APPENDIX D PROGRAM WEIBULL	208
	APPENDIX E PDP-8 STAIRCASE REDUCTION	225
	APPENDIX F PDP-8 GOODMAN DIAGRAM PROGRAM	226
	APPENDIX G PDP-8 VON MISES-HENCKY REDUCTION PROGRAM	227
	APPENDIX H PDP-8 AXIAL STAIRCASE REDUCTION PROGRAM	228
	APPENDIX I PDP-8 AXIAL LOAD PROGRAM	229
8.0	DETAILED TEST DATA	230
	8.1 WIRE FATIGUE MACHINE DATA	231
	8.2 WIEDEMANN FATIGUE MACHINE	324
	8.3 AXIAL FATIGUE MACHINE DATA	369
9.0	REDUCED TEST DATA	383
	9.1 WIRE FATIGUE MACHINE DATA	384
	9.2 WIEDEMANN FATIGUE MACHINE DATA	444
	9.3 AXIAL FATIGUE MACHINE DATA	473
10.0	DISTRIBUTION LIST	493

LIST OF FIGURES

		Page
2.1-1	Calibration chart for Wire Machine #1	30
2.1-2	Calibration chart for Wire Machine #2	31
2.1-3	Calibration chart for Wire Machine #3	32
2.1-4	Calibration chart for Wire Mcahine #4	33
2.2-1	Upper Pan Counter-Weight System	37
2.2-2	Bearing Housing Assembly	38
2.2-3	Lower Pan Weight Assembly	39
2.2-4	Specimen Loading Free-body Diagram	40
2.2-5	Notch sensitivity of normalized steel specimens [5, p. 9]	44
2.2-6	Notch sensitivity of quenched and tempered alloy steel specimens (Based on Data of Gough) [5, p. 9]	44
2.2-7	Stress concentration factor, K_t, for a grooved shaft in bending (r/D from 0.001 to 0.050) [5, p.48],	45
2.2-8	Stress concentration factor, K_t, for a grooved shaft in bending (r/D from 0.050 to 1.000)[5, p. 49]	46
2.2-9	R. R. Moore rotating beam fatigue machine bearing housing	54
2.2-10	Average notch sensitivity curves [5, p. 10, Fig. 4]	60
2.2-11	Stress concentration factor, K_t, for a grooved shaft in bending (r/d from 1.01 to ∞)[5, p. 47]	61
2.2-12	Stress concentration factor, K_t, for a grooved shaft in bending (r/d from 1.005 to ∞ and r/d from 0.3 to 100) [5, p. 50]	62
2.3-1	Goodman diagrams showing various theories defining the safe design region for combined-stress fatigue	73
2.3-2	Goodman diagram (empirical) showing the estimates of the mean of the stress vector, S_v, at different stress ratios, r_s	77

LIST OF FIGURES (Continued) Page

3.2-1 Statistical S-N surface for 35 specimens; D = 0.040 in., AISI 4340 steel wire for results summarized in Tables 3.2-1 and 3.2-2. 97

3.2-2 Statistical S-N surface for 35 specimens; D = 0.040 in., AISI 4130 steel wire for results summarized in Tables 3.2-1 and 3.2-3. 98

3.2-3 Statistical S-N surface for 35 specimen; D = 0.040 in., AISI 1038 steel wire for results summarized in Tables 3.2-1 and 3.2-4. 99

3.2-4 Statistical S-N surface for 35 specimen; D = 0.040 in., AISI 1018 steel wire for results summarized in Tables 3.2-1 and 3.2-5. 100

3.2-5 Staircase test results obtained with the Wiedemann machine for AISI 1038 steel, d = 0.2700 in., r = 0.062 in., and 3 x 10^6 cycles of life (Group No. 163) 105

3.3-1 Experimentally determined S-N diagrams using ONR research results for AISI 4130 steel rod in reversed bending, D = 0.0375, d = 0.0937", and r = 0.250". 113

3.3-2 Experimentally determined S-N diagram using ONR research results for AISI 4130 grooved steel rod in reversed bending, D = 0.375", d = 0.0937" and r = 0.125". . . . 114

3.3-3 Modifying factors for surface finish for steels [6, Fig. 5.26, p. 167]. 122

3.3-4 S-N diagram plotted for AISI 4130 steel rod D = 0.375", d = 0.0937" and r = 0.250", using Shigley's recommendations 127

3.3-5 Severity of K_f' at 10^3 cycles [7, Fig. 13.16, P. 260] . 131

3.3-6 S-N diagram for AISI 4130 steel rod, D = 0.375", d = 0.0937", r = 0.250" and r = 0.125" using Juvinall's recommendations 134

3.3-7 Notch sensitivity versus notch radius. Vertical lines represent observed "points". Dashed line represents Neuber's theory [16, p. 47, Fig. 24]. . . . 146

3.3-8 Neuber grain size constants for steel and aliuminum for use in Eq. (3.3-25), [7, p. 254, Fig. 13.20] . . . 148

LIST OF FIGURES (Continued) Page

3.3-9 Notch sensitivity values versus notch radius [7, p. 255, Fig. 13.21] 150

3.3-10 Notch sensitivity values versus hole or fillet radius [5, p. 9, Fig. 8] 151

3.3-11 Notch sensitivity of quenched and tempered alloy steel versus notch radius [5, p. 9, Fig. 9] 152

3.3-12 Neuber's theoretical stress concentration factor relationships [Ref. 6, p. 66] 153

3.3-13 Notch sensitivity factor, q, for AISI 1038 steel rod subjected to fully reversed bending (See Table 3.3-9) 156

3.3-14 Fatigue stress concentration factor, K_f, vs r/D for a grooved shaft in bending AISI 1038 steel rod, endurance at 3×10^6 cycles, rod diameter D = 0.375In., base diameter, d = 0.2700 in. varied notch radii, r . . 157

3.3.-15 Notch sensitivity versus notch radius [18, p. 526, Fig. 4] 158

3.3-16 Notch sensitivity values for normalized steels versus notch radius [18, p. 527, Fig. 6]. 159

3.3-17 Relations among K_f, K and S_{Max} for notched AISI 4130 steel [15, p. 416, Fig. 4.25]. 160

3.4-1 Example of plot of a stress vector distribution for a stress ratio, $r_s = 1$. 165

3.4-2 Distribution Goodman strength diagram for 2.0×10^6 cycles of life with AISI 1018 steel ungrooved specimens 168

VOLUME II

LIST OF FIGURES

Page

9.1-1 Calibration Chart of Stress Vs. Measured Strain for Calibration of Fatigue Research Machines (See Table 9). 392

9.1-2 Cycles-to-Failure distribution of Group No. 129 using Wire Fatigue Machine No. 1 for 35 specimens of .040 in. diameter AISI 4130 steel wire. Fixed alternating stress level of 67,700 psi. Bend angle 19.5 degrees. Coast-down cycles 100. 393

9.1-3 Cycles-to-failure distribution of Group No. 129 using Wire Fatigue Machine No. 1 for 35 specimens of .040 in. dimaeter AISI 4130 steel wire. Fixed alternating stress level of 67,700 psi. Bend angle 19.5 degrees. Coast down cycles 100. 394

9.1-4 Cycles-to-failure distribution, SL = 67700 psi, Group No. 129 395

9.1-5 Cycles-to-failure distribution of Group No. 130, using Wire Machine No. 1 for 35 specimens of .040 in. diameter AISI 4130 steel wire. Fixed alternating stress level of 70,000 psi. Bend angle 20.0 degrees. Coast down cycles 200 396

9.1-6 Cycles-to-failure distribution of Group No. 130 using Wire Machine No. 1 for 35 specimens of .040 in. diameter AISI 4130 steel wire. Fixed alternating stress level of 70,000 psi. Bend angle 20.0 degrees. Coast down cycles 200 397

9.1-7 Cycles-to-failure distribution, Group 130, SL 70,000 psi 398

9.1-8 Cycles-to-failure distribution of Group No. 131 using Wire Machine No. 1 for 35 specimens of .040 in. diameter AISI 4130 steel wire. Fixed alternating stress level of 72,500 psi. Bend angle 20.5 degrees. Coast down cycles 100 399

LIST OF FIGURES (Cont.) Page

9.1-9 Cycles-to-failure distribution of Group No. 131 using Wire Machine No. 1 for 35 specimens of .040 in. diameter AISI 4130 steel wire. Fixed alternating stress level of 72,500 psi. Bend angle 20.5 degrees. Coast down cycles 100 400

9.1-10 Cycles-to-failure distribution, Group 131, SL = 72,500 psi 401

9.1-11 Cycles-to-failure distribution of Group No. 132 using Wire Machine No. 1 for 35 specimens of .040 in. diameter AISI 4130 steel wire. Fixed alternating stress level of 74,700 psi. Bend angle 21.0 degrees. Coast down cycles 200 402

9.1-12 Cycles-to-failure distribution of Group No. 132 using Wire Machine No. 1 for 35 specimens of .040 in. diameter AISI 4130 steel wire. Fixed alternating stress level of 74,700 psi. Bend angle 21.0 degrees. Coast down cycles 200 403

9.1-13 Cycles-to-failure distribution, Group 132, SL = 74,700 psi 404

9.1-14 Cycles-to-failure distribution of Group No. 133, using Wire Machine No. 1 for 35 specimens of .040 in. diameter AISI 4130 steel wire. Fixed alternating stress level of 77,800 psi. Bend angle 21.5 degrees. Coast down cycles 200 405

9.1-15 Cycles-to-failure distribution of Group No. 133 using Wire Machine No. 1 for 35 specimens of .040 in. diameter AISI 4130 steel wire. Fixed alternating stress level of 77,800 psi. Bend angle 21.5 degrees. Coast down cycles 200 406

9.1-16 Cycles-to-failure distribution, Group 133, SL = 77,800 psi 407

9.1-17 Cycles-to-failure distribution of Group No. 136 using Wire Fatigue Machine No. 2 for 35 specimens of .040 in. diameter AISI 1038 steel wire. Fixed alternating stress level of 64,500 psi. Bend angle 17.0 degrees. Coast down cycles 100 408

9.1-18 Cycles-to-failure distribution of Group No. 136 using Wire Fatigue Machine No. 2 for 35 specimens of .040 in. diameter AISI 1038 steel wire. Fixed Alternating stress level of 64,500 psi. Bend angle 17.0 degress. Coast-down cycles 100. 409

LIST OF FIGURES (Cont.) Page

9.1-19 Cycles-to-failure distribution, SL = 64,500 psi, Group 136 410

9.1-20 Cycles-to-failure distribution of Group No. 137 using Wire Machine No. 2 for 35 specimens of .040 in. diameter AISI 1038 steel wire. Fixed alternating stress level of 67,200 psi. Bend angle 17.5 degrees. Coast down cycles 100 411

9.1-21 Cycles-to-failure distribution of Group No. 137 using Wire Machine No. 2 for 35 specimens of .040 in. diameter AISI 1038 steel wire. Fixed alternating stress level of 67,200 psi. Bend angle 17.5 degrees. Coast down cycles 100 412

9.1-22 Cycles-to-failure distribution, Group 137, SL = 67,200 psi 413

9.1-23 Cycles-to-failure distribution of Group No. 138 using Wire Machine No. 2 for 35 specimens of .040 in. diameter AISI 1038 steel wire. Fixed alternating stress level of 69,200 psi. Bend angle 18.0 degrees. Coast down cycles 200 414

9.1-24 Cycles-to-failure distribution of Group No. 138 using Wire Machine No. 2 for 35 specimens of .040 in. diameter AISI 1038 steel wire. Fixed alternating stress level of 69,200 psi. Bend angle 18.0 degrees. Coast down cycles 200 415

9.1-25 Cycles-to-failure distirbution, Group 138, SL = 69,200 psi 416

9.1-26 Cycles-to-failure distribution of Group No..139 Using Wire Machine No. 2 for 35 specimens of .040 in. diameter AISI 1038 steel wire. Fixed alternating stress level of 72,300 psi. Bend angle 18.5 degrees. Coast down cycles 200 417

9.1-27 Cycles-to-failure distribution of Group No. 139 using Wire Machine No. 2 for 35 specimens of .040 in. diameter AISI 1038 steel wire. Fixed alternating stress level of 72,300 psi. Bend angle 18.5 degrees. Coast down cycles 200 418

9.1-28 Cycles-to-failure distribution, Group 139, SL = 72,300 psi. 419

LIST OF FIGURES (Cont.) Page

9.1-29 Cycles-to-failure distribution of Group No. 143 using Wire Machine No. 3 for 35 specimens of .040 in. diameter AISI 1018 steel wire. Fixed alternating stress level of 57,200 psi. Bend angle 15.5 degrees. Coast down cycles 200 420

9.1-30 Cycles-to-failure distribution of Group No. 143 using Wire Machine No. 3 for 35 specimens of .040 in. diameter AISI 1018 steel wire. Fixed alternating stress level of 57,200 psi. Bend angle 15.5 degrees. Coast down cycles 200 421

9.1-31 Cycles-to-failure distribution, Group 143, SL = 57,200 psi 422

9.1-32 Cycles-to-failure distribution of Group No. 144 using Wire Machine No. 3 for 35 specimens of .040 in. diameter AISI 1018 steel wire. Fixed alternating stress level of 60,000 psi. Bend angle 16.0 degrees. Coast down cycles 100 423

9.1-33 Cycles-to-failure distribution of Group No. 144 using Wire Machine No. 3 for 35 specimens of .040 in. diameter AISI 1018 steel wire. Fixed alternating stress level of 60,000 psi. Bend angle 16.0 degrees. Coast down cycles 100 424

9.1-34 Cycles-to-failure distribution, Group 144, SL = 60,000 psi 425

9.1-35 Cycles-to-failure distribution of Group No. 145 using Wire Machine No. 3 for 35 specimens of .040 in. diameter AISI 1018 steel wire. Fixed alternating stress level of 62,800 psi. Bend angle 16.5 degrees. Coast down cycles 200 426

9.1-36 Cycles-to-failure distribution of Group No. 145 using Wire Machine No. 3 for 35 specimens of .040 in. diameter AISI 1018 steel wire. Fixed alternating stress level of 62,800 psi. Bend angle 16.5 degrees. Coast down cycles 200 427

9.1-37 Cycles-to-failure distribution, Group 14., SL = 62,800 psi 428

LIST OF FIGURES (Cont.) Page

9.1-40 Cycles-to-failure distribution of Group No. 150 using Wire Machine No. 4 for 35 specimens of .040 in. diameter AISI 4340 steel wire. Fixed alternating stress level of 73,500 psi. Bend angle 20.5 degrees. Coast down cycles 100. 429

9.1-41 Cycles-to-failure distribution of Group No. 150 using Wire Machine No. 4 for 35 specimens of .040 in. diameter AISI 4340 steel wire. Fixed alternating stress level of 73,500 psi. Bend angle 20.5 degrees. Coast down cycles 100 430

9.1-42 Cycles-to-failure distribution, SL = 73,500 psi, Group 150 431

9.1-43 Cycles-to-failure distribution of Group No. 151 using Wire Fatigue Machine No. 4 for 35 specimens of .040 in. diameter AISI 4340 steel wire. Fixed alternating stress level of 78,100 psi. Bend angle 21.5 degrees. Coast down cycles 100 432

9.1-44 Cycles-to-failure distribution of Group No. 151 using Wire Fatigue Machine No. 4 for 35 specimens of .040 in. diameter AISI 4340 steel wire, Fixed alternating stress level of 78,100 psi. Bend angle 21.5 degrees. Coast down cycles 100 433

9.1-45 Cycles-to-failure distribution, SL = 78,100 psi, Group 151 434

9.1-46 Cycles-to-failure distribution of Group No. 152 using Wire Fatigue Machine No. 4 for 35 specimens of .040 in. diamter AISI 4340 steel wire. Fixed alternating stress level of 80,100 psi. Bend angle 22.0 degrees. Coast down cycles 100 435

9.1-47 Cycles-to-failure distribution of Group No. 152 using Wire Fatigue Machine No. 4 for 35 specimens of .040 in. diameter AISI 4340 steel wire. Fixed alternating stress level of 80,100 psi. Bend angle 22.0 degrees. Coast down cycles 100 436

9.1-48 Cycles-to-failure distribution, Group 152, SL = 80,100 psi 437

9.1-49 Cycles-to-failure distribution of Group No. 153 using Wire Fatigue Machine No. 4 for 35 specimens of .040 in. diameter AISI 4340 steel wire. Fixed alternating stress level of 84,700 psi. Bend angle 23.0 degrees. Coast down cycles 100 438

LIST OF FIGURES (Cont.) Page

9.1-50 Cycles-to-failure distribution of Group No. 153 using Wire Fatigue Machine No. 4 for 35 specimens of .040 in. diameter AISI 4340 steel wire. Fixed alternating stress level of 84,700 psi. Bend angle 23.0 degrees. Coast down cycles 100.. 439

9.1-51 Cycles-to-failure distribution, SL = 84,700, Group 135 440

9.1-52 Cycles-to-failure distribution of Group No. 154 using Wire Fatigue Machine No. 4 for 35 specimens of .040 in. diameter AISI 4340 steel wire. Fixed alternating stress level of 90,000 psi. Bend angle 24.0 degrees. Coast down cycles 100 441

9.1-53 Cycles-to-failure distribution of Group No. 154 using Wire Fatigue Machines No. 4 for 35 specimens of .040 in. diameter AISI 4340 steel wire. Fixed alternating stress level of 90,000 psi. Bend angle 24.0 degrees. Coast down cycles 100 442

9.1-54 Cycles-to-failure distribution, SL = 90,000 psi, Group 154 443

9.2-1 Cycles-to-failure distribution of Group No. 89 using the Wiedemann Fatigue Machine for 36 specimens of .0937 in. notch diameter and .125 in notch radius AISI 4130 steel rod. Fixed alternating stress level of 75,000 psi 445

9.2-2 Cycles-to-failure distribution of Group No. 89 using the Wiedemann Fatigue Machine for 36 specimens of .0937 in. notch diameter and .125 in. notch radius AISI 4130 steel rod. Fixed alternating stress level of 75,000 psi 446

9.2-3 Cycles-to-failure distribution, SL = 75,000, Group 89 447

9.2-4 Cycles-to-failure distribution of Group No. 90 using the Wiedemann Fatigue Machine for 37 specimens of .0937 in. notch diameter and .125 in. notch radius AISI 4130 steel rod. Fixed alternating stress level of 85,000 psi 448

LIST OF FIGURES (Cont.) Page

9.2-5 Cycles-to-failure distribution of Group No. 90 using the Wiedemann Fatigue Machine for 37 specimens of .0937 in. notch diameter and .125 in. notch radius AISI 4130 steel rod. Fixed alternating stress level of 85,000 psi 449

9.2-6 Cycles-to-failure distribution, SL = 85,000 psi, Group 90 450

9.2-7 Cycles-to-failure distribution of Group No. 91 using the Wiedemann Fatigue Machine for 37 specimens of .0937 in. notch diameter and .125 in. notch radius AISI 4130 steel rod. Fixed alternating stress level of 90,000 451

9.2-8 Cycles-to-failure distribution of Group No. 91 using the Wiedemann Fatigue Machine for 37 specimens of .0937 in. notch diameter and .125 in. notch radius AISI 4130 steel rod. Fixed alternating stress level of 90,000 452

9.2-9 Cycles-to-failure distribution, SL = 95,000 psi, Group 91 453

9.2-10 Cycles-to-failure distribution of Group No. 93 using the Wiedemann Fatigue Machine for 35 specimens of .0937 in. notch diameter and .250 in. notch radius AISI 4130 steel rod. Fixed alternating stress level of 70,000 psi 454

9.2-12 Cycles-to-failure distribution, SL = 70,000 psi, Group 93 456

9.2-13 Cycles-to-failure distribution of Group No. 94 using the Wiedemann Fatigue Machine for 35 specimens of .0937 in. notch diameter and .250 in. notch radius AISI 4130 steel rod. Fixed alternating stress level of 80,000 psi 457

9.2-14 Cycles-to-failure distribution of Group No. 94 using the Wiedemann Fatigue Machine for 35 specimens of .0937 in. notch diameter and .250 in. notch radius AISI 4130 steel rod. Fixed alternating stress level of 80,000 psi 458

9.2-15 Cycles-to-failure distribution, SL = 80,000 psi, Group 94 459

LIST OF FIGURES (Cont.) Page

9.2-16 Cycles-to-failure distribution of Group No. 95 using the Wiedemann Fatigue Machine for 34 specimens of .0937 in. notch diameter and .250 in. notch radius AISI 4130 steel rod. Fixed alternating stress level of 95,000 psi 460

9.2-17 Cycles-to-failure distribution of Group No. 95 using the Wiedemann Fatigue Machine for 34 specimens of .0937 in. notch diameter and .250 in. notch radius AISI 4130 steel rod. Fixed alternating stress level of 95,000 psi 461

9.2-18 Cycles-to-failure distribution, SL = 95,000 psi, Group 95 462

9.2-19 Endurance strength data for AISI 1038 steel rod, Group No. 162, groove diameter d = 0.2700 in., groove radius r = 0.31 in. with cut-off at 3×10^6 cycles 464

9.2-20 Endurance strength data for AISI 1038 rod, Group No. 163, groove diameter d = 0.2700 in., groove radius r = 0.062 in. with cut-off at 3×10^6 cycles 466

9.2-21 Endurance strength data for AISI 1038 steel rod, Group No. 164, groove diameter d = 0.2700 in., groove radius r = 0.125 in. with cut-off at 3×10^6 cycles 468

9.2-22 Endurance strength data for AISI 1038 steel rod, Group No. 165, groove diameter d = 0.2700 in., groove radius r = 0.250 in., cut-off at 3×10^6 cycles 470

9.2-23 Endurance strength data for AISI 1038 steel rod, Group No. 166, groove diameter d = 0.2700 in., groove radius r = 1.87 in. with cut-off at 3×10^6 cycles 472

9.3.-1 Staircase plot of endurance strength data for Group 159, AISI 1018 steel specimens, d = 0.075 in. and groove radius = 2.70 in. tested at stress ratio r_s = 1.0 475

LIST OF FIGURES (Cont.)

Page

9.3-2 Staircase plot of endurance strength data for Group 160, AISI 1018 steel specimens, d = 0.075 in., and groove radius = 2.70 in., tested at a stress ratio r_s = 2.0 477

9.3-3 Staircase plot of endurance strength data for Group 161, AISI 1018 steel specimens, d = 0.075 in., and groove radius = 2.70 in., tested at a stress ratio of infinity 479

9.3-4 Staircase plot of endurance strength data for Group 63, AISI 4130 steel specimens, d = 0.048 in., groove radius = 2.70 in., tested at stress ratio r_s = 0.2 485

LIST OF TABLES

		Page
2.0-1	Summary of experimental research program for the Office of Naval Research	8
2.1-1	Test program for Wire Fatigue Machines	34
2.2-1	Computer output (sample) for pan weight calculations of Wiedemann Fatigue Machine (Modified)	49
2.2-2	Computer output (sample) for pan weight calculations of Wiedemann Fatigue Machine (Unmodified)	65
2.2-3	Cycles-To-Failure on Wiedemann Machines	70
2.2-4	Notch sensitivity fatigue test data - staircase testing on Wiedemann Machines	71
2.3-1	Ratio of experimental endurance strength to static ultimate strength for staircase-test starting-stress determination	75
2.3-2	Axial Fatigue Machine test program for AISI 1018 steel specimens and references for the raw and the reduced data for groups of 35 specimens	81
3.2-1	The University of Arizona experimentally determined distributional static strength data for Wire	92
3.2-2	The University of Arizona experimentally determined cycles-to-failure parameters for AISI 4340 steel wire under pure reversed bending fatigue testing conditions for design use	93
3.2-3	The University of Arizona experimentally determined cycles-to-failure parameters for AISI 4130 steel wire under pure reversed bending fatigue testing conditions for design use	94
3.2-4	The University of Arizona experimentally determined cycles-to-failure parameters for AISI 1038 steel wire under pure reversed bending fatigue testing conditions for design use	95
3.2-5	The University of Arizona experimentally determined cycles-to-failure parameters for AISI 1018 steel wire under pure reversed bending fatigue testing condistions for design use	96

LIST OF TABLES (Continued)

		Page
3.2-6	K-S and Chi-Squared test results for Weibull distribution	101
3.2-7	Reduced data for Group 163, AISI 1038 steel. Wiedemann Fatigue Machine	107
3.3-1	The University of Arizona experimentally determined distributional static strength data for ungrooved steel rod	112
3.3-2	The University of Arizona experimentally determined cycles-to-failure parameters for AISI 4130 steel rod under pure reversed bending fatigue testing conditions for design use	115
3.3-3	The University of Arizona experimentally determined cycles-to-failure parameters for AISI 4130 steel rod under pure reversed bending fatigue testing conditions for design use	116
3.3-4	The University of Arizona experimentally determined staircase parameters for AISI 1038 steel rod under pure reversed bending, fatigue testing conditions for 3×10^6 cycles of life	117
3.3-5	Values of fatigue-notch factor and fatigue-notch sensitivity	139
3.3-6	Rotating beams with circumferential grooves [17, p. 16, Table 1]	140
3.3-7	Check of computed strength-reduction factor (k') with strength-reduction factor determined directly by fatigue tests [18, p. 517]	143
3.3-8	Stress concentration factor, K_t; fatigue notch factors, K_f; and notch sensitivity indices q for various alloys in rotating bending [15, p. 104, Table 3.3]	145
3.3-9	The University of Arizona experimentally determined distributional fatigue notch sensitivity design data for AISI 1038 steel rod in fully reversed bending	155

VOLUME II

LIST OF TABLES

Page

8.1-1 Wire Fatigue Research Machines 232

8.1-2 Wire Fatigue Research Machines 241

8.1-3 Wire Fatigue Research Machines 250

8.1-4 Wire Fatigue Research Machines 259

8.1-5 Static calibration data for Wire Fatigue Research Machine calibration specimen 268

8.1-6 Cycles-to-failure data of Group No. 129 using Wire Fatigue Machine No. 1 for 35 specimens of .040 in. diameter AISI 4130 steel wire. Fixed Aleternating stress level of 67.7 Kpsi. Bend angle 19.5°. Coast-down cycles 200 272

8.1-7 Cycles-to-failure data of Group No. 130 using Wire Fatigue Machine No. 1 for 35 specimens of .040 in. diameter AISI 4130 steel wire. Fixed Alternating stress level of 70,000 psi. Bend angle 20°. Coast-down cycles 200. 274

8.1-8 Cycles-to-failure data for Group No. 131 using Wire Fatigue Machine No. 1 for 35 specimens of .040 in. diameter AISI 4130 steel wire. Fixed Alternating stress level of 72,500 psi. Bend angle 20.5°. Coast-down cycles 200. 276

8.1-9 Cycles-to-failure data of Group No. 132 using Wire Fatigue Machine No. 1 for 35 specimens of .040 in. diameter AISI 4130 steel wire. Fixed Alternating stress level of 74,700 psi. Bend angle 21.0°. Coast-down cycles 200. 278

8.1-10 Cycles-to-failure data of Group No. 133 using Wire Fatigue Machine No. 1 for 35 specimens of .040 in. diameter AISI 4130 steel wire. Fixed Alternating stress level of 77,800 psi. Bend angle 21.5°. Coast-down cycles 200. 280

8.1-11 Static ultimate strength test data of Group No. 134 using the Riehle Machine 35 specimens of AISI 4130 steel 282

LIST OF TABLES (Cont.) Page

8.1-12 Test data for hardness and ultimate strength elongation of Group No. 134. 35 specimens of AISI 4130 steel. D = .040 in.; L = 10 in.. 284

8.1-13 Cycles-to-failure data of Group No. 136 using Wire Fatigue Machine No. 2 for 35 specimens of .040 in. diameter AISI 1038 steel wire. Fixed Alternating stress level of 64,500 psi. Bend angle 17°. Coast-down cycles 200 286

8.1-14 Cycles-to-failure data of Group No. 137 using Wire Fatigue Machine No. 2 for 35 specimens of 0.40 in. diameter AISI 1038 steel wire. Fixed alternating stress level of 67,200 psi. Bend angle 17.5° Coast-down cycles 200 288

8.1-15 Cycles-to-failure data of Group No. 138 using Wire Fatigue Machine No. 2 for 35 specimens of .040 in. diameter AISI 1038 steel wire. Fixed alternating stress level of 69,200 psi. Bend angle 18.0°. Coast-down cycles 200. 290

8.1-16 Cycles-to-failure data of Group No. 139 using Wire Fatigue Machine No. 2 for 35 specimens of .040 in. diameter AISI 1038 steel wire. Fixed alternating stress level of 72,300 psi. Bend angle 18.5°. Coast-down cycles 200. 292

8.1-17 Static ultimate strength test data of Group No. 141 using the Riehle Machine, 35 specimens of AISI 1038 steel 294

8.1-18 Test data for hardness and ultimate strength elongation of Group No. 141. 35 specimens of AISI 1038 steel, D = .040 in.; L = 10 in. 296

8.1-19 Cycles-to-failures data of Group No. 143 using Wire Fatigue Machine No. 3 for 35 specimens of .040 in. diameter ASIS 1018 steel wire. Fixed alternating stress level of 57,200 psi. Bend angle 15.5°. Coast-down cycles 200 298

8.1-20 Cycles-to-failures data of Group No. 144 using Wire Fatigue Machine No. 3 for 35 specimens of .040 in. diameter AISI 1018 steel wire. Fixed alternating stress level of 60,000 psi. Bend angle 16.0°. Coast-down cycles 200 300

LIST OF TABLES (Cont.) Page

8.1-21 Cycles-to-failure data of Group No. 145 using Wire Fatigue Machine No. 3 for 35 specimens of .040 in. diameter AISI 1018 steel wire. Fixed alternating stress level of 62,800 steel wire. Bend angle 16.5°. Coast-down cycles 200 302

8.1-22 Static ultimate strength test data of Group No. 148 using the Riehle Machine, 35 specimens of AISI 1018 steel 304

8.1-23 Test data for hardness and ultimate strength elongation of Group No. 148. 35 specimens of AISI 1018 steel. D = .040 in.; L = 10 in. 306

8.1-24 KHN hardness data for Group No. 148-2 using Tukon Micro-Hardness Tester for 10 specimens of.040 in. diameter. AISI 1018 steel wire 308

8.1-25 Cycles-to-failure data of Group No. 155 using Wire Fatigue Machine No. 4 for 35 specimens of .040 in. diameter AISI 4340 steel wire. Fixed alternating stress level of 73,500 psi. Bend angle 20.5°. Coast-down cycles 200 309

8.1-26 Cycles-to-failure data of Group No. 151 using Wire Fatigue Machine No. 4 for 35 specimens of .040 in. diameter AISI 4340 steel wire. Fixed alternating stress level of 78,100 psi. Bend angle 21.5°. Coast-down cycles 100 311

8.1-27 Cycles-to-failure data of Group No. 152 using Wire Fatigue Machine No. 4 for 35 specimens of .040 in. diameter AISI 4340 steel wire. Fixed alternating stress level of 80,100 psi. Bend angle 22.0°. Coast-down cycles 100. 313

8.1-28 Cycles-to-failure data of Group No. 153 using Wire Fatigue Machine No. 4 for 35 specimens of .040 in. diameter AISI 4340 steel wire. Fixed alternating stress level of 84,700 psi. Bend angle 23.0°. Coast-down cycles 200. 315

8.1-29 Cycles-to-failure data of Group No. 154 using Wire Fatigue Machine No. 4 for 35 specimens of .040 in. diameter AISI 4340 steel wire. Fixed alternating stress level of 90,000 psi. Bend angle 24.0°. Coast-down cycles 200 317

LIST OF TABLES (Cont.) Page

8.1-30 Static ultimate strength test data of Group No. 155 using the Riehle Machine, 35 specimens of AISI 4340 steel. 319

8.1-31 Test data for hardness and ultimate strength elongation of Group No. 155. 35 specimens of AISI 4340 steel. D = .040 in.; L = 10 in. 321

8.1-32 KHN hardness data for Group No. 155-2 using Tukon Micro-Hardness Tester for 10 specimens of .040 in. diameter AISI 4340 steel wire 323

8.2-1 Cycles-to-failure data of Group No. 89 using the Wiedemann Machine. 36 specimens of AISI 4130 steel rod of test section diameter, d = .0937 in., Radius, r = .125 in. Upper added pan load = 15.79 lbs Alternating stress = 75,000 psi. 325

8.2-2 Inspection data for critical and major characteristics of Group No. 89. 36 specimens of AISI 4130 steel D = .375 in.; L = 3.50 in. 327

8.2-2 Inspection data for critical and major characteristics of Group No. 90. 37 specimens of AISI 4130 steel D = .375 in.; L = 3.5 in. 329

8.2-4 Cycles-to-failure data of Group No. 90 using the Wiedemann Machine. 37 specimens of AISI 4130 steel rod of test section diameter, d = .0937 in., Radius, r = .125 in. Upper added pan load = 15.44 lbs. Alternating stress = 85,000 psi. 331

8.2-5 Inspection data for critical and major characteristics of Group No.91. 35 specimens of AISI 4130 steel D = .375 in.; L = 3.50 in. , Drawing No. 200 333

8.2-6 Cycles-to-failure data of Group No. 91 using the Wiedemann Machine. 37 specimens of AISI 4130 steel rod of test section diameter, d = .0937 in., Radius, r = .125 in. Upper added pan load = 15.10 lbs Alternating stress = 95,000 psi. 335

8.2-7 Inspection data for critical and major characteristics of Group No. 93. 35 specimens of AISI 4130 steel D = .375 in.; L = 3.50 in. Drawing No. 200 337

LIST OF TABLES (Cont.) Page

8.2-8 Cycles-to-failure data of Group No. 93 using the Wiedemann Machine. 35 specimens of AISI 4130 steel rod of test section diameter, d = .0937 in., Radius, r = .250 in. Upper added pan load = 15.96 lbs. Alternating stress = 70,000 psi. 339

8.2-9 Inspection data for critical and major characteristics of Group No. 94. 35 specimens of AISI 4130 steel D = .37 in.; L = 3.50 in. Drawing No. 200 341

8.2-10 Cycles-to-failure data of Group No. 94 using the Wiedemann Machine. 35 specimens of AISI 4130 steel rod of test section diameter, d = .0937 in., Radius, r = .250 in. Upper added pan load = 15.621 lbs. Alternating stress = 80,000 psi 343

8.2-11 Cycles-to-failure data of Group No. 95 using the Wiedemann Machine. 34 specimens of AISI 4130 steel rod of test section diameter, d = .0937 in., Radius, r = .250 in. Upper added pan load = 15.10 lbs. Alternating stress = 95,000 psi. 345

8.2-12 Inspection data for critical and major characteristics of Group No. 95. 34 specimens of AISI 4130 steel D = .375 in.; L = 3.00 in. Drawing No. 200 347

8.2-13 Staircase method data of Group No. 162 using the R. R. Moore Machine. 35 specimens of AISI 1038 steel rod with test section diameter d = .2700 in., Radius, r = .031 in. Cutoff at 3 x 10^6 cycles 349

8.2-14 Inspection data for critical and major characteristics of Group No. 162. 38 specimens of AISI 1038 steel,D = .375 in.; L = 2.75 in. Drawing No. 200. . . 351

8.2-15 Staircase method data of Group No. 163 using the R. R. Moore Machine. 37 specimens of AISI 1038 steel rod with test section diameter, d = .2700 in., Radius, r = .062 in., Cutoff at 3 x 10^6 cycles 353

8.2-16 Inspection data for critical and major characteristics of Group No. 163. 37 specimens of AISI 1038 steel. D = .375 in.; L = 2.75 in. Drawing No. 200 355

8.2-17 Staircase method data of Group No. 164 using the R. R. Moore Machine. 37 specimens of AISI 1038 steel rod with test section diameter, d = 0.2700 in., Radius, r = 0.125 in. Cutoff at 3 x 10^6 cycles. . 357

LIST OF TABLES (Cont.) Page

8.2-18 Inspection data for critical and major characteristics of Group No. 164. 37 specimens of AISI 1038 steel. D = .375 in.; L = 2.75 in. Drawing No. 200 359

8.2-19 Staircase method data of Group No. 165 using the R. R. Moore Machine. 36 specimens of AISI 1038 steel rod with test section diameter, d = .2700 in., Radius r = .250 in. Cutoff at 3 x 10^6 cycles 361

8.2-20 Inspection data for critical and major characteristics of Group No. 165. 36 specimens of AISI 1038 steel. D = .375 in.; L = 2.75 in. Drawing No. 200 363

8.2-21 Staircase method data of Group No. 166 using the R. R. Moore Machine. 35 specimens of AISI 1038 steel rod with test section diameter, d = .2700 in., Radius r = 1.87 in. Cutoff at 3 x 10^6 cycles 365

8.2-22 Inspection data for critical and major characteristics of Group No. 166. 35 specimens of AISI 1038 steel. D = .373 in.; L = 2.75 in. Drawing No. 200 367

8.3-1 Static ultimate strength test data of Group No. 156 using the Tinius Olsen Machine. 35 specimens of AISI 1018 steel. 270

8.3-2 Test data for hardness and ultimate strength elongation of Group No. 156. 35 specimens of AISI 1018 steel. D = .373 in.; L = 9.0 in. + 1/16. Drawing No. 100 372

8.3-3 Staircase method data of Group No. 159 using the Axial Fatigue Machine. 35 specimens of AISI 1018 steel rod with test section diameter, d = 0.075 in., Radius r = 2.70 in. Stress ratio r_s = 1.0. Cutoff at 2 x 10^6 cycles 374

8.3-4 Staircase method data of Group No. 160 using the Axial Fatigue Machine. 35 specimens of AISI 1018 steel rod with test section diameter, d = 0.075 in., Radius r = 2.70 in. Stress ratio r_s = 2.0. Cutoff at 2 x 10^6 cycles 376

8.3-5 Staircase method data of Group No. 161 using the Axial Fatigue Machine. 36 specimens of AISI 1018 steel rod with test section diameter, d = 0.075 in., Radius r = 2.70 in. Stress ratio $r_s = \infty$. Cutoff at 2 x 10^6 cycles 378

LIST OF TABLES (Cont.) Page

8.3-6 Staircase method data of Group No. 63 using the Axial Fatigue Machine. 25 specimens of AISI 4130 steel rod with test section diameter, d = 0.047 in., Radius r = 2.70 in. Stress ratio r_s = 0.2. Cutoff at 2 x 10^6 cycles 380

9.1-1 Angle of deflection vs. mean measured strain in Wire Fatigue Research Machine calibration specimen for each one of the four machines. 385

9.1-2 Summary of static axial calibration data for the 0.040 in. Diameter wire specimen used in calibrating the Wire Fatigue Machine 386

9.1-3 Calculation of the standard deviation for strain for each stress level given in Table 7. 387

9.1-4 Static axial stress versus measured strain for the Wire specimen used in calibrating the Wire Fatigue Research Machines. Mean wire diameter - D = .04063 in. 389

9.1-5 Actual specimen stress versus test specimen deflection angle for each Wire Fatigue Research Machine 390

9.1-6 Reduced data for Group 87, AISI 1038 steel. Wire Fatigue Machine No. 2. 391

9.2-1 Reduced data for Group 162, AISI 1038 steel. Wiedemann Fatigue Machine 463

9.2-2 Reduced data for Group 163, AISI 1038 steel. Wiedemann Fatigue Machine 465

9.2-3 Reduced data for Group 164, AISI 1038 steel. Wiedemann Fatigue Machine 467

9.2-4 Reduced data for Group 165, AISI 1038 steel, Wiedemann Fatigue Machine 469

9.2-5 Reduced data for Group 166, AISI 1038 steel. Wiedemann Fatigue Machine. 471

9.3-1 Reduced data for Group 159, AISI 1018 steel. Axial Fatigue Machine. 474

9.3-2 Reduced data for Group 160, AISI 1018 steel. Axial Fatigue Machine 476

LIST OF TABLES (Cont.) Page

9.3-3 Reduced data for Group 161, AISI 1018 steel. Axial Fatigue Machine 478

9.3-4 Reduced data for Group 32, AISI 4130 steel. Axial Fatigue Machine 480

9.3-5 Reduced data for Group 33, AISI 4130 steel. Axial Fatigue Machine 481

9.3-6 Reduced data for Group 34, AISI 4130 steel. Axial Fatigue Machine 482

9.3-7 Reduced data for Group 62, AISI 4130 steel. Axial Fatigue Machine 483

9.3-8 Reduced data for Group 63, AISI 4130 steel. Axial Fatigue Machine. 484

9.3-9 Reduced data for Group 64, AISI 4130 steel. Axial Fatigue Machine 486

9.3-10 Reduced data for Group 111, AISI 1038 steel. Axial Fatigue Machine 487

9.3-11 Reduced data for Group 112, AISI 1038 steel. Axial Fatigue Machine 488

9.3-12 Reduced data for Group 113, AISI 1038 steel. Axial Fatigue Machine 489

9.3-13 Reduced data for Group 114, AISI 1038 steel. Axial Fatigue Machine 490

9.3-14 Reduced data for Group 115, AISI 1038 steel. Axial Fatigue Machine 491

1.0 INTRODUCTION

1.1 PRIOR RESEARCH

Research under the Office of Naval Research Contract N00014-67-A-0209-002 was initiated on 1 February 1967. This program has included both theoretical and experimental research. In the theoretical research, the interactions among stress and strength phenomena in the design and life of dynamic and rotary machinery have been investigated, and a method was developed for applying the strength-stress relationship to optimize the design of machinery for a finite life at a specified level of reliability. The experimental research program has included the testing of specimens of various materials and geometry to support and validate the results of the theoretical research.

During the first reporting period a literature search was conducted to survey the extent and nature of the interactions among the design phenomena important to dynamic and rotary machinery, to assess the availability of data in statistical form, and to assess the state of development of the probabilistic design-by-reliability theory and methods. The Design-by-Reliability Methodology was discussed in the First Progress Report (1), and the applicable mathematical equations were given. That report also included discussions on the definition of failure mechanisms in shafts, bearings, and other mechanical components and the methodology whereby conventional designs could be improved. An experimental research program was proposed for the development of statistically described fatigue strength properties of materials. Testing machines to accomplish the experimental program were identified and their availability was confirmed.

During the second reporting period, 1 February 1968 - 31 January 1969, the testing machines were calibrated and experimental fatigue testing was initiated. The initial material selected for study was AISI 4340 cold rolled and annealed steel. Specimens appropriate for

each type of testing machine were obtained and their physical and geometric properties were evaluated. The description of the machine calibration procedures and results, the procurement and preparation of test specimens and the results of fatigue testing accomplished during the second period are described in the Second Technical Report (2).

During the third reporting period, 1 February 1969 - 31 August 1970, emphasis was placed upon generating statistical data needed in the design of dynamic and rotary machinery for specified levels of reliability. Static tensile, and endurance strength parameter distributions and cycles-to-failure distributions at fixed stress levels were obtained for AISI 4340 and 4130 steel. Specimens tested included 0.0625 in. diameter wires subjected to reversed bending on the Wire Fatigue Machines, 0.0937 in. diameter rods subjected to reversed bending on the Wiedemann Machine, 0.065 in. diameter rods subjected to combined mean and alternating axial loads on the Axial Fatigue Machine, and 0.270 in. diameter rods subjected to reversed bending on the Ann Arbor Machine. The Wire Fatigue Machines were recalibrated for the diameter of wires being tested, and the Ann Arbor Machine was calibrated. A literature search was conducted to compile the published data on the materials tested and the results of the experimental program were compared with the published data as part of the analysis program. Distributional S-N diagrams were prepared which are directly useable by designers. Descriptions and results of the research accomplished during the third operating period is contained in the Third Technical Report (3).

During the period 1 February 1970 - 31 August 1971 the experimental research was expanded to include specimens made of two new materials: AISI 1018 and AISI 1038 steel. Testing included static tensile tests, and hardness and geometry measurements needed to determine the distributional parameters of strength and dimensions. Fatigue tests included both endurance-strength tests and cycles-to-failure tests needed for the preparation of Goodman strength diagrams

and S-N diagrams. Concurrent research included an investigation of stress concentration through photoelastic models. The analysis verified that specimens fabricated with relief angles and subjected to fatigue tests provided valid data. In order to strengthen the analysis of fatigue testing data, a manual method of fitting a three-parameter Weibull distribution was developed. Thus the evaluation of the distributions of fatigue data would include the normal, the log-normal, and the Weibull distributions. In addition to the usual goodness-of-fit tests for the normal and lognormal distributions, an automatic plot of a data histogram overscribed by a theoretical curve having the estimated parameters was developed and used. Specific examples using the data generated with design-by-reliability method to optimize designs of rotating mechanical components were developed and included in the Fourth Technical Report (4).

1.2 OBJECTIVES FOR THIS REPORT

The objectives for the period 1 September 1971 - 31 August 1972 were to continue the theoretical and experimental research of wire and rod steel specimens in order to provide designers with the capability to improve the design of dynamic rotary mechanical components. Specific objectives for each type of research machine were as follows:

1.2.1 WIRE RESEARCH MACHINES

The objective was to generate static and dynamic strength distributions for wire specimens and to compile the data in a form directly useable by designers. Tasks conducted in order to achieve the objective included:

1. Static tensile tests to determine the distributions of the yield, ultimate and breaking strengths of wire specimens of AISI 4340, 4130, 1018 and 1038 steels.

2. Cycles-to-failure tests to determine the distribution of fatigue cycle life at various levels of reversed alternating bending stress.

3. Stress-to-failure tests to determine the distribution of fatigue endurance strength for 3×10^6 cycles.

4. Construction of distributional S-N diagrams for the given specimen materials and geometry.

1.2.2 WIEDEMANN RESEARCH MACHINES

The objective was to generate and analyze dynamic distributional strength data for AISI 4130 and 1038 steel rods with various groove radii.

Tasks included:

1. Cycles-to-failure tests to determine the distribution of fatigue life for each specimen material and geometry subjected to reversed alternating bending stress.

2. Stress-to-failure tests to determine the distribution of the endurance strength for 3×10^6 cycles of life.

3. Construction of distributional S-N diagrams for the specimen materials and geometries tested.

4. Analyze the endurance strength parameters for the different specimen groove radii to determine the effect of groove radii on fatigue life.

5. Develop notch sensitivity and fatigue stress concentration factors for the different specimen materials and geometries tested.

6. Completion of a theoretical study of notch sensitivity and associated stress concentration factors and comparison with the distributional values obtained from the experimental data.

1.2.3 AXIAL FATIGUE RESEARCH MACHINE

The objective was to generate endurance strength distributions for AISI 1018 steel rods and develop the associated distributional Goodman diagram.

Tasks included:

1. Staircase tests to determine the distribution of the endurance strength for 2×10^6 cycles of life for specimens subjected to various ratios of axial alternating and mean loads.

2. Construction of a distributional Goodman strength diagram.

3. Determination of failure governing criteria which correlate with the Goodman strength diagram.

2.0 EXPERIMENTAL RESEARCH PROGRAM AND DATA

The experimental program undertaken during the Fifth Phase of this research program is presented in Sections 2.1 through 2.3. A cross-reference between the test program and the generated and reduced data is also presented. The static, cycles-to-failure, and staircase strength data was used to generate S-N diagrams, Goodman diagrams, and fatigue stress concentration and notch sensitivity factors.

Table 2.0-1 provides a list of the research completed, in progress, or scheduled for initiation. In the next final report a cross-reference of all of the research completed will be provided. This table will be broken down by Data State, i.e., Raw Data, Reduced Data, Staircase Plot, and Distribution Plot, and by Data Type, i.e., Static Ultimate Strength, Staircase, Endurance, Break Length, Diameter, Hardness, Cycles to Failure, Yield Strength, and Elongation.

2.1 WIRE RESEARCH MACHINE

The wire research machines were the same as those used in previous phases of this research. The calibration, and the details about the research program and data for this period of research are given next.

2.1.1 CALIBRATION OF THE WIRE FATIGUE RESEARCH MACHINES

The calibration procedures for the wire fatigue research machines were the same as those described in the Third Technical Report [3, pp. 38-84]. The calibration data for Machines Number 1, 2, 3, and 4 appear in Tables 10.1-1 through 10.1-4 of Section II of this report.

Preceding page blank

Table 2.0-1 Summary of experimental research program for the Office of Naval Research*

Group No.	Sample Size	Test Machine	Test Type	Material Tested Steel	Type Data	Loading	Specimen d in.	Geometry r in.	Status*
1	34	Wiedemann	Reversed Bending	AISI 4340	Cycles to Failure	Fixed Stress 60,300 psi	0.1800	0.250	C
2	28	Wiedemann	Reversed Bending	AISI 4340	Cycles to Failure	Fixed Stress 57,570 psi	0.2700	0.250	C
3	31	Wiedemann	Reversed Bending	AISI 4340	Cycles to Failure	Fixed Stress 66,300 psi	0.1800	0.250	C
4	30	Wiedemann	Reversed Bending	AISI 4340	Cycles to Failure	Fixed Stress 66,300 psi	0.2700	0.031	C
5	33	Wiedemann	Reversed Bending	AISI 4340	Cycles to Failure	Fixed Stress 66,300 psi	0.2700	0.250	C
6	31	Wiedemann	Reversed Bending	AISI 4340	Cycles to Failure	Fixed Stress 66,300 psi	0.2700	∞	
7	30	Wiedemann	Reversed Bending	AISI 4340	Cycles to Failure	Fixed Stress 66,300 psi	0.1800	0.031	C
8	33	Riehle	Static Ultimate	AISI 4340	Pounds Tensile Force	Increasing Static Load	0.2700	∞	C
9	63	Wiedemann	Reversed Bending	AISI 4340	Endurance	Staircase 5 x 106 cycles	0.0937	0.250	C
10	26	Riehle	Breaking Strength	AISI 4340	Pounds Tensile Force	Increasing Static Load	Dia, at Fracture	---	C

* C = Test complete
IP = Test in progress
P = Test planned

Table 2.0-1 (Cont.) Summary of experimental research program for the Office of Naval Research

Group No.	Sample Size	Test Machine	Test Type	Material Tested Steel	Type Data	Loading	Specimen d in.	Geometry r in.	Status*
11	12	Wiedemann	Reversed Bending	AISI 4340	Endurance	Staircase 10^6 cycles	0.1800	∞	P
12	30	Axial Fatigue	Push-Pull	AISI 4340	Cycles to Failure	$s_a/s_m = 1$ $s_a = 47,000$ psi	0.0740	∞	C
13	30	Axial Fatigue	Push-Pull	AISI 4340	Cycles to Failure	$s_a/s_m = 1$ $s_a = 47,000$ psi	0.0740	∞	C
12 & 13	60	Axial Fatigue	Push-Pull	AISI 4340	Cycles to Failure	$s_a/s_m = 1$ $s_a = 47,100$ psi	0.0740	∞	C
14	27	Axial Fatigue	Push-Pull	AISI 4340	Cycles to Failure	$s_a/s_m = 2$ $s_a = 47,100$ psi	0.0740	∞	C
15	50	Riehle	Static Ultimate	AISI 4340 (wire)	Pounds Tensile Force	Increasing Static Load	0.0625	∞	C
16	50	Riehle	Static Ultimate	AISI 4340 (wire)	Pounds Tensile Force	Increasing Static Load	0.0937	∞	C
17	55	Wiedemann	Reversed Bending	AISI 4340	Endurance	Staircase 5×10^6 cycles	0.0937	∞	C

* C = Test complete
IP = Test in progress
P = Test planned

Table 2.0-1 (Cont.) Summary of experimental research program for the Office of Naval Research

Group No.	Sample Size	Test Machine	Test Type	Material Tested Steel	Type Data	Loading	Specimen d in.	Geometry r in.	Status*
18	56	Wiedemann	Reversed Bending	AISI 4340	Endurance	Staircase 5×10^6 cycles	0.0937	0.031	C
19	67	Wire Fatigue	Reversed Bending	AISI 4340 (wire)	Endurance	Staircase 10^6 cycles	0.0937	∞	C
20	100	Wire Fatigue	Reversed Bending	AISI 4340 (wire)	Endurance	Staircase 10^6 cycles	0.0937	∞	P
21	100	Wire Fatigue	Reversed Bending	AISI 4340 (wire)	Endurance	Staircase 2×10^6 cycles	0.0625	∞	C
22	100	Wire Fatigue	Reversed Bending	AISI 4340 (wire)	Endurance	Staircase 2×10^6 cycles	0.0625	∞	C
23	27	Wiedemann	Reversed Bending	AISI 4340	Endurance	Staircase 5×10^6 cycles	0.0937	0.063	C
24	100	Wire Fatigue	Reversed Bending	AISI 4340 (wire)	Cycles to Failure	Fixed Stress 80,800 psi	0.0625	∞	C
25	100	Wire Fatigue	Reversed Bending	AISI 4340 (wire)	Cycles to Failure	Fixed Stress 68,000 psi	0.0625	∞	C
26	29	Wiedemann	Reversed Bending	AISI 4340	Endurance	Staircase 5×10^6 cycles	0.0937	0.125	C
27	22	Wiedemann	Reversed Bending	AISI 4340	Endurance	Staircase 5×10^6 cycles	0.1800	0.0625	C

Table 2.0-1 (Cont.) Summary of experimental research program for the Office of Naval Research

Group No.	Sample Size	Test Machine	Test Type	Material Tested Steel	Type Data	Loading	Specimen d in.	Geometry r in.	Status*
28	29	Wiedemann	Reversed Bending	AISI 4340	Endurance	Staircase 5×10^6 cycles	0.1800	0.125	C
29	29	Ann Arbor	Reversed Bending	AISI 4340	Endurance	Staircase 5×10^6 cycles	0.2700	0.0625	C
30	25	Ann Arbor	Reversed Bending	AISI 4340	Endurance	Staircase 5×10^6 cycles	0.2700	0.0937	C
31	24	Axial Fatigue	Push-Pull	AISI 4130	Combined Stress $s_a/s_m = \infty$	Staircase 10^6 cycles	0.0664	∞	C
32	27	Axial Fatigue	Push-Pull	AISI 4130	Combined Stress $s_a/s_m = 2$	Staircase 10^6 cycles	0.0651	∞	C
33	25	Axial Fatigue	Push-Pull	AISI 4130	Combined Stress $s_a/s_m = 1$	Staircase 10^6 cycles	0.0647	∞	C
34	28	Axial Fatigue	Push-Pull	AISI 4130	Combined Stress $s_a/s_m = 1/2.5$	Staircase 10^6 cycles	0.0642	∞	C
35	21	Axial	Push-Pull	AISI 4130	Combined Stress $s_a/s_m = 1/10$	Staircase 10^6 cycles	0.0628	∞	C

Table 2.0-1 (Cont.) Summary of experimental research program for the Office of Naval Research

Group No.	Sample Size	Test Machine	Test Type	Material Tested Steel	Type Data	Loading	Specimen d in.	Geometry r in.	Status*
36	34	Riehle	Static Ultimate	AISI 4130	Pounds Tensile Force	Increasing Static Load	0.1800	∞	C
37	100	Wire Fatigue	Reversed Bending	AISI 4340 (wire)	Cycles to Failure	Fixed Stress 89,000 psi	0.0625	∞	C
38	100	Wire Fatigue	Reversed Bending	AISI 4340 (wire)	Cycles to Failure	Fixed Stress 101,000 psi	0.0625	∞	C
39	81	Wire Fatigue	Reversed Bending	AISI 4340 (wire)	Endurance	Staircase 5×10^5 cycles	0.0625	∞	C
40	95	Wire Fatigue	Reversed Bending	AISI 4340 (wire)	Endurance	Staircase 10^7 cycles	0.0625	∞	C
41	100	Wire Fatigue	Reversed Bending	AISI 4340 (wire)	Endurance	Staircase 3×10^5 cycles	0.0625	∞	C
42	50	Axial Fatigue	Push-Pull	AISI 4340	Endurance $s_a/s_m = \infty$	Staircase 10^6 cycles	0.0620	∞	C
43	24	Axial Fatigue	Push-Pull	AISI 4340	Cycles to Failure $s_a/s_m = \infty$	Fixed Stress $s_a = 47,100$ psi	0.0740	∞	C
44	24	Axial Fatigue	Push-Pull	AISI 4340	Endurance $s_a/s_m = 1$	Staircase 10^6 cycles	0.0695	∞	C

Table 2.0-1 (Cont.) Summary of experimental research program for the Office of Naval Research

Group No.	Sample Size	Test Machine	Test Type	Material Tested Steel	Type Data	Loading	Specimen d in.	Geometry r in.	Status*
45	29	Axial Fatigue	Push-Pull	AISI 4340	Endurance $s_a/s_m = 1/2.5$	Staircase 10^6 cycles	0.0645	∞	C
46	30	Axial Fatigue	Push-Pull	AISI 4340	Endurance $s_a/s_m = 1/10$	Staircase 10^6 cycles	0.0645	∞	C
47	23	Riehle	Static Ultimate	AISI 4340	Pounds Tensile Force	Increasing Static Load	Diameter Varied	∞	C
48	63	Wire Fatigue	Reversed Bending	AISI 4340 (wire)	Endurance	Staircase 7.5×10^5 cycles	0.0625	∞	C
49	100	Wire Fatigue	Reversed Bending	AISI 4340 (wire)	Endurance	Staircase 10^6 cycles	0.0625	∞	C
50	100	Wire Fatigue	Reversed Bending	AISI 4340 (wire)	Endurance	Staircase 1.5×10^6 cycles	0.0625	∞	C
51	100	Wire Fatigue	Reversed Bending	AISI 4340 (wire)	Endurance	Staircase 10^6 cycles	0.0625	∞	C
52	100	Wire Fatigue	Reversed Bending	AISI 4340 (wire)	Endurance	Staircase 10^5 cycles	0.0625	∞	C
53	68	Wire Fatigue	Reversed Bending	AISI 4340 (wire)	Endurance	Staircase 3×10^6 cycles	0.0625	∞	C
54	100	Wire Fatigue	Reversed Bending	AISI 4340 (wire)	Cycles to Failure	Fixed Stress $s_a = 75{,}000$ psi	0.0625	∞	C

Table 2.0-1 (Cont.) Summary of experimental research program for the Office of Naval Research

Group No.	Sample Size	Test Machine	Test Type	Material Tested Steel	Type Data	Loading	Specimen d in.	Geometry r in.	Status*
55-1	35	Tinius Olsen	Static Ultimate	AISI 4340	Pounds Tensile Force	Increasing Static Load	0.250	∞	P
55-2	35	Tinius Olsen & Wilson	Static Ultimate	AISI 4340	Hardness and % Elongation	Increasing Static Load	0.250	∞	P
56-1	35	Tinius Olsen	Static Ultimate	AISI 4130	Pounds Tensile Force	Increasing Static Load	0.250	∞	C
56-2	35	Tinius Olsen & Wilson	Static Ultimate	AISI 4130	Hardness and % Elongation	Increasing Static Load	0.250	∞	C
57-1	35	Tinius Olsen	Static Ultimate	AISI 1038	Pounds Tensile Force	Increasing Static Load	0.250	∞	C
57-2	35	Tinius Olsen & Wilson	Static Ultimate	AISI 1038	Hardness and % Elongation	Increasing Static Load	0.250	∞	C
58-1	35	Tinius Olsen	Static Ultimate	AISI 1018	Pound Tensile Force	Increasing Static Load	0.250	∞	C
58-2	35	Tinius Olsen & Wilson	Static Ultimate	AISI 1018	Hardness and % Elongation	Increasing Static Load	0.250	∞	C
59-1	35	Riehle	Static Ultimate	AISI 4130 (wire)	Pounds Tensile Force	Increasing Static Load	0.0626	∞	C
59-2	35	Tukon	Static Ultimate	AISI 4130 (wire)	Hardness	Increasing Static Load	0.0626	∞	P

Table 2.0-1 (Cont.) Summary of experimental research program for the Office of Naval Research

Group No.	Sample Size	Test Machine	Test Type	Material Tested Steel	Type Data	Loading	Specimen d in.	Geometry r in.	Status*
60-1	40	Tinius Olsen & Wilson	Static Ultimate	AISI 1038 (wire)	Pounds Tensile Load	Increasing Static Load	0.0626	∞	C
60-2	35	Tukon	Static Ultimate	AISI 1038 (wire)	Hardness	Increased Static Load	0.0626	∞	P
61-1	35	Tinius Olsen	Static Ultimate	AISI 1018 (wire)	Pounds Tensile Load	Increased Static Load	0.0626	∞	C
61-2	35	Tukon	Static Ultimate	AISI 1018 (wire)	Hardness	Increased Static Load	0.0626	∞	C
62	35	Axial Fatigue	Push-Pull	AISI 4130	Combined Stress $r_s = 0.1$	Staircase 2×10^6 cycles	0.05 ±	∞	C
63	35	Axial Fatigue	Push-Pull	AISI 4130	Combined Stress $r_s = 0.2$	Staircase 2×10^6 cycles	0.05 ±	∞	P
64	35	Axial Fatigue	Push-Pull	AISI 4130	Combined Stress $r_s = \infty$	Staircase 2×10^6 cycles	0.0664	1.87	C
65	35	Wiedemann	Reversed Bending	AISI 4130	Endurance-Notch Sensitivity	Staircase 3×10^6 cycles	0.0937	0.0625	C
66	35	Wiedemann	Reversed Bending	AISI 4130	Endurance-Notch Sensitivity	Staircase 3×10^6 cycles	0.0937	0.0310	C
67	36	Wire Fatigue #1	Reversed Bending	AISI 4130 (wire)	Cycles to Failure	Fixed Stress 60,000 (13.9)	0.0626	∞	C

Table 2.0-1 (Cont.) Summary of experimental research program for the Office of Naval Research

Group No.	Sample Size	Test Machine	Test Type	Material Tested Steel	Type Data	Loading	Specimen d in.	Geometry r in.	Status*
68	35	Wire Fatigue #2	Reversed Bending	AISI 4130	Cycles to Failure	Fixed Stress 55,000 (11.8)	0.0626	∞	C
69	35	Wire Fatigue #3	Reversed Bending	AISI 4130	Cycles to Failure	Fixed Stress 70,000 (14.85)	0.0626	∞	C
70	35	Wire Fatigue #4	Reversed Bending	AISI 4130	Cycles to Failure	Fixed Stress 65,000 (14.6)	0.0626	∞	C
71	35	Wire Fatigue #5	Reversed Bending	AISI 4130	Cycles to Failure	Fixed Stress 80,000 (17.5)	0.0626	∞	P
72	5	Riehle	Ultimate Strength	AISI 4340 (new)	Pounds Tensile Load	Increasing Static	0.250	∞	P
73	5	Tinius Olsen	Ultimate Strength	AISI 4340 (new)	Ultimate Load	Increasing Static	0.250	∞	P
74	35	Wiedemann	Reversed Bending	AISI 4130	Endurance Notch Sensitivity	Staircase 3×10^6 cycles	0.0937	0.125	C
75	35	Wiedemann	Reversed Bending	AISI 4130	Endurance Notch Sensitivity	Staircase 3×10^6 cycles	0.0937	0.250	C
76	35	Wiedemann	Reversed Bending	AISI 4130	Endurance Notch Sensitivity	Staircase 3×10^6 cycles	0.0937	0.250	C
77	35	Wire Fatigue #1	Reversed Bending	AISI 1038	Cycles to Failure	Fixed Stress 55,000 (12.7)	0.0626	∞	C

Table 2.0-1 (Cont.) Summary of experimental research program for the Office of Naval Research

Group No.	Sample Size	Test Machine	Test Type	Material Tested Steel	Type Data	Loading	Specimen d in.	Geometry r in.	Status*
78	35	Wire Fatigue	Reversed Bending	AISI 1038	Cycles to Failure	Fixed Stress 75,000	0.0626	∞	C
79	35	Wire Fatigue #4	Reversed Bending	AISI 1038	Cycles to Failure	Fixed Stress 60,000	0.0626	∞	C
80	35	Wire Fatigue #4	Reversed Bending	AISI 1038	Cycles to Failure	Fixed Stress 65,000 (14.6)	0.0626	∞	C
81	35	Wire Fatigue #4	Reversed Bending	AISI 1038	Cycles to Failure	Fixed Stress 70,000 (15.6)	0.0626	∞	C
82	35	Wiedemann	Reversed Bending	AISI 4130	Cycles to Failure	Fixed Stress (to be determined)	0.0937	0.031	P
83	35	Wiedemann	Reversed Bending	AISI 4130	Cycles to Failure	Fixed Stress (to be determined)	0.0937	0.031	P
84	35	Wiedemann	Reversed Bending	AISI 4130	Cycles to Failure	Fixed Stress (to be determined)	0.0937	0.031	P
85	35	Wiedemann	Reversed Bending	AISI 4130	Cycles to Failure	Fixed Stress (to be determined)	0.0937	0.031	P
86	70	Wire Fatigue #3	Reversed Bending	AISI 4130	Endurance	Staircase 2×10^6 cycles	0.0626	∞	C
87	70	Wire Fatigue #2	Reversed Bending	AISI 1038	Endurance	Staircase 2×10^6 cycles	0.0626	∞	C

Table 2.0-1 (Cont.) Summary of experimental research program for the Office of Naval Research

Group No.	Sample Size	Test Machine	Test Type	Material Tested Steel	Type Data	Loading	Specimen d in.	Geometry r in.	Status*
88	35	Wiedemann	Reversed Bending	AISI 4130	Cycles to Failure	Fixed Stress (to be determined)	0.0937	0.125	C
89	35	Wiedemann	Reversed Bending	AISI 4130	Cycles to Failure	Fixed Stress (to be determined)	0.0937	0.125	C
90	35	Wiedemann	Reversed Bending	AISI 4130	Cycles to Failure	Fixed Stress (to be determined)	0.0937	0.125	C
91	35	Wiedemann	Reversed Bending	AISI 4130	Cycles to Failure	Fixed Stress (to be determined)	0.0937	0.125	P
92	35	Wiedemann	Reversed Bending	AISI 4130	Cycles to Failure	Fixed Stress (to be determined)	0.0937	0.250	P
93	35	Wiedemann	Reversed Bending	AISI 4130	Cycles to Failure	Fixed Stress (to be determined)	0.0937	0.250	C
94	35	Wiedemann	Reversed Bending	AISI 4130	Cycles to Failure	Fixed Stress (to be determined)	0.0937	0.250	C
95	35	Wiedemann	Reversed Bending	AISI 4130	Cycles to Failure	Fixed Stress (to be determined)	0.0937	0.250	C
96	35	Wiedemann	Reversed Bending	AISI 4130	Cycles to Failure	Fixed Stress (to be determined)	0.0937	1.870	P
97	35	Wiedemann	Reversed Bending	AISI 4130	Cycles to Failure	Fixed Stress (to be determined)	0.0937	1.870	P

Table 2.0-1 (Cont.) Summary of experimental research program for the Office of Naval Research

Group No.	Sample Size	Test Machine	Test Type	Material Tested Steel	Type Date	Loading	Specimen d in.	Geometry r in.	Status*
98	35	Wiedemann	Reversed Bending	AISI 4130	Cycles to Failure	Fixed Stress (to be determined)	0.0937	1.870	P
99	35	Wiedemann	Reversed Bending	AISI 4130	Cycles to Failure	Fixed Stress (to be determined)	0.0937	1.870	P
100	35	Ann Arbor	Reversed Bending	AISI 4340	Cycles to Failure	Fixed Stress (to be determined)	0.2700	0.031	P
101	35	Ann Arbor	Reversed Bending	AISI 4340	Cycles to Failure	Fixed Stress	0.2700	0.031	P
102	35	Ann Arbor	Reversed Bending	AISI 4340	Cycles to Failure	Fixed Stress	0.2700	0.031	P
103	35	Ann Arbor	Reversed Bending	AISI 4340	Cycles to Failure	Fixed Stress	0.2700	0.031	P
104	35	Wiedemann	Reversed Bending	AISI 4130	Cycles to Failure	Fixed Stress	0.0937	0.062	P
105	35	Wiedemann	Reversed Bending	AISI 4130	Cycles to Failure	Fixed Stress	0.0937	0.062	P
106	35	Wiedemann	Reversed Bending	AISI 4130	Cycles to Failure	Fixed Stress	0.0937	0.062	P
107	35	Wiedemann	Reversed Bending	AISI 4130	Cycles to Failure	Fixed Stress	0.0937	0.062	P

Table 2.0-1 (Cont.) Summary of experimental research program for the Office of Naval Research

Group No.	Sample Size	Test Machine	Test Type	Material Tested Steel	Type Date	Loading	Specimen d in.	Geometry r in.	Status*
108	35	Ann Arbor	Reversed Bending	AISI 4340	Endurance	Staircase 2×10^6 cycles	0.2700	0.031	P
109	35	Ann Arbor	Reversed Bending	AISI 4340	Endurance	Staircase 2×10^6 cycles	0.2700	0.250	P
110	35	Ann Arbor	Reversed Bending	AISI 4340	Endurance	Staircase 2×10^6 cycles	0.2700	1.870	P
111	35	Axial Fatigue	Push-Pull	AISI 1038	Combined Stress $r_s = 0.1$	Staircase 2×10^6 cycles	0.065	2.70	C
112	35	Axial Fatigue	Push-Pull	AISI 1038	Combined Stress $r_s = 0.4$	Staircase 2×10^6 cycles	0.068	2.70	C
113	35	Axial Fatigue	Push-Pull	AISI 1038	Combined Stress $r_s = 1.0$	Staircase 2×10^6 cycles	0.075	2.70	C
114	35	Axial Fatigue	Push-Pull	AISI 1038	Combined Stress $r_s = 2.0$	Staircase 2×10^6 cycles	0.075	2.70	C
115	35	Axial Fatigue	Push-Pull	AISI 1038	Combined Stress $r_s = \infty$	Staircase 2×10^6 cycles	0.075	2.70	C
116	35	Wiedemann	Reversed Bending	AISI 4130	Endurance	Staircase 3×10^6 cycles	0.2700	0.031	IP

Table 2.0-1 (Cont.) Summary of experimental research program for the Office of Naval Research

Group No.	Sample Size	Test Machine	Test Type	Material Tested Steel	Type Date	Loading	Specimen d in.	Geometry r in.	Status*
117	35	Wiedemann	Reversed Bending	AISI 4130	Endurance	Staircase 3×10^6 cycles	0.2700	0.062	IP
118	35	Wiedemann	Reversed Bending	AISI 4130	Endurance	Staircase 3×10^6 cycles	0.2700	0.125	IP
119	35	Wiedemann	Reversed Bending	AISI 4130	Endurance	Staircase 3×10^6 cycles	0.2700	0.250	IP
120	35	Wiedemann	Reversed Bending	AISI 4130	Endurance	Staircase 3×10^6 cycles	0.2700	0.187	IP
121	35	Wire Fatigue #4	Reversed Bending	AISI 1018	Endurance	Staircase 2×10^6 cycles	0.0626	∞	C
122	35	Wire Fatigue	Reversed Bending	AISI 1018	Cycles to Failure	Fixed Stress	0.0626	∞	C
123	35	Wire Fatigue	Reversed Bending	AISI 1018	Cycles to Failure	Fixed Stress	0.0626	∞	C
124	35	Wire Fatigue	Reversed Bending	AISI 1018	Cycles to Failure	Fixed Stress	0.0626	∞	C
125	35	Wire Fatigue	Reversed Bending	AISI 1018	Cycles to Failure	Fixed Stress 50,000	0.0626	∞	C
126	35	Wire Fatigue	Reversed Bending	AISI 1018	Cycles to Failure	Fixed Stress 55,000	0.0626	∞	C

Table 2.0-1 (Cont.) Summary of experimental research program for the Office of Naval Research

Group No.	Sample Size	Test Machine	Test Type	Material Tested Steel	Type Date	Loading	Specimen d in.	Geometry r in.	Status*
127	35	Tinius Olsen	Ultimate Strength	AISI 1018 (wire)	Pounds Tensile Force	Increasing Static Load	0.0626	∞	C
128	70	Wire Fatigue	Reversed Bending	AISI 4130	Endurance	Staircase 2×10^6 cycles	0.040	∞	P
129	35	Wire Fatigue	Reversed Bending	AISI 4130	Cycles to Failure	Fixed Stress 67,700	0.040	∞	C
130	35	Wire Fatigue	Reversed Bending	AISI 4130	Cycles to Failure	Fixed Stress 70,000	0.040	∞	C
131	35	Wire Fatigue	Reversed Bending	AISI 4130	Cycles to Failure	Fixed Stress 72,500	0.040	∞	C
132	35	Wire Fatigue	Reversed Bending	AISI 4130	Cycles to Failure	Fixed Stress 74,700	0.040	∞	C
133	35	Wire Fatigue	Reversed Bending	AISI 4130	Cycles to Failure	Fixed Stress 77,800	0.040	∞	C
134	35	Riehle	Ultimate Strength	AISI 4130	Pound tensile Force	Increasing Static	0.040	∞	C
135	70	Wire Fatigue	Reversed Bending	AISI 4130	Endurance	Staircase 2×10^6 cycles	0.040	∞	P

Table 2.0-1 (Cont.) Summary of experimental research program for the Office of Naval Research

Group No.	Sample Size	Test Machine	Test Type	Material Tested Steel	Type Data	Loading	Specimen d in.	Geometry r in.	Status*
136	35	Wire Fatigue	Reversed Bending	AISI 1038	Cycles to Failure	Fixed Stress 64,500	0.040	∞	C
137	35	Wire Fatigue	Reversed Bending	AISI 1038	Cycles to Failure	Fixed Stress 67,200	0.040	∞	C
138	35	Wire Fatigue	Reversed Bending	AISI 1038	Cycles to Failure	Fixed Stress 69,200	0.040	∞	C
139	35	Wire Fatigue	Reversed Bending	AISI 1038	Cycles to Failure	Fixed Stress 72,300	0.040	∞	C
140	35	Wire Fatigue	Reversed Bending	AISI 1038	Cycles to Failure	Fixed Stress No Test	0.040	∞	C
141	35	Riehle	Ultimate Strength	AISI 1038 (wire)	Pounds Tensile Force	Increasing Static	0.040	∞	P
142	70	Wire Fatigue	Reversed Bending	AISI 1018	Endurance	Staircase 2×10^6 cycles	0.040	∞	P
143	35	Wire Fatigue	Reversed Bending	AISI 1018	Cycles to Failure	Fixed Stress 57,200	0.040	∞	C
144	35	Wire Fatigue	Reversed Bending	AISI 1018	Cycles to Failure	Fixed Stress 60,000	0.040	∞	C

Table 2.0-1 (Cont.) Summary of experimental research program for the Office of Naval Research

Group No.	Sample Size	Test Machine	Test Type	Material Tested Steel	Type Data	Loading	Specimen d in.	Geometry r in.	Status*
145	35	Wire Fatigue	Reversed Bending	AISI 1018	Cycles to Failure	Fixed Stress 62,800	0.040	∞	C
146	35	Wire Fatigue	Reversed Bending	AISI 1018	Cycles to Failure	Fixed Stress No Test	0.040	∞	P
147	35	Wire Fatigue	Reversed Bending	AISI 1018	Cycles to Failure	Fixed Stress No Test	0.040	∞	P
148	35	Riehle	Ultimate Strength	AISI 1018 (wire)	Pounds Tensile Force	Increasing Static	0.040	∞	C
148-2	10	Tukon	Static Ultimate	AISI 1018 (wire)	Hardness	Increasing Static	0.040	∞	C
149	70	Wire Fatigue	Reversed Bending	AISI 4340	Endurance	Staircase 2×10^6 cycles	0.040	∞	C
150	35	Wire Fatigue	Reversed Bending	AISI 4340	Cycles to Failure	Fixed Stress 73,500	0.040	∞	C
151	35	Wire Fatigue	Reversed Bending	AISI 4340	Cycles to Failure	Fixed Stress 78,100	0.040	∞	C
152	35	Wire Fatigue	Reversed Bending	AISI 4340	Cycles to Failure	Fixed Stress 80,100	0.040	∞	C

Table 2.0-1 (Cont.) Summary of experimental research program for the Office of Naval Research

Group No.	Sample Size	Test Machine	Test Type	Material Tested Steel	Type Data	Loading	Specimen d in.	Geometry r in.	Status*
153	35	Wire Fatigue	Reversed Bending	AISI 4340	Cycles to Failure	Fixed Stress 84,700	0.040	∞	C
154	35	Wire Fatigue	Reversed Bending	AISI 4340	Cycles to Failure	Fixed Stress 90,000	0.040	∞	C
155	35	Riehle	Ultimate Strength	AISI 4340 (wire)	Pounds Tensile Force	Increasing Static	0.040	∞	C
155-2	10	Tukon	Static Ultimate	AISI 4340 (wire)	Hardness	Increasing Static	0.040	∞	C
156	35	Tinius Olsen	Ultimate Strength $r_s = 0.0$	AISI 1018	Pounds Tensile Force	Increasing Static	0.250	∞	C
157	35	Axial Fatigue	Push-Pull	AISI 1018	Combined Stress $r_s = 0.2$	Staircase 2×10^6 cycles	0.070	∞	IP
158	35	Axial Fatigue	Push-Pull	AISI 1018	Combined Stress $r_s = 0.4$	Staircase 2×10^6 cycles	0.070	∞	IP
159	35	Axial Fatigue	Push-Pull	AISI 1018	Combined Stress $r_s = 1.0$	Staircase 2×10^6 cycles	0.075	∞	C

Table 2.0-1 (Cont.) Summary of experimental research program for the Office of Naval Research

Group No.	Sample Size	Test Machine	Test Type	Material Tested Steel	Type Data	Loading	Specimen d in.	Geometry r in.	Status*
160	35	Axial Fatigue	Push-Pull	AISI 1018	Combined Stress $r_s = 2.0$	Staircase 2×10^6 cycles	0.075	∞	C
161	35	Axial Fatigue	Push-Pull	AISI 1018	Combined Stress $r_s = \infty$	Staircase 2×10^6 cycles	0.075	∞	C
162	35	Wiedemann	Reversed Bending	AISI 1038	Endurance	Staircase 3×10^6 cycles	0.375	0.031	C
163	35	Wiedemann	Reversed Bending	AISI 1038	Endurance	Staircase 3×10^6 cycles	0.375	0.062	C
164	35	Wiedemann	Reversed Bending	AISI 1038	Endurance	Staircase 3×10^6 cycles	0.375	0.125	C
165	35	Wiedemann	Reversed Bending	AISI 1038	Endurance	Staircase 3×10^6 cycles	0.375	0.250	C
166	35	Wiedemann	Reversed Bending	AISI 1038	Endurance	Staircase 3×10^6 cycles	0.375	1.870	C
167	35	Ann Arbor	Reversed Bending	AISI 1018	Endurance	Staircase 2×10^6 cycles	0.375	0.031	IP
168	35	Ann Arbor	Reversed Bending	AISI 1018	Endurance	Staircase 2×10^6 cycles	0.375	0.062	IP

Table 2.0-1 (Cont.) Summary of experimental research program for the Office of Naval Research

Group No.	Sample Size	Test Machine	Test Type	Material Tested Steel	Type Data	Loading	Specimen d in.	Geometry r in.	Status*
169	35	Ann Arbor	Reversed Bending	AISI 1018	Endurance	Staircase 2×10^6 cycles	0.375	0.125	IP
170	35	Ann Arbor	Reversed Bending	AISI 1018	Endurance	Staircase 2×10^6 cycles	0.375	0.250	IP
171	35	Ann Arbor	Reversed Bending	AISI 1018	Endurance	Staircase 2×10^6 cycles	0.375	1.870	IP
172	35	Wiedemann	Reversed Bending	AISI 1038	Endurance Notch Sensitivity	Staircase 3×10^6 cycles	0.375	0.031	IP
173	35	Wiedemann	Reversed Bending	AISI 1038	Endurance Notch Sensitivity	Staircase 3×10^6 cycles	0.375	0.062	IP
174	35	Wiedemann	Reversed Bending	AISI 1038	Endurance Notch Sensitivity	Staircase 3×10^6 cycles	0.375	0.125	IP
175	35	Wiedemann	Reversed Bending	AISI 1038	Endurance Notch Sensitivity	Staircase 3×10^6 cycles	0.375	0.250	IP
176	35	Wiedemann	Reversed Bending	AISI 1038	Endurance Notch Sensitivity	Staircase 3×10^6 cycles	0.375	1.87	IP

Table 2.0-1 (Cont.) Summary of experimental research program for the Office of Naval Research

Group No.	Sample Size	Test Machine	Test Type	Material Tested Steel	Type Data	Loading	Specimen d in.	Geometry r in.	Status*
177	35	Tinius Olsen	Static Tensile	AISI 4340	Ultimate Strength	Increasing Static	0.250	0.0375	P

The static stress versus measured strain data are given in Table 8.1-5 and summarized in Table 9.1-2. The calculations for the standard deviation of strain are given in Table 9.1-3. The results of the static axial calculations which related the measured strain to a known stress are presented in Table 9.1-4. A "Stress Versus Measured Strain" chart was constructed from the values in Table 9.1-4 and is given in Figure 9.1-1. The line in Figure 9.1-1 gives the relationship between the mean strain and pan weight. This also verifies the linearity of the strain gages used. The least squares technique was used to calculate the best fit straight line giving a Y (stress) intercept of 4,267 psi and a slope of 55,379 x 10^6 psi/inch/inch of strain.

Thus the equation which relates the measured strain in μ-in./in. to the actual stress in psi in the 0.040 in. diameter wire specimens is:

$$\text{Stress} = \text{Measured strain} \times 55{,}379 \times 10^6 + 4{,}267. \qquad (2.1\text{-}1)$$

Eq. (2.1.-1) provides the means for determining the applied stress for each deflection angle utilized in the in-machine calibration. The mean strain measured for the selected deflection angles for all machines, shown in Table 9.1-1, were converted to stresses as shown in Table 9.1-5 and plotted for each machine in Figs. 2.1-1 through 2.1-4 to provide the calibration curves. The curves compared well with the results of the previous calibration.

2.1.2 RESEARCH PROGRAM AND DATA

The Table 2.1-1 provides a cross-reference between the test program and the data generated and reduced. The raw and reduced data can be found in Volume II of this report. Each data type is broken down by Wire Fatigue Machines, Wiedemann Fatigue Machines, and Axial Fatigue Machine, and by Materials AISI 4130, 4340, 1038 and 1018 steel.

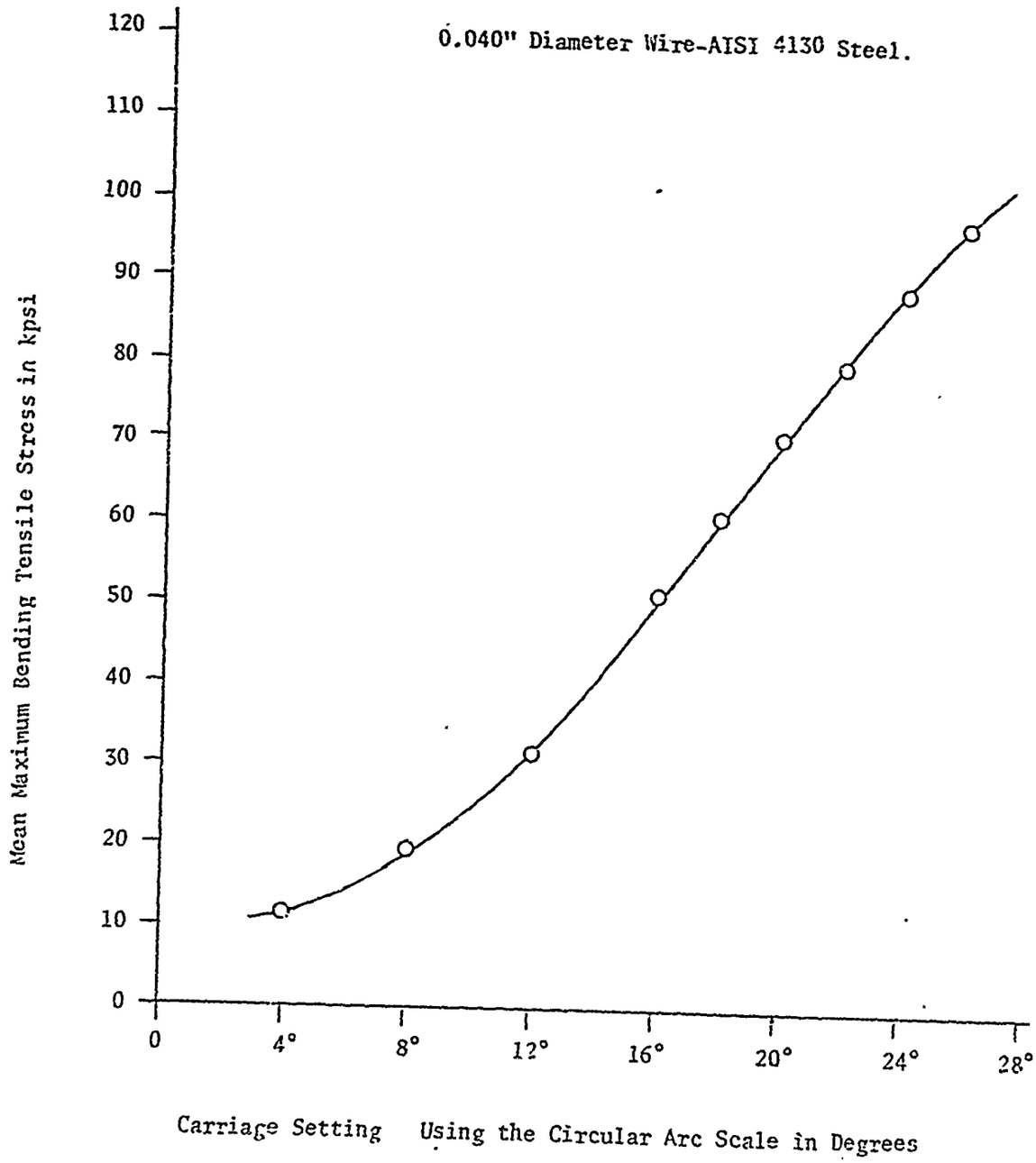

Fig. 2.1-1 Calibration chart for Wire Machine #1.

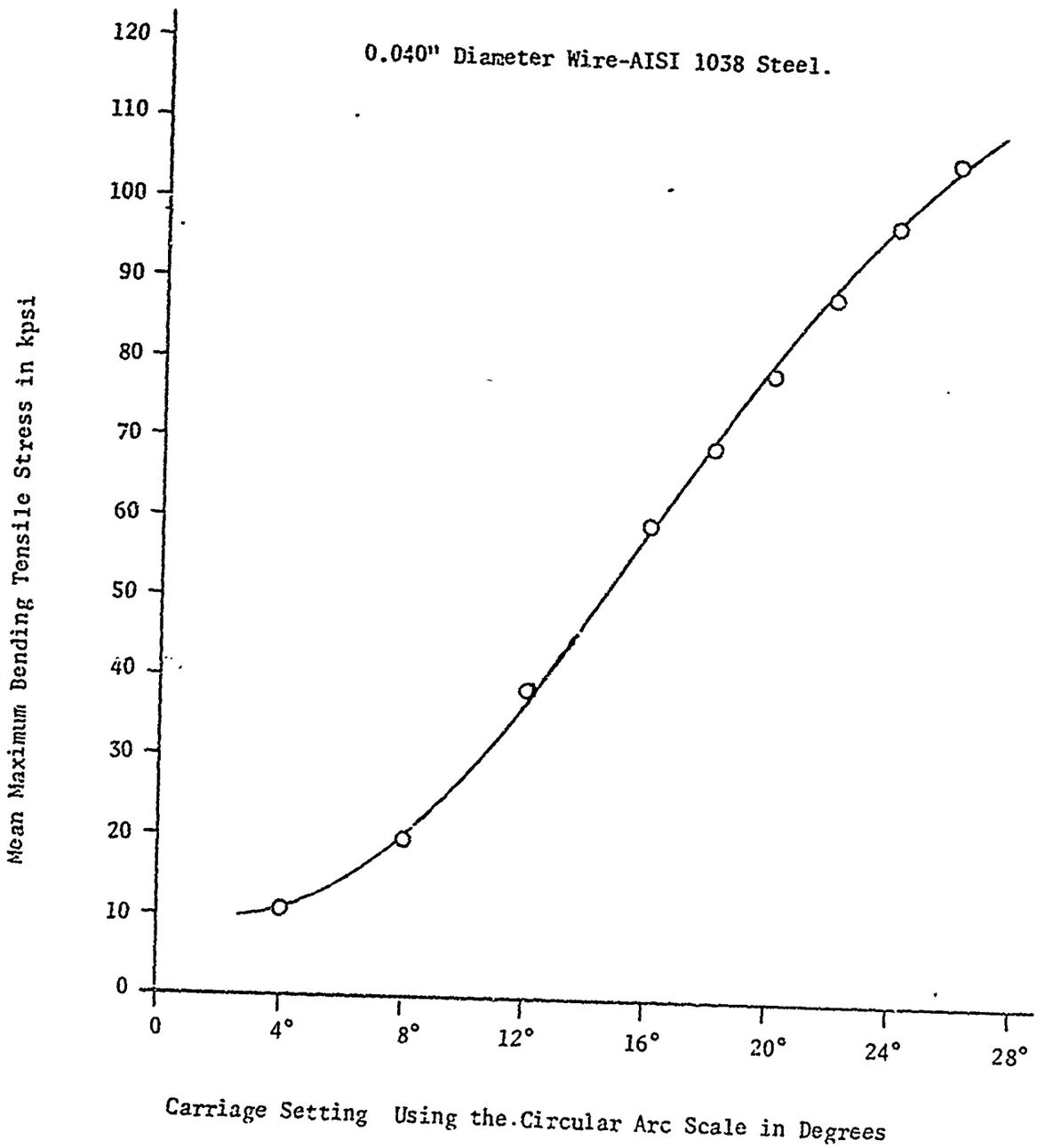

Fig. 2.1-2 Calibration chart for Wire Machine #2.

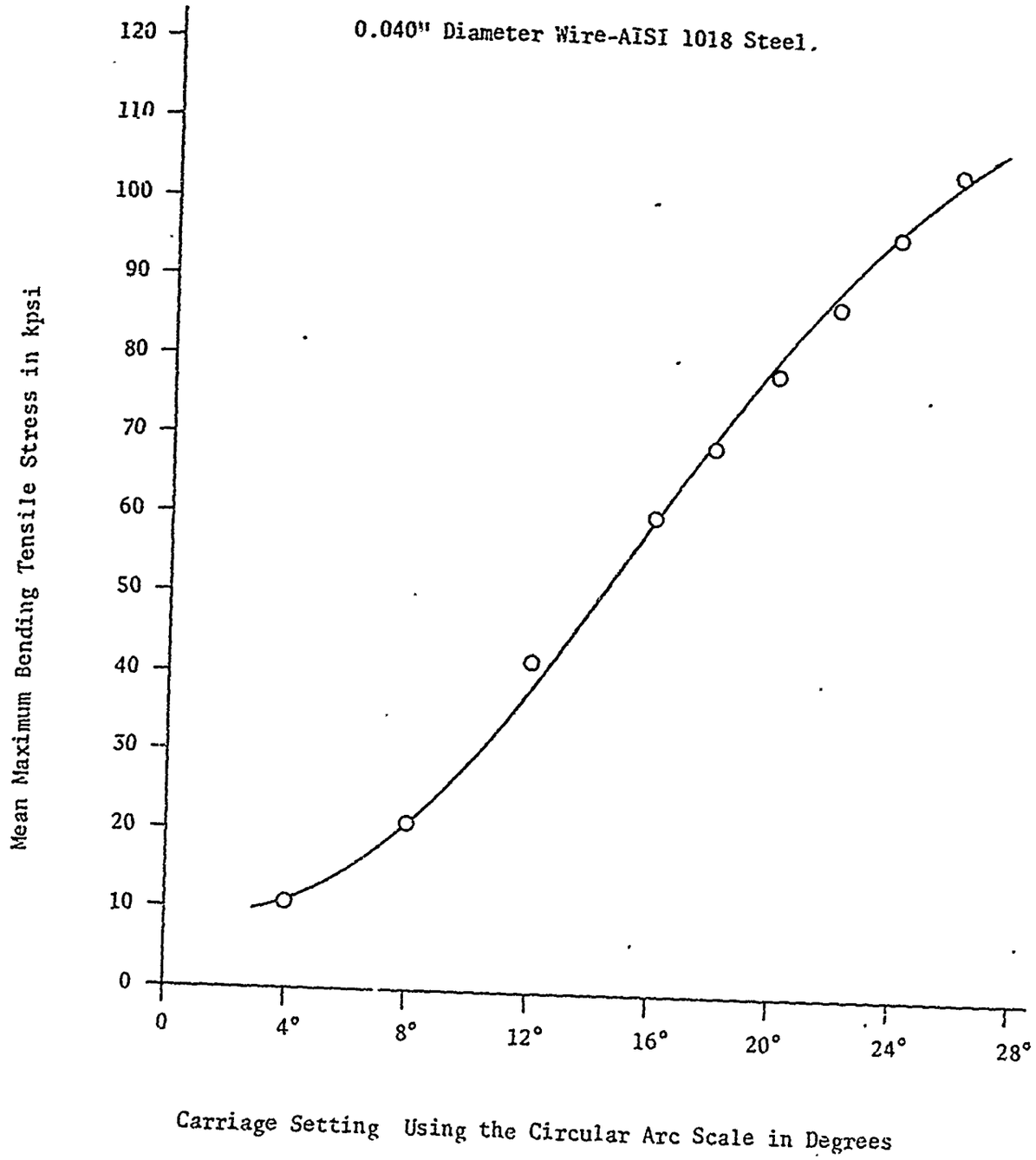

Fig. 2.1-3 Calibration chart for Wire Machine #3.

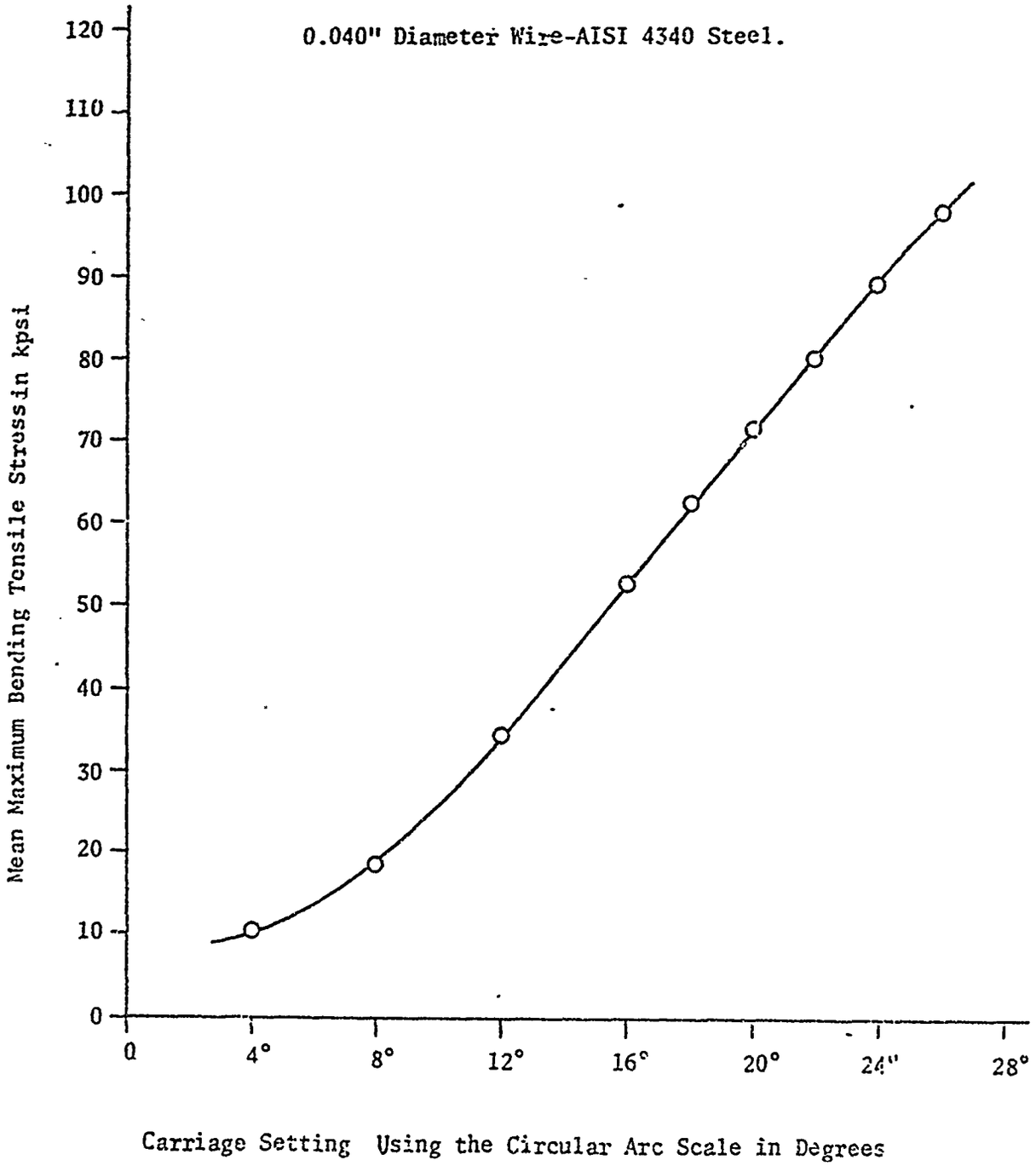

Fig. 2.1-4 Calibration chart for Wire Machine #4.

Table 2.1-1 Test Program for Wire Fatigue Machines

Group No.	Stress Level	Stress psi	Sample Size	Section II Raw Data Table No.	Cross Reference Reduced Data Figure No.
A. AISI 4130 Steel Wire - .040 in. diameter					
128	1 - Endurance	---------	70		
129	2	67,700	35	8.1-6	9.1-2 thru 9.1-4
130	3	70,000	35	8.1-7	9.1-5 thru 9.1-7
131	4	72,500	35	8.1-8	9.1-8 thru 9.1-10
132	5	74,700	35	8.1-9	9.1-11 thru 9.1-13
133	6	77,800	35	8.1-10	9.1-14 thru 9.1-16
134	7 - Ult. Strength	------	35	8.1-11	
B. AISI 1038 Steel Wire - .040 in. diameter					
135	1 - Endurance	------	70		
136	2	64,500	35	8.1-13	9.1-17 thru 9.1-19
137	3	67,200	35	8.1-14	9.1-20 thru 9.1-22
138	4	69,200	35	8.1-15	9.1-23 thru 9.1-25
139	5	72,300	35	8.1-16	9.1-26 thru 9.1-28
140	6	NO TEST			
141	7 - Ult. Strength	-------	35	8.1-17	
C. AISI 1018 Steel Wire - .040 in. diameter					
142	1 - Endurance	-------	70		
143	2	57,200	35	8.1-19	9.1-29 thru 9.1-31
144	3	60,000	35	8.1-20	9.1-32 thru 9.1-34
145	4	62,800	35	8.1-21	9.1-35 thru 9.1-37
146	5	NO TEST			
147	6	NO TEST			
148	7 - Ult. Strength	-------	35	8.1-22	

Table 2.1-1 (Cont.) Test Program for Wire Fatigue Machines

Group No.	Stress Level	Stress psi	Sample Size	Section II Raw Data Table No.	Cross Reference Reduced Data Figure No.
D. AISI 4340 Steel Wire - .040 in. diameter					
149	1 - Endurance	-------	70		
150	2	73,500	35	8.1-25	9.1-40 thru 9.1-42
151	3	78,100	35	8.1-26	9.1-43 thru 9.1-45
152	4	80,100	35	8.1-27	9.1-46 thru 9.1-48
153	5	84,700	35	8.1-28	9.1-49 thru 9.1-51
154	6	90,000	35	8.1-29	9.1-52 thru 9.1-54
155	7 - Ult. Strength	------	35	8.1-30	

2.2 WIEDEMANN RESEARCH MACHINES

The research machines were the same as those used in previous phases of this research. The calibration, and the details of the research program and data for this period of research are given next.

2.2.1 CALIBRATION OF THE WIEDEMANN FATIGUE RESEARCH MACHINES

Calibration procedures of the Wiedemann fatigue research machines are presented next in two parts: Wiedemann (Modified) and Wiedemann (Unmodified).

2.2.1.1 WIEDEMANN (MODIFIED)

An analysis was performed to determine the correct loading schedule required to apply a desired maximum, nominal bending stress to specimens of this research. This investigation required that freebody diagrams be constructed for the components of the system using actual measured weights and forces. The components of the system consist of the following:

a) The auxilliary upper-pan counter-weight system. Fig. 2.2-1
b) The bearing and housing assembly. Fig. 2.2-2
c) The lower pan weight system. Fig. 2.2-3
d) Specimen loading freebody diagram. Fig. 2.2-4

The equations of force were written for each of the above component systems treated as freebody diagrams. By Figs. 2.2-1 thru 2.2-4 , and their attendent calculations the validity of the previous calculations provided in ONR Report 2 [2, pp. 67-83], were ascertained.

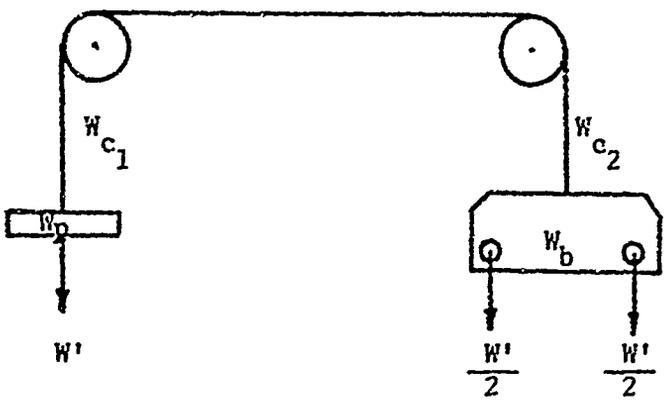

Fig. 2.2-1 Upper Pan Counter-Weight System.

W_p = pan weight = 0.067 pounds

W_c = wire weight: W_{c_1} = 0.0028 pounds, W_{c_2} = 0.0018 pounds

W_b = bracket weight = 0.068 pounds

W' = pan added weight, pounds

When unloaded $W' = 0$, and for $\Sigma F_y = 0$

$$(W_p + W_{c_1}) - (W_b + W_{c_2}) = 0, \qquad (2.2\text{-}1)$$

or

$$(0.067 + .0028) - (0.068 + 0.0018) = 0,$$

therefore

$$0.0698 - 0.0698 = 0.$$

Thus the system depicted in Fig. 2.2-1 is in balance and does not contribute to the specimen loading.

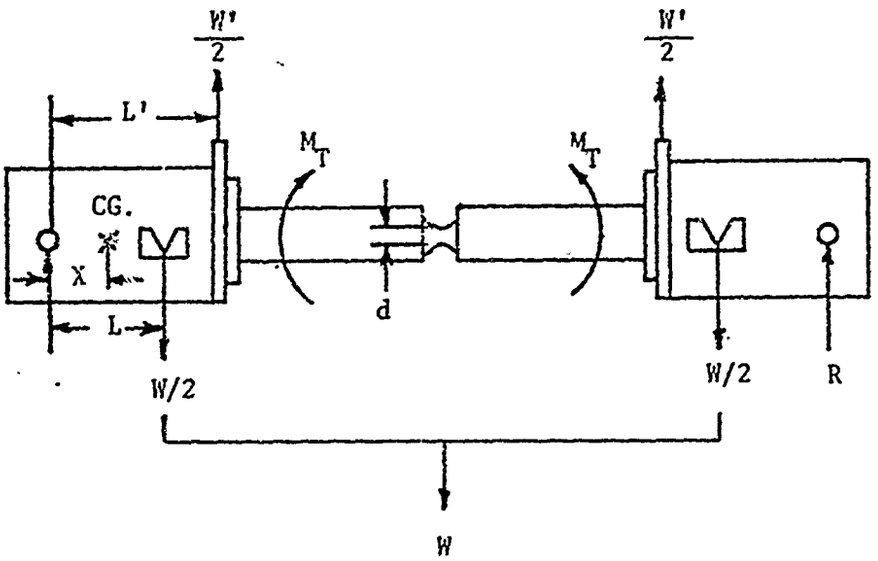

Fig. 2.2-2 Bearing Housing Assembly.

L = length of moment arm for lower pan load = 4 in.

L' = length of moment arm for upper pan load = 4.655 in.

d = diameter of specimen (test section)

W = lower pan load

W' = upper pan load

S = applied stress in specimen

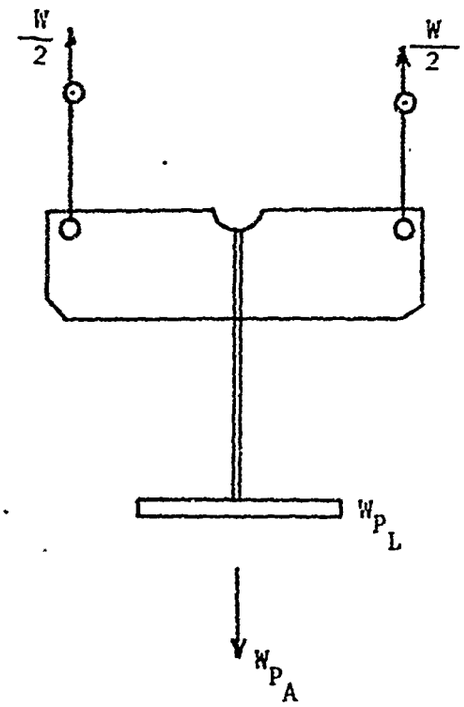

Fig. 2.2-3 Lower Pan Weight Assembly.

W_{P_L} = weight of lower pan and linkage, 5.960 pounds

W_{P_A} = added weight to lower pan, pounds

$W/2$ = load applied to each bearing housing

For $\Sigma F_y = 0$, (Fig. 2.2-3),

$$2(W/2) - (W_{P_L} + W_{P_A}) = 0 \qquad (2.2\text{-}2)$$

or

$$W = W_{P_L} + W_{P_A} .$$

Since W_{P_L} was determined to be 5.960 lb ,

$$W = 5.960 + W_{P_A} . \qquad (2.2\text{-}3)$$

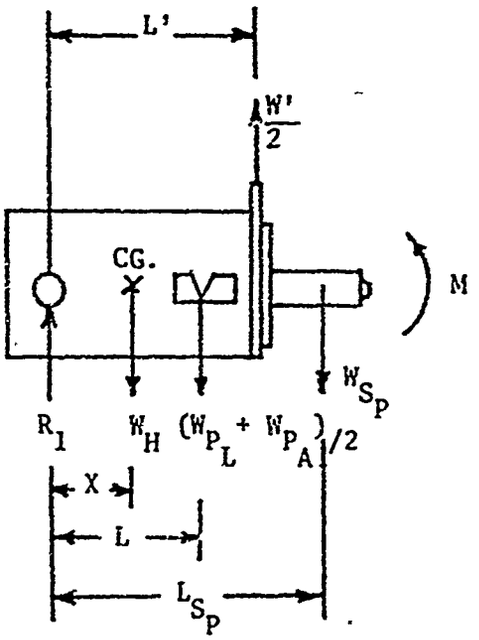

Fig. 2.2-4 Specimen Loading Free-body Diagram.

W' = upper pan added weight, pounds

L' = upper pan moment arm = 4.655 in.

W_H = weight of bearing housing at C. G. = 4.219 lb.

X = bearing housing moment arm = 2.074 in.

W_{P_L} = weight of lower pan and linkage = 5.960 lb.

L = lower pan and linkage moment arm = 4.000 in.

W_{P_A} = lower pan added weight, pounds

W_{S_P} = weight of specimen (1/2 specimen) = 0.0358 lb.

L_{S_P} = specimen moment arm = 4.967 in.

R_1 = reaction force at bearing, pounds

M = bending moment at specimen test section, in - lb.

Determination of M, the Bending Moment, at the Specimen Groove

From $\Sigma M_{R_1} = 0$ (Fig. 2.2-4)

$$W_H X + \frac{(W_{P_L} + W_{P_A})}{2} L + W_{S_P} (L_{S_P}) - \frac{W'}{2} L' - M = 0,$$

or

$$4.219(2.074) + \frac{(5.960 + W_{P_A})}{2} 4 + 0.0358(4.967) - \frac{W'}{2} (4.655) = M.$$

$$M = 8.750 + 11.920 + 2\ W_{P_A} + 0.178 - 2.328\ W'.$$

Therefore

$$M = 20.85 + 2\ W_{P_A} - 2.33\ W'.^{*} \qquad (2.2\text{-}4)$$

Determination of the Nominal Stress in a Specimen

The maximum fiber bending stress in the specimen test section is given by

$$S = \frac{M}{I/C}, \qquad (2.2\text{-}5)$$

where

$$I/C = \frac{\pi d^3}{32}$$

for round test specimens and d is the test section diameter. Substitution for I/C in Eq. (2.2-5) and rearrangement yields

$$S = \frac{32\ M}{\pi d^3}. \qquad (2.2\text{-}6)$$

Substitution of Eq. (2.2-4) into Eq. (2.2-6) yields

$$S = \frac{20.85 + 2\ W_{P_A} - 2.33\ W'}{\pi d^3/32},$$

* All figures were rounded to the second decimal place.

or

$$S = \frac{212.45 + 20.38\ W_{P_A} - 23.74\ W'}{d^3}. \qquad (2.2\text{-}7)$$

Thus, if an ungrooved specimen of diameter d is to be tested, pan weights, W_{P_A} and W', can be chosen to give the desired bending stress using Eq. (2.2-7).

To calculate the upper pan weight, W', corresponding to various stress levels the following form of Eq. (2.2-7) is useful:

$$W' = 8.95 + 0.86\ W_{P_A} - 0.042\ S\ d^3. \qquad (2.2\text{-}8)$$

In order to reduce the number of variables in Eq. (2.2-8) and to simplify calculations, the lower pan added weight can be held constant and the upper pan added weight varied to obtain the desired bending stress. The lower pan added weight was chosen to be 11.00 pounds; thus Eq. (2.2-8) becomes

$$W' = 8.95 + 0.86(11.00) - 0.042\ S\ d^3,$$

or

$$W' = 18.39 - 0.042\ S\ d^3. \qquad (2.2\text{-}9)$$

Eq. (2.2-9) can be used to determine the upper pan weight given the bending stress and the specimen test diameter for ungrooved specimens.

Determination of the Actual Stress in a Grooved Specimen

If the specimen to be tested is grooved, the expression which gives the pan weight is needed. The stress concentration factor must be taken into account, and if fatigue is involved the fatigue notch factor must also be considered.

The procedure is as follows:

1. Obtain the theoretical stress concentration factor, K_t, for the notch configuration and material employed.
2. Obtain the fatigue notch factor from

$$K_f = q(K_t - 1) + 1, \tag{2.2-10}$$

where q, the notch sensitivity, and K_t are obtained from published tables and figures such as Peterson's Stress Concentration Design Factors [5; p. 9, Figs. 8 and 9; pp. 48-49, Figs. 39-40]. In this report, please see Figs. 2.2-5 thru 2.2-8.

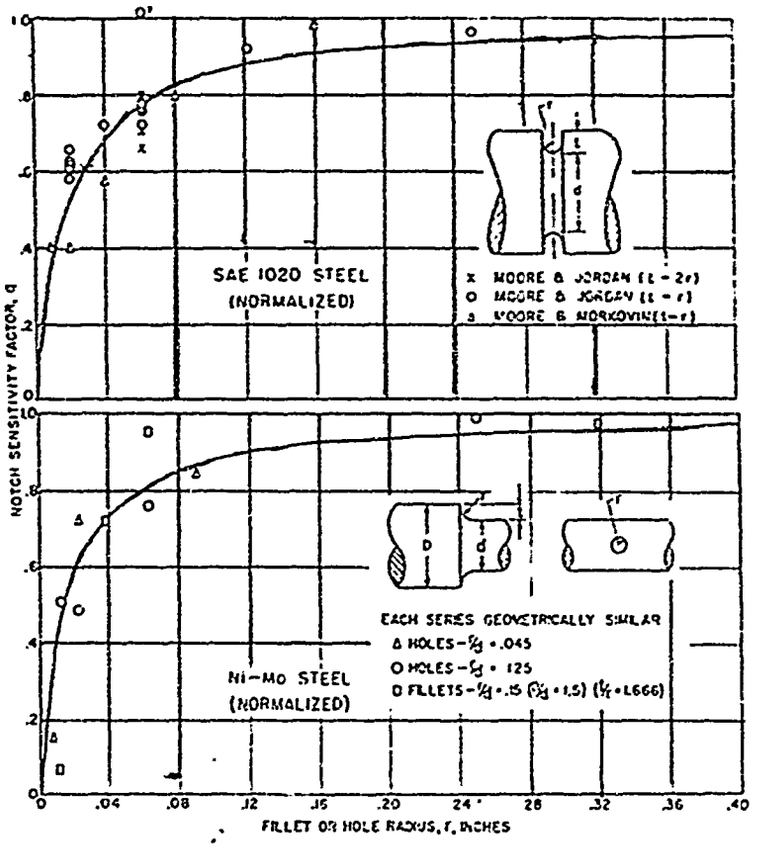

Fig. 2.2-5 Notch sensitivity of normalized steel specimens. [5, p. 9]

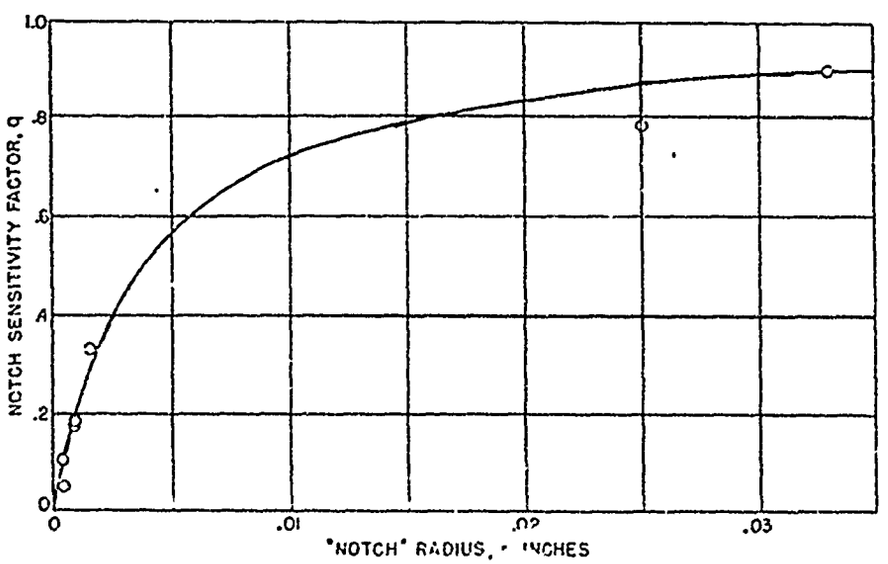

Fig. 2.2-6 Notch sensitivity of quenched and tempered alloy steel specimens (Based on Data of Gough) [5, p. 9]

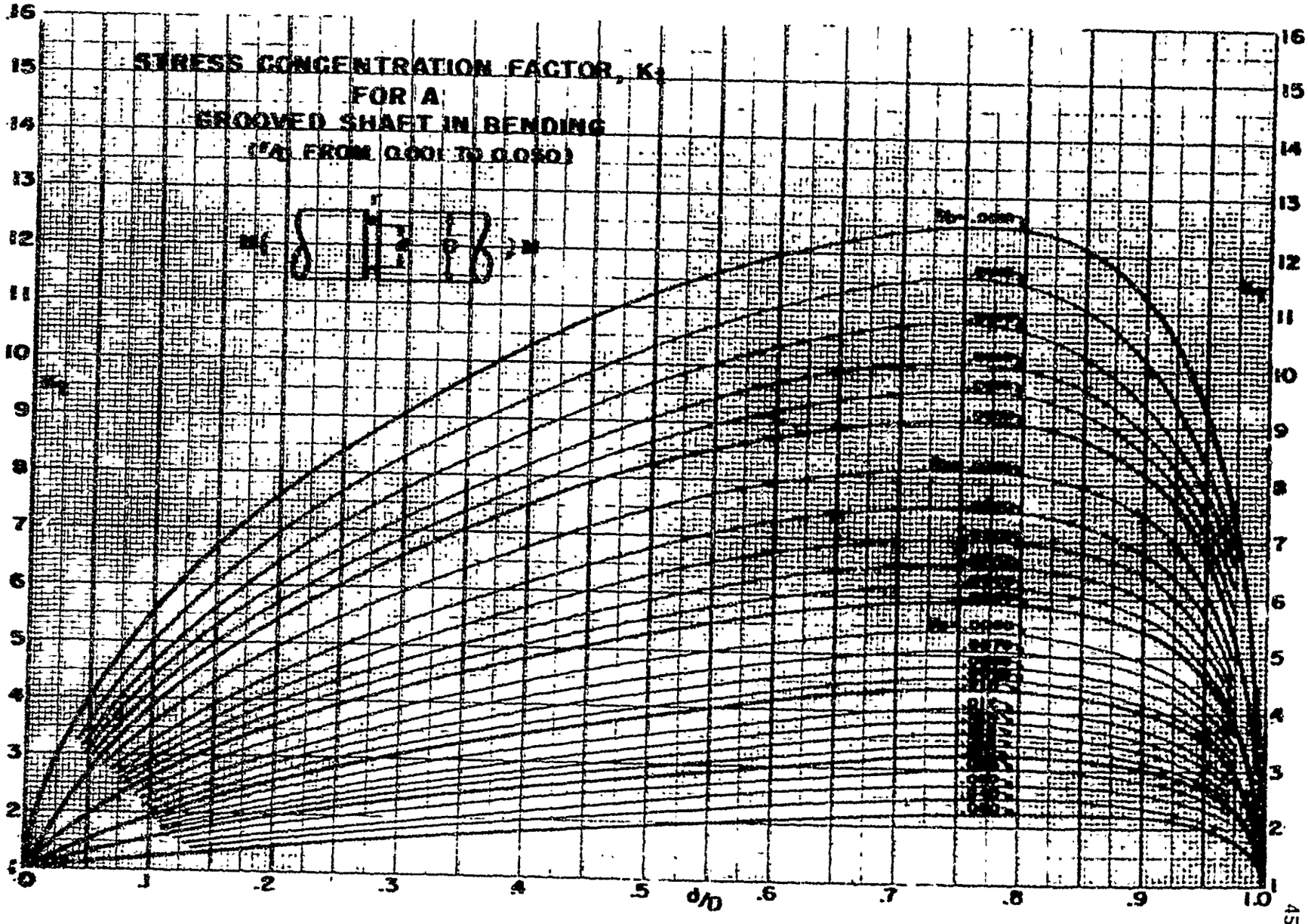

Fig. 2.2-7 Stress concentration factor, K_t, for a grooved shaft in bending (r/D from 0.001 to 0.050)[5, p.48].

Reproduced from best available copy.

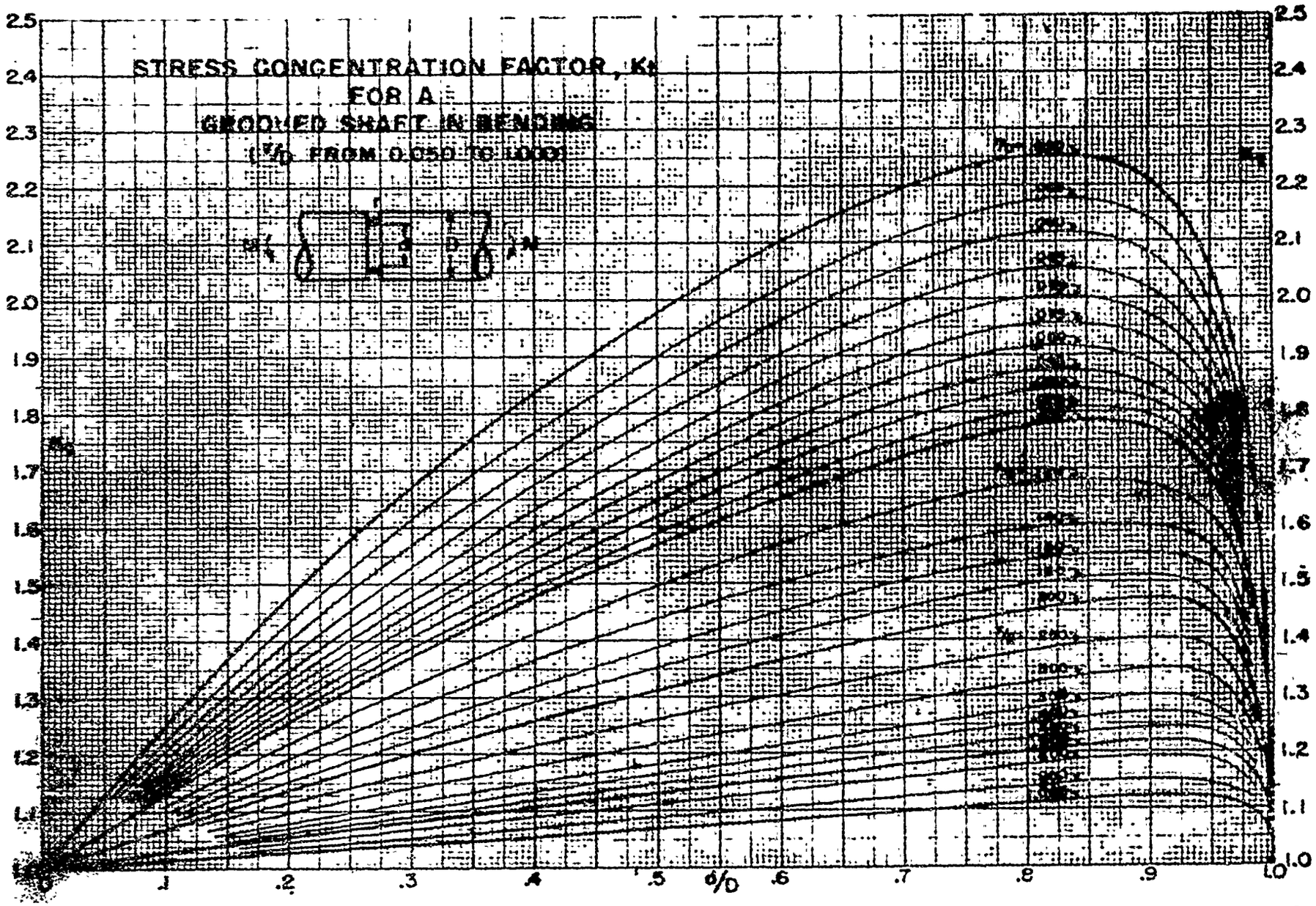

Fig. 2.2-8 Stress concentration factor, K_t, for a grooved shaft in bending (r/D from 0.050 to 1.000)[5, p. 49].

3. Obtain an estimate of the stress in the groove from

$$S_g = K_f S_{gn}, \tag{2.2-11}$$

where S_{gn}, the nominal grooved stress, is calculated by using Eq. 2.2-6.

If the specimen configuration is known then the pan loading for a desired bending stress may be calculated. Since the fatigue notch factor K_f, is greater than one, the actual grooved stress will be greater than the nominal grooved stress. It should be clear that Eq.(2.2-10)gives only an estimate of the fatigue notch factor so that Eq.(2.2-11) will also give only an estimate of the actual grooved stress. To find the actual K_f, two lots of specimens are tested: One lot grooved and one lot ungrooved; however, both lots have the same groove base diameter.

Then

$$K_f = \frac{S_{\text{nominal for ungrooved specimens}}}{S_{\text{nominal for grooved specimens}}} \tag{2.2-12}$$

In Eq.(2.2-12) $S_{nominal}$ is either the endurance limit or endurance strength at an arbitrarily large number of cycles.

Eq.(2.2-12) gives the actual value of the fatigue notch factor to be used in actual stress and notch sensitivity calculations. So when testing grooved specimens divide the nominal ungrooved stress by the estimated fatigue notch factor to obtain the stress to be used in Eq. (2.2-9).

Thus

$$W' = 18.39 - 0.042 \frac{S_{gn}}{K_f} d^3. \tag{2.2-13}$$

Eq. (2.2-13) gives the desired pan weights for calculating stresses for grooved specimens.

Thumb Rules for Estimating Starting Stress Levels for Staircase Testing

The method of staircase type testing to obtain endurance limits of grooved and ungrooved specimens is a good one. However, the time involved and the expense of manufacturing test specimens are critical. Therefore, it is worthwhile to obtain thumb rules for estimating the best staircase test starting point so that realistic initial stress levels are employed and the number of test specimens used is minimized.

After investigating staircase test data for ungrooved specimens it was found that a starting stress level of about 0.54 of the ultimate strength is the optimum starting point. Therefore, when staircase testing ungrooved specimens, a starting stress level of

$$S_{st} = 0.54\ S_{Ultimate} \tag{2.2-14}$$

is recommended to be used in Eq. (2.2-9) in place of S.

For staircase testing grooved specimens the following relationship is suggested for a starting stress:

$$S_{st} = 0.54\ S_{Ultimate}\ . \tag{2.2-15}$$

This stress is recommended to be used in Eq. (2.2-13) in place of S_{gn}.

COMPUTER PROGRAM TO DETERMINE THE WEIGHT TO BE ADDED TO THE UPPER PAN TO OBTAIN THE DESIRED SPECIMEN NOMINAL STRESS

A computer program and accompanying output is given in Appendix A.* This output gives the added pan weight needed to achieve a desired stress level in the base diameter of test specimens. Estimates of the groove stress and pan weights to be added are also given. It is recommended that this program be consulted before any testing takes place.

*Excerpts from Appendix A are given in Table 2.2-1.

Table 2.2-1 Computer Output (Sample) for Pan Weight Calculations of Wiedemann Fatigue Machine (Modified).[1]

RAD[3] inches	CKF[4]	SN[5]	SU[6]	WUPA[7] pounds
1.870	1.000	0	0	18.39
1.870	1.000	1000	1000	18.36
1.870	1.000	2000	2000	18.32
1.870	1.000	3000	3000	18.29
⋮	⋮	⋮	⋮	⋮
.031	1.280	0	0	18.39
.031	1.280	1228	1000	18.36
.031	1.280	2456	2000	18.32
.031	1.280	3684	3000	18.24
⋮	⋮	⋮	⋮	⋮
.062	1.156	0	0	18.39
.062	1.156	1156	1000	18.36
.062	1.156	2312	2000	18.32
.062	1.156	3408	3000	18.29
⋮	⋮	⋮	⋮	⋮
.125	1.100	0	0	18.39
.125	1.100	1100	1000	18.36
.125	1.100	2200	2000	18.32
.125	1.100	3300	3000	18.26
⋮	⋮	⋮	⋮	⋮
.250	1.047	0	0	18.39
.250	1.047	1047	1000	18.36
.250	1.047	2095	2000	18.36
.250	1.047	3142	3000	18.29
⋮	⋮	⋮	⋮	⋮

1. Computer program can be found in Appendix A.
2. The groove base diameter, d, is 0.0937 in for all groove radii.
3. RAD = specimen groove radius.
4. CKF = dynamic stress concentration factor.
5. SN = stress in base of groove.
6. SU = nominal stress in base of groove.
7. WUPA = upper pan weight to be added.

Use Appendix A as follows:

Ungrooved Specimens

1. For ungrooved specimens, find the $S_{Ultimate}$ value of the material and calculate S using Eq. (2.2-14) or S = 0.54 $S_{Ultimate}$.
2. Enter the Table in Appendix A whose first column has values RAD = 1.870, or a groove radius of 1.870 in. which results in practically no stress concentration, hence it is equivalent to no groove. Go down the SU column in this table and stop at the value closest to that found in Step 1, then read off the value of WUPA in the adjacent column at the right. This is the weight that has to be added to the upper pan, with the lower pan weight fixed at 11.00 pounds, to obtain the starting stress level for staircase testing, and is the value given by Eq. (2.2-9) with S = 0.54 $S_{Ultimate}$ substituted in it.
3. The SU value used in Step 2 to arrive at the WUPA value is the stress to be entered in the staircase plot.
4. If the specimen does not fail at or before the chosen number of cut-off cycles of 3×10^6 cycles, run a fresh specimen at a stress level 2,000 psi higher. Do this by getting the WUPA value for SU 2,000 psi higher than that used in the specimen just run. If the specimen fails before the chosen number of cut-off cycles, run a fresh specimen at a stress level 2,000 psi lower. Do this by getting the WUPA value for 2,000 psi lower than that used in the specimen just run. Continue the test until 35 useful specimens are run. Have the test results checked by your supervisor prior to terminating the tests.

Grooved Specimens

1. For grooved specimens find the ultimate value of the material and calculate S_{gn} using Eq. (2.2-15).

2. Calculate K_f using Eq. (2.2-10) after getting an estimate for q, for the material to be tested, from Figs. 2.2-5 and 2.2-6 and for K_t using Figs. 2.2-7 and 2.2-8. Such K_f values are given in the second column of Table 2.2-1 headed CKF.

3. Divide the S_{gn} value found in Step 1 by the K_f value found in Step 2, or find S_{gn}/K_f.

4. Enter the Table in Appendix A where the first column has values RAD equal to the groove radius of the specimens to be tested. Go down the SU column and stop at the value closest to that found in Step 3, then read off the value WUPA in the adjacent column at the right. This is the weight that has to be added to the upper pan to obtain the starting stress for staircase testing. This value is the one that would be obtained if Eq.(2.2.-13) were used.

5. The SU value used in Step 4 to arrive at the WUPA value is the stress to be entered in the staircase plot.

6. If the specimen does not fail at or before the chosen number of cut-off cycles of 3×10^6 cycles, run a fresh specimen at a stress level 2,000 psi higher. Do this by getting the WUPA value for SU 2,000 psi higher than that used in the specimen just run. If the specimen fails before the chosen number of cut-off cycles, run a fresh specimen at a stress level 2,000 psi lower than that used in the specimen just run. Continue the test until 35 useful specimens are run. Have the test results checked by your supervisor prior to terminating the tests.

CONCLUSIONS

This study verifies that the calibration and the loading schedule appearing on ONR Technical Report 4 [4, pp. 212-220] are correct.

2.2.1.2 WIEDEMANN (UNMODIFIED)

An analysis was performed to determine the correct loading schedule required to apply a desired maximum bending stress to specimens of this research for the unmodified machine.

The first step in the calibration procedure was to weigh the bearing housings, loading pan and pan linkage so that the contribution of each component to the bending moment in the test specimen could be calculated.

The next step in the calibration was to determine the moments due to the bearing housings and loading linkage. The procedure was to support the bearing at its normal pivots and measure the force, F, exerted at the end of the housing shown in Fig. 2.2-9 . Knowing the distance from the pivot to the end of the housing, L, the moment in the specimen was calculated for the housing only. The moment due to the linkage and load pan was obtained by taking the product of one-half the weight of the linkage and the distance from the knife edges to the pivot point.

Determination of Bending Moment

Due to the Bearing Housing

The bending moment, M_{B_O}, at the specimen groove due to the bearing housing is

$$M_{B_O} = (F + W_{S_P})\ L, \qquad (2.2\text{-}16)$$

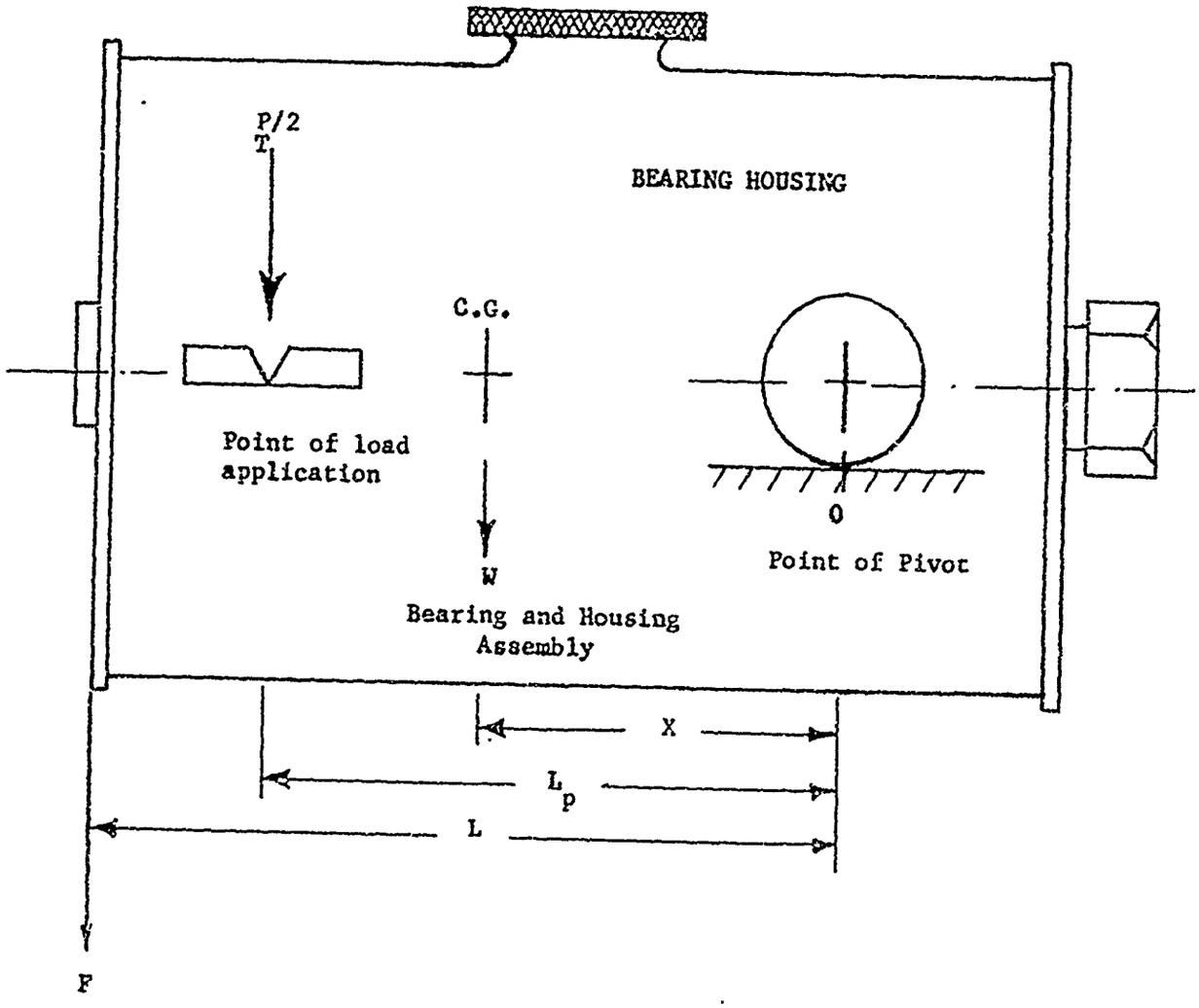

Fig. 2.2-9 R. R. Moore rotating beam fatigue machine bearing housing.

where

M_{B_0} = bending moment due to the bearing housing and one-half of specimen weight, in. - lb

F = force component due to bearing housings = 1.6 lb

W_{S_p} = Weight of one-half test specimen = 0.0358 lb

L = moment arm for force F = 4.655 in.

Substitution of the above values into Eq. (2.2-16) gives

$$M_{B_0} = (1.6 + 0.0358)\ (4.665),$$

$$M_{B_0} = 1.6358 \times 4.655,$$

$$M_{B_0} = 7.61 \text{ in. lb}$$

Determination of Bending Moment

Due to the Pan and Linkage

The bending moment due to the weight of the pan and accompanying linkage is calculated from

$$M_{P_0} = \frac{p}{2}\ (L_p), \qquad (2.2\text{-}17)$$

where

M_{P_0} = bending moment at the specimen due to the pan and linkage, in. - lb

p = weight of pan + linkage = 1.575 + 4.375 = 5.950 lb

L_p = length of moment arm for pan load = 4.00 in.

Substitution of these values into Eq. (2.2-17) yields

$$M_{P_0} = \frac{5.950}{2}\ (4.00),$$

$$M_{P_0} = 11.90 \text{ in.} - \text{lb}.$$

Thus the bending moment in the specimen contributed by the pan and linkage is 11.90 in. - lb.

Determination of the Total Bending Moment Due to the Bearing Housings, Pan and Linkage

The total bending moment contributed by the bearing housings, the pan, and the linkage is calculated as

$$M_{T_0} = M_{B_0} + M_{P_0}, \qquad (2.2\text{-}18)$$

where

M_{T_0} = the total bending moment due to the bearing housings and the pan-linkage assembly, in. - lb

M_{B_0} = 7.61 in. - lb

M_{P_0} = 11.90 in. - lb

Substitution of these values into Eq. (2.2-18) yields

$$M_{T_0} = 7.61 + 11.90,$$

$$M_{T_0} = 19.51 \text{ in.} - \text{lb}$$

Determination of the Equivalent Pan Load

The equivalent pan load, P_e, may be defined as the force acting at the knife edge supports of the bearing housings due to the weight of the bearing housings and pan-linkage assembly. It is this force that produces a bending moment, M_T, in the test specimen prior to loading of the pan and testing. It is necessary to determine this load so that the actual stress produced in the test specimen by the addition of a pan load may be determined. The equivalent pan load may be determined as follows:

$$P_e = \frac{2\,M_{T_0}}{L_p}, \qquad (2.2\text{-}19)$$

where

M_{T_0} = 19.51 in. - lb,

L_p = 4.00 in.

Substitution of these values into Eq.(2.2-19) yields

$$P_e = \frac{2(19.51)}{4},$$

$$P_e = 9.76 \text{ lb.}$$

Determination of the Center of Gravity of the Bearing Housing

The center of gravity, X, may be determined by taking the summation of moments around the pivot point of the bearing assembly as follows:

$$\Sigma M_0 = 0,$$

$$M_{B_0} - W_{D_B}(X) = 0, \qquad (2.2\text{-}20)$$

where

W_{D_B} = weight of the bearing housing = 4.221 lb

X = center of gravity, in.

M_{B_0} = 7.61 in. - lb .

Substitution of these values into Eq. (2.2-20)

$$7.61 - 4.221\,(X) = 0,$$

$$X = \frac{7.61}{4.221},$$

$X = 1.804$ in.

Determination of Stress in an Ungrooved Specimen

Knowing the total pan weight and its accompanying moment arm it is now possible to calculate the stress in the ungrooved test specimen from

$$S = \frac{M}{I/C}, \tag{2.2-21}$$

where

$$I/C = \frac{\pi d^3}{32},$$

for round test specimens and d is the specimen test section diameter. Substitution of Eq. (2.2-22) into Eq. (2.2-21) yields

$$S = \frac{32\ M}{\pi d^3}, \tag{2.2-23}$$

Now substitution of M into Eq. (2.2-23) gives

$$S = \frac{32(\frac{1}{2}\ P_T)\ L_P}{\pi d^3}, \tag{2.2-24}$$

where

P_T is the total pan weight or the pan added weight plus the equivalent pan load. Use of this definition in Eq. (2.2-24) yields

$$S = \frac{32(\frac{1}{2})(W_{P_A} + 9.76)\ 4.00}{\pi d^3}.$$

Determination of Added Pan Weight - Stress Relationship for Ungrooved Specimen

It is desired to establish a relationship for determining the amount of weight to be added to the pan to achieve the desired maximum bending stress. Rearrangement of Eq. (2.2-25) yields

$$W_{P_A} = \frac{\pi d^3 S}{64} - 9.76.$$

Thus Eq. (2.2-26) provides a way to calculate the needed added pan weight to give the desired maximum bending stress in ungrooved specimens.

Determination of the Maximum Stress in a Grooved Specimen

If the specimen to be tested is grooved, the expression which gives the pan weight for a desired maximum stress in the specimen groove is needed. The stress concentration factor must be taken into account, and if fatigue is involved the notch factor must also be considered.

The procedure is as follows:

1. Obtain the theoretical stress concentration factor, K_t, for the groove configuration and type of loading employed.
2. Obtain the fatigue notch factor from

$$K_f = q(K_t - 1) + 1, \qquad (2.2\text{-}27)$$

where q, the notch sensitivity factor, and K_t, are obtained from published tables and figures such as those in Peterson [5 ; p.9, Figs. 8 and 9 and p. 10; Fig. 10; pp. 47-50, Figs. 38 thru 41]. These are given here as Figs. 2.2-5 thru 2.2-8 and Figs. 2.2-10 thru 2.2-12.

3. Obtain an estimate of the stress in the groove from

$$S_g = K_f S_{g_n}, \qquad (2.2\text{-}28)$$

where S_{gn}, the nominal groove stress, is calculated by using Eq. (2.2-23).

If the specimen configuration is known then the pan loading for a desired bending stress may be calculated. Since the fatigue notch factor, K_f, is greater than one, the actual groove stress will be greater that the nominal groove stress. It should be clear that

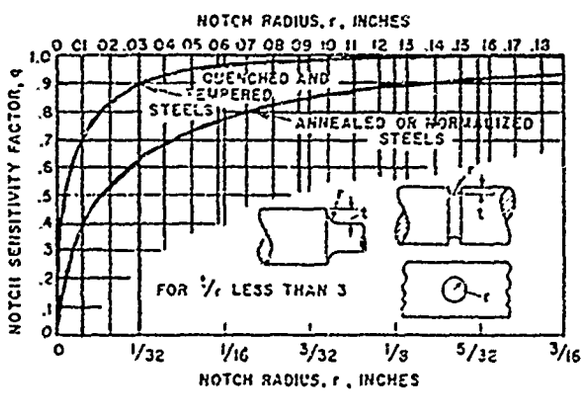

Fig. 2.2-10 Average notch sensitivity curves [5, p. 10, Fig. 4].

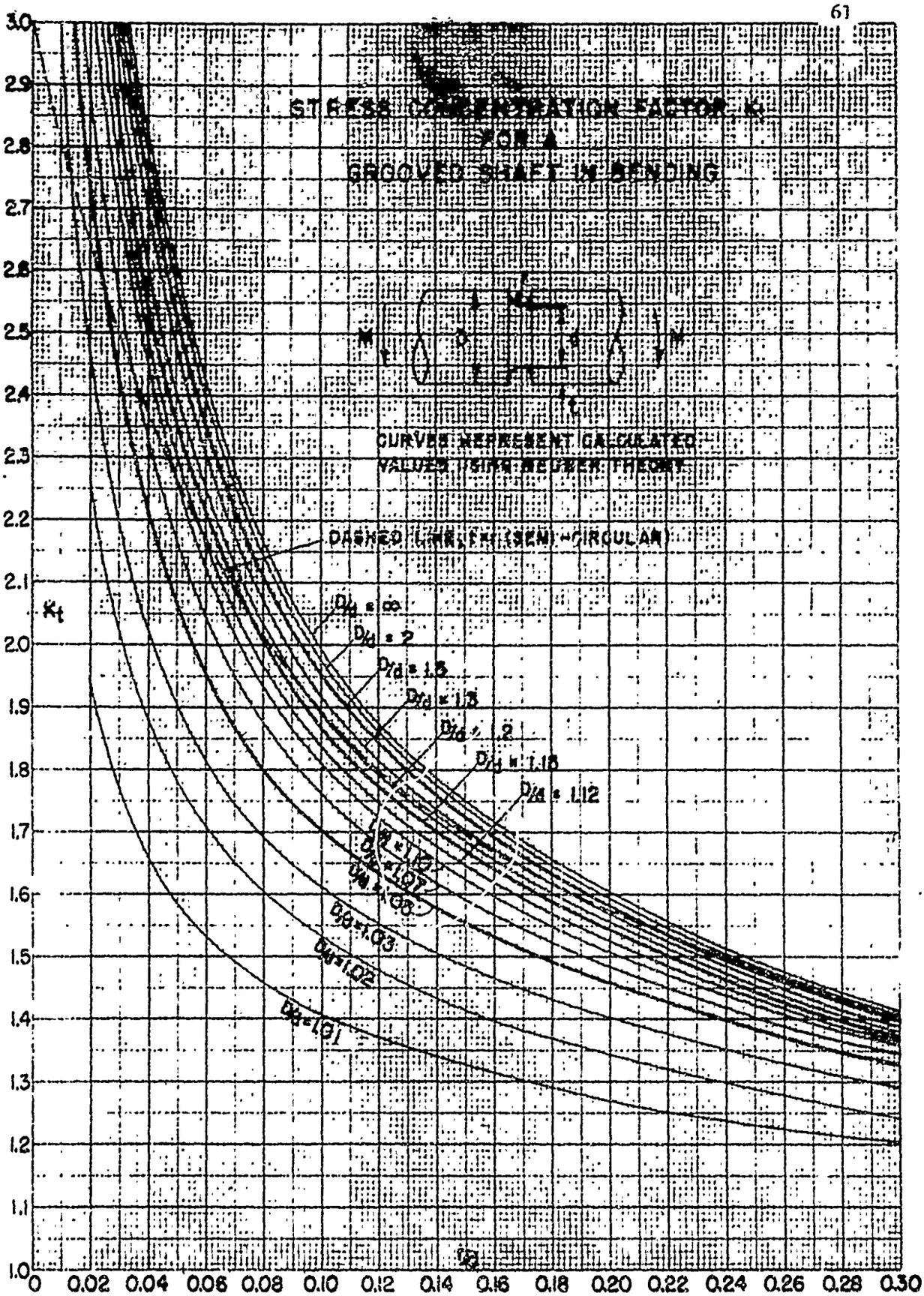

Fig. 2.2-11 Stress concentration factor, K_t, for a grooved shaft in bending (r/d from 1.01 to ∞)[5, p. 47].

Reproduced from best available copy.

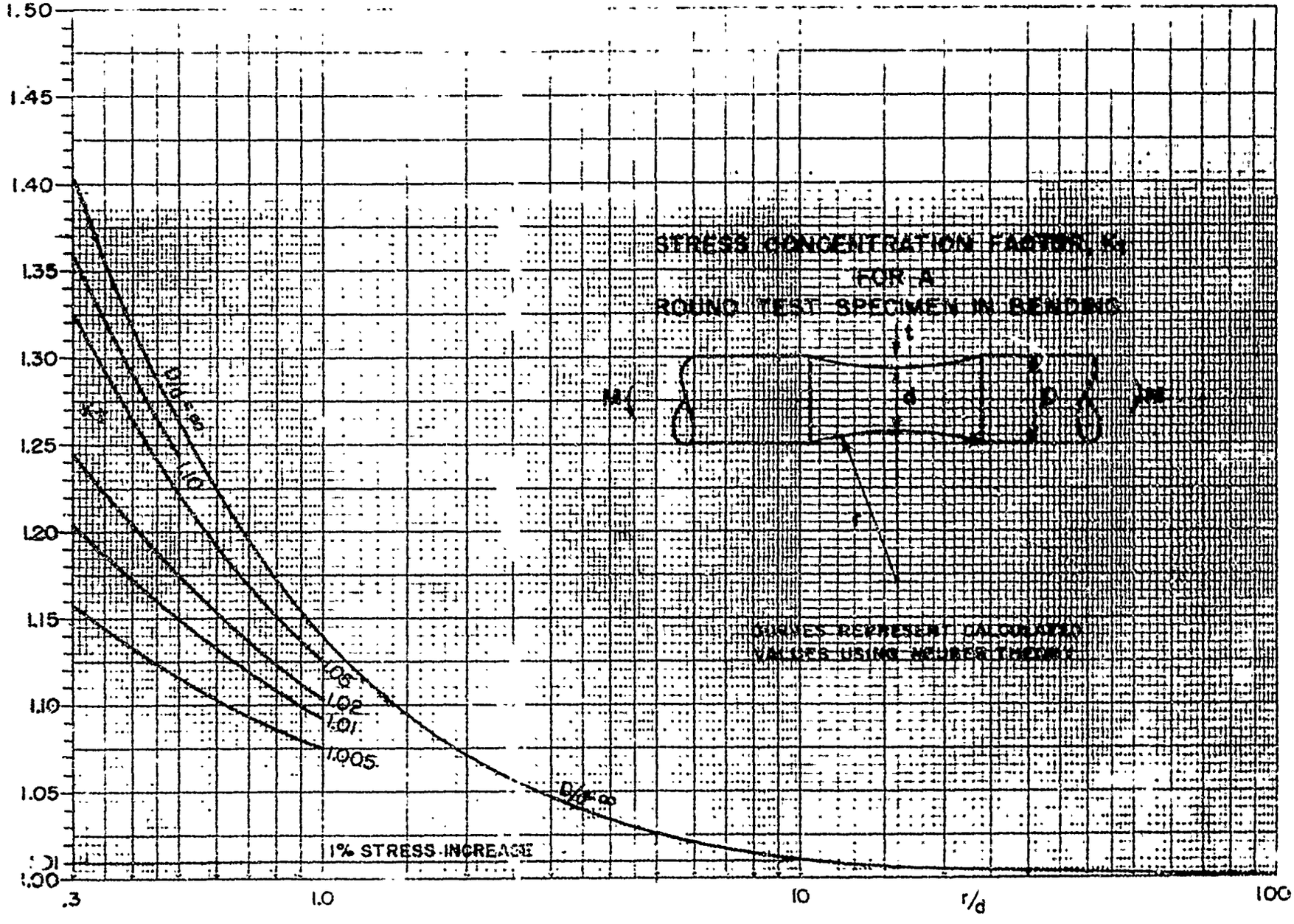

Fig. 2.2-12 Stress concentration factor, K_t, for a grooved shaft in bending(r/d from 1.005 to ∞ and r/d from 0.3 to 100) [5, p. 50].

Eq. (2.2-27) gives only an estimate of the fatigue notch factor so that Eq. (2.2-28) will also give only an estimate of the actual groove stress. To find the actual K_f two lots of specimens are tested: one lot grooved and one lot ungrooved; however, both lots have the same groove diameter.

Then

$$K_f = \frac{S_{\text{nominal for ungrooved specimen}}}{S_{\text{nominal for grooved specimen}}} . \qquad (2.2\text{-}29)$$

In Eq. (2.2-29) $S_{nominal}$ is either the endurance limit or the endurance strength at an arbitrarily large number of cycles. Eq. (2.2-29) however, is restricted to the case of completely reversed bending. Eq. (2.2-29) gives the actual value of K_f to be used in stress and notch sensitivity calculations. So when testing grooved specimens divide the nominal ungrooved stress by the estimated fatigue notch factor to obtain the stress to be used in Eq. (2.2-26).

Thus

$$W_{P_A} = \frac{\pi d^3}{64} \frac{S_{g_n}}{K_f} - 9.76 . \qquad (2.2\text{-}30)$$

Eq. (2.2-30) gives the desired added pan weight for calculating the stress for grooved specimens.

THUMB RULES FOR ESTIMATING STARTING STRESS LEVEL FOR STAIRCASE-TESTING

The method of staircase type testing to obtain endurance limits of grooved and ungrooved specimens is a good one. However, the time involved and the expense of manufacturing test specimens are critical. Therefore, it is worthwhile to obtain thumb rules for estimating the best staircase test starting point so that realistic initial stress levels are employed and the number of test specimens used is minimized.

After investigating staircase test data for ungrooved specimens it was found that a starting stress level of about 0.54 of the ultimate

strength is the optimum starting point. Therefore, when staircase-testing ungrooved specimens, a starting stress level of

$$S = 0.54\ S_{Ultimate}, \tag{2.2-31}$$

is recommended for use in Eq. (2.2-26).

For staircase-testing grooved specimens, a starting stress level of

$$S_{g_n} = 0.54\ S_{Ultimate}, \tag{2.2-32}$$

is recommended for use in Eq. (2.2-30).

Computer Program to Determine Pan Added Weights

In Appendix B, Table 2.2-2 will be found a computer program and accompanying output. This output gives the pan weight needed to achieve a desired stress level. Estimates of the grooved stress and pan weights are also given. It is recommended that this program be consulted before any testing takes place. Table 2.2-2 provides excerpts from Appendix B.

Use Appendix B as follows:

Ungrooved Specimens

1. For ungrooved specimens, find the $S_{Ultimate}$ value of the material and calculate S using Eq.(2.2-31), or $S = 0.54\ S_{Ultimate}$.
2. Enter Appendix B table whose first column has values RAD = 1.870. or a groove radius of 1.870 in. which results in practically no stress concentration, hence it is equivalent to no groove. Go down the SU column in this table and stop at the value closest to that found in Step 1, then read off the value of WPA in the adjacent column at the right. This is the weight that has to be added to the pan

Table 2.2-2 Computer Output (Sample) for Pan Weight Calculations of Wiedemann Fatigue Machine (Unmodified).*

RAD** inches	CKF	SN	SU	WPA pounds
.031	1.510	0	0	-9.76
.031	1.510	1510	1000	-8.79
.031	1.510	3020	2000	-7.83
.031	1.510	4530	3000	-6.86
⋮	⋮	⋮	⋮	⋮
.062	1.390	0	0	-9.76
.062	1.390	1390	1000	-8.79
.062	1.390	2780	2000	-7.83
.062	1.390	4170	3000	-6.86
⋮	⋮	⋮	⋮	⋮
.125	1.243	0	0	-9.76
.125	1.243	1243	1000	-8.79
.125	1.243	2486	2000	-7.83
.125	1.243	3729	3000	-6.86
⋮	⋮	⋮	⋮	⋮
.250	1.142	0	0	-9 76
.250	1.142	1142	1000	-8.79
.250	1.142	2284	2000	-7.83
.250	1.142	3426	3000	-6.86
⋮	⋮	⋮	⋮	⋮
1 870	1.000	0	0	-9.76
1.870	1.000	1000	1000	-8.79
1.870	1.000	2000	2000	-7.83
1.870	1.000	3000	3000	-6.86
⋮	⋮	⋮	⋮	⋮

*Complete tables are found in Tables 10.2-6 thru 10.2-10 computer program can be found in Appendix B.

**The groove base diameter, d, is 0.2700 in. for all groove radii.

to obtain the starting stress level for staircase testing, and is the value given by Eq. (2.2-26) with S = 0.54 $S_{Ulitmate}$ substituted in it.

3. The SU value used in Step 2 to arrive at the WPA value is the stress to be entered in the staircase plot.

4. If the specimen does not fail at or before the chosen number of cutoff cycles of 3×10^6 cycles, run a fresh specimen at a stress level 2,000 psi higher. Do this by getting the WPA value for SU 2,000 psi higher than that used in the specimen just run. If the specimen fails before the chosen number of cutoff cycles, run a fresh specimen at a stress level 2,000 psi lower. Do this by getting the WPA value for 2,000 psi lower than that used in the specimen just run. Continue the test until 35 useful specimens are run.

Grooved Specimens

1. For grooved specimens find that ultimate value of the material and calculate S_{g_n} using Eq. (2.2-32).

2. Calculate K_f using Eq. (2.2-27) after getting an estimate for q, for the material to be tested, from Figs. 2.2-5, 2.2-6, or 2.2-10, and for K_f using Figs. 2.2-7, 2.2-8, 2.2-11, or 2.2-12. Such K_f values are given in the second column of Table 2.2-2 headed CKF.

3. Divide the value S_{g_n} found in Step 1 by the K_f value found in Step 2, or find S_{g_n}/K_f.

4. Enter Appendix B table where the first column has values RAD equal to the groove radius of the specimens to be tested. Go down the SU column and stop at the value closest to that found in Step 3, then read off the value WPA in the adjacent column at the right. This is the weight that has to be added to the pan to obtain the starting stress for staircase testing. This value is the one that would be obtained if Eq. (2.2-30) were used.

5. The SU value used in Step 3 to arrive at the WPA value is the stress to be entered in the staircase plot.

6. If the specimen does not fail at or before the chosen number of cutoff cycles of 3×10^6 cycles, run a fresh specimen at a stress level 2,000 psi higher. Do this by getting the WPA value for SU 2,000 psi higher than that used in the specimen just run. If the specimen fails before the chosen number of cutoff cycles, run a fresh specimen at a stress level 2,000 psi lower. Do this by getting the WPA value for 2,000 lower than that used in the specimen just run. Continue the test until 35 useful specimens are run.

CONCLUSIONS

This study indicates that this calibration report and the associated loading schedule should replace those appearing in ONR Technical Report No. 2. [2, pp. 67-73].

RECOMMENDATIONS

For any research using the unmodified R. R. Moore Reliability Research Machine the following equations are recommended:

1. To obtain the ungrooved specimen maximum bending stress use

$$S = \frac{32\left(\frac{1}{2}\right)(W_{P_A} + 9.76) \quad 4.00}{\pi d^3} \qquad (2.2\text{-}25)$$

2. To obtain the added pan weight for a desired maximum bending for ungrooved specimens use

$$W_{P_A} = \frac{\pi d^3 S}{64} - 9.76 \ . \qquad (2.2\text{-}26)$$

3. To obtain the added pan weight for a desired maximum bending stress for grooved specimens use

$$W_{P_A} = \frac{\pi d^3 S_{g_n}}{64 K_f} - 9.76 \qquad (2.2\text{-}30)$$

4. To obtain a starting stress level for staircase testing of ungrooved specimens use the instructions on pages 71-74.

5. To obtain a starting stress level for staircase testing of grooved specimens use the instructions on pages 74-75.

2.2.2 RESEARCH PROGRAM AND DATA

Tables 2.3.-3 and 2.2-4 provide a cross-reference for the Wiedemann machines test program, and the data generated and reduced. The test program in these tables are broken down by data type, i.e., Cycles-to-failure and Staircase testing data.

Table 2.2-3 Cycles-To-Failure on Wiedemann Machines.

Group No.	Notch Radius Inches + .001 - .002	Sample Size	Volume II Section Cross Reference: Raw Data Table No.	Reduced Data Table No.	Reduced Data Figure No.
AISI 4130 Steel Rod D = 0.375 in. diameter. d = 0.0937 in. dia. of Notch					
82	0.031	35	Test to be re-run		
83	0.031	35	Test to be re-run		
84	0.031	35	Test to be re-run		
85	0.031	35	Test to be re-run		
104	0.062	35	Test to be re-run		
105	0.062	35	Test to be re-run		
106	0.062	35	Test to be re-run		
107	0.062	35	Test to be re-run		
88	0.125	35	Test to be re-run		
89	0.125	35	8.2-11		9.2-1 to 9.2-3
90	0.125	35	8.2-14		9.2-4 to 9.2-6
91	0.125	35	8.2-16		9.2-7 to 9.2-9
92	0.250	35	Test to be re-run		
93	0.250	35	8.2-18		9.2-10 to 9.2-12
94	0.250	35	8.2-20		9.2-13 to 9.2-15
95	0.250	35	8.2-21		9.2-16 to 9.2-18

Table 2.2-4 Notch Sensitivity Fatigue Test Data - Staircase Testing on Wiedemann Machines

Group No.	Notch Radius Inches + .001 - .002	Sample Size	Volume II Section Cross Reference		
			Raw Data Table No.	Reduced Data Table No.	Reduced Data Figure No.
AISI 1038 Steel Rod D = 0.375 in. diameter. d = 0.2700 in. dia. of Notch					
162	0.031	35	8.2-23	9.2-1	9.2-19
163	0.062	35	8.2-25	9.2-2	9.2-20
164	0.125	35	8.2-27	9.2-3	9.2-21
165	0.250	35	8.2-29	9.2-4	9.2-22
166	1.870	35	8.2-31	9.2-5	9.2-23

2.3 AXIAL FATIGUE RELIABILITY RESEARCH MACHINE

2.3.1 AXIAL FATIGUE TESTING TO GENERATE GOODMAN DIAGRAMS

The axial fatigue machine can apply a constant mean tensile load onto which a constant amplitude alternating tensile-compressive load can be superimposed along the longitudinal axis of a test specimen. The application of the combined loads provides the capability to determine the endurance strength of the test specimens and to investigate the effects of interaction between alternating and mean loads. When the endurance strength calculated at specified ratios of alternating to mean stresses are plotted on a biaxial graph, a strength surface known as the distributional Goodman diagram results, as shown in Fig. 2.3-1.

Four different theories are presented in Fig. 2.3.-1. The first one is the modified Goodman line joining the mean of the endurance strength, at a specific cycles of life, to the mean of the static ultimate strength of the material. This a conservative design criterion for combined-stress fatigue and may be used when fracture is the failure mode. The second is a modification of the previous one, in that the line joins the means of the endurance strength to the mean of the static yield strength instead of the ultimate. This is also a conservative combined-stress design criterion and may be used when yield is the failure mode. The third criterion is the Gerber parabola passing through the mean of the endurance strength and the mean of the static ultimate strength. This parabola results from the maximum principal shear stress theory of failure [6, p. 183]. This theory is optimistic relative to the first two criteria and yet is closer to the actual fatigue strength. This criterion is not recommended for stresses beyond the yield strength. The fourth criterion is an ellipse, resulting from the von Mises-Hencky failure criterion [7, p. 85], which passes through the mean of the endurance strength and the mean of the static ultimate strength. This criterion is the closest to the actual combined-stress fatigue strength of most steels. Again this criterion is not recommended for stresses beyond the yield strength, however, for lack of better criteria, it is being used to represent fracture as well.

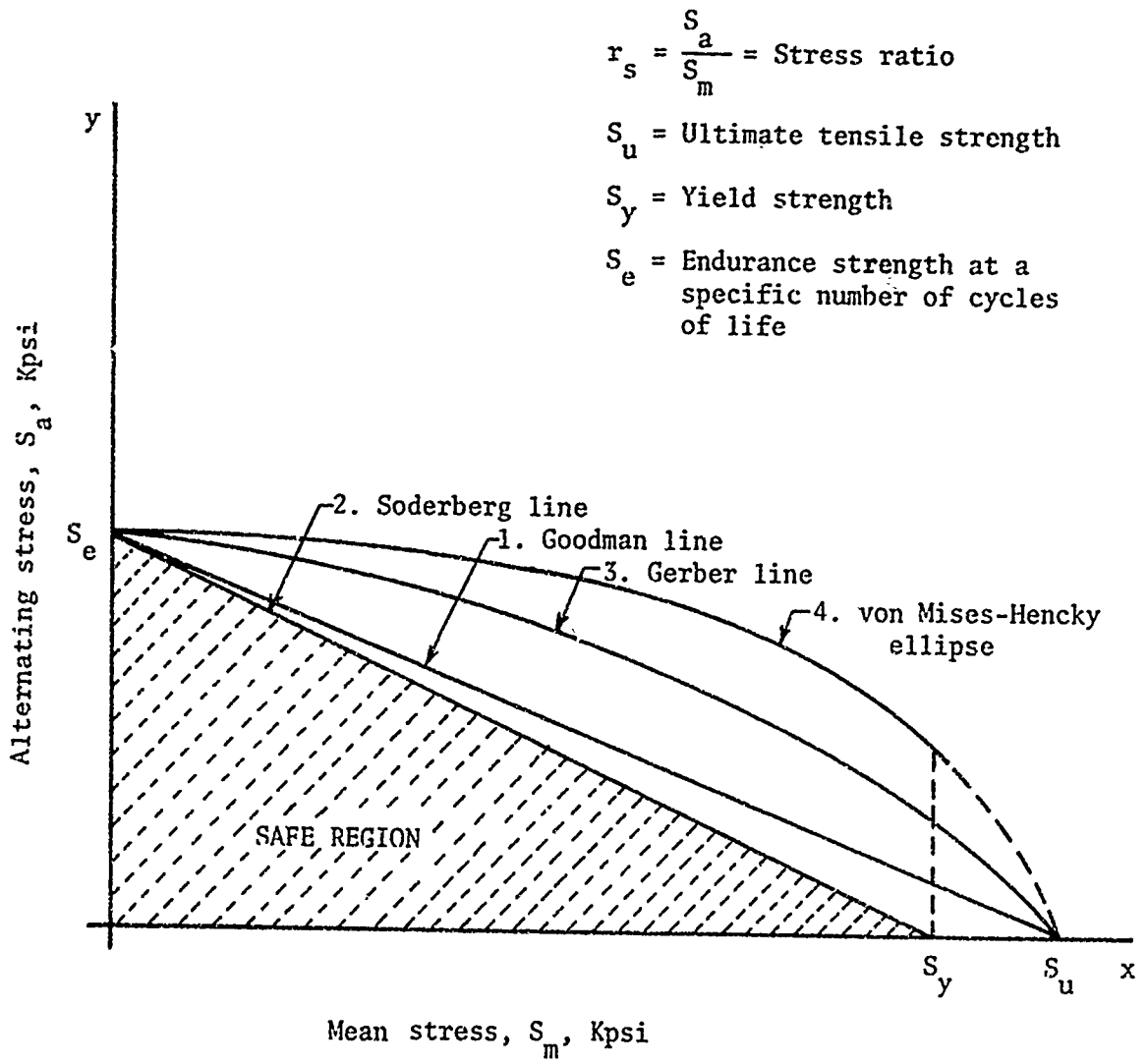

Fig. 2.3-1 Goodman diagrams showing various theories defining the safe design region for combined-stress fatigue.

The axial fatigue machine was used to obtain experimental data to determine the strength distributions for a specific cycles of life for specimens of a specified steel and geometry for construction of distributional Goodman diagrams. In order to obtain sufficient data points to adequately define the strength surface, axial fatigue tests are conducted at stress ratios of infinity, 2.0, 1.0, 0.4 and 0.2. The static ultimate strength distribution is used for the strength distribution at a stress ratio of zero.

2.3.1.1 DETERMINATION OF ENDURANCE STRENGTH DISTRIBUTION AT THE STRESS RATIO $r_s = \infty$

First an estimate of the endurance strength mean is required. Table 2.3.1 was developed to obtain the ratio between the endurance strength mean and the ultimate strength mean, based on experimental data for the four materials researched. The results indicate that the value $\overline{S}_e/\overline{S}_u = 0.45$ is a representative one. Consequently the following equation was developed for the estimate of the mean of the endurance strength from a knowledge of the mean of the static ultimate strength:

$$\overline{S}_e = 0.45\ \overline{S}_u . \qquad (2.3\text{-}1)$$

Knowing $\overline{S}_u$ from the experimental data for static ultimate strength, $\overline{S}_e$ can be calculated from Eq. (2.3-1). The starting load for the staircase test may then be obtained from

$$\overline{P}_a = \overline{S}_e \cdot \overline{A}, \qquad (2.3\text{-}2)$$

where

$\overline{P}_a$ = mean alternating load in lb.

$\overline{A}$ = mean cross sectional area of the test specimen in in^2.

Table 2.3-1 Ratio of experimental endurance strength to static ultimate strength for staircase-test starting-stress determination.

Material	Mean of Static Ultimate Strength, $\overline{S}_u$ psi	Mean of Endurance Strength, $\overline{S}_e$ psi	$\overline{S}_e/\overline{S}_u$
AISI 1018	60,000	26,000	0.434
AISI 1038	69,000	31,000	0.449
AISI 4130	105,000	40,000	0.381
AISI 4340	116,000	49,000	0.423

The staircase method of testing requires that if the first specimens fails before 2×10^6 cycles, the next specimen is loaded to a stress level one increment higher. This increment has been chosen to be approximately 1,000 psi.

2.3.1.2 DETERMINATION OF STRENGTH DISTRIBUTION AT STRESS RATIOS OTHER THAN ∞

For stress ratios other than ∞ it is necessary to apply a mean load as well as an alternating load. This is done by determining the mean as well as the alternating loads as follows:

Previous experimental research at The University of Arizona provides substantial evidence that the actual strength distribution for axial fatigue lie in between the Gerber parabola and the von Mises-Hencky ellipse. The equation of the Gerber parabola is

$$\frac{S_a}{S_e} + \left(\frac{S_m}{S_u}\right)^2 = 1, \qquad (2.3\text{-}3)$$

and the equation of the von Mises-Hencky ellipse is

$$\left(\frac{S_a}{S_e}\right)^2 + \left(\frac{S_m}{S_u}\right)^2 = 1. \qquad (2.3\text{-}4)$$

The data appears to favor the ellipse, furthermore a slightly higher stress vector, $S_v m$ value will provide a good starting stress with the first few specimens being failures. Thus as an estimate of the mean of S_v for starting staircase testing a value favoring the von Mises-Hencky ellipse is used for a specific stress ratio. Dividing Eq. (2.3-4) by $(S_m)^2$ gives

$$\frac{S_a^{\,2}}{S_m^{\,2}\ S_e^{\,2}} + \frac{1}{S_u^{\,2}} = \frac{1}{S_m^{\,2}}, \qquad (2.3\text{-}5)$$

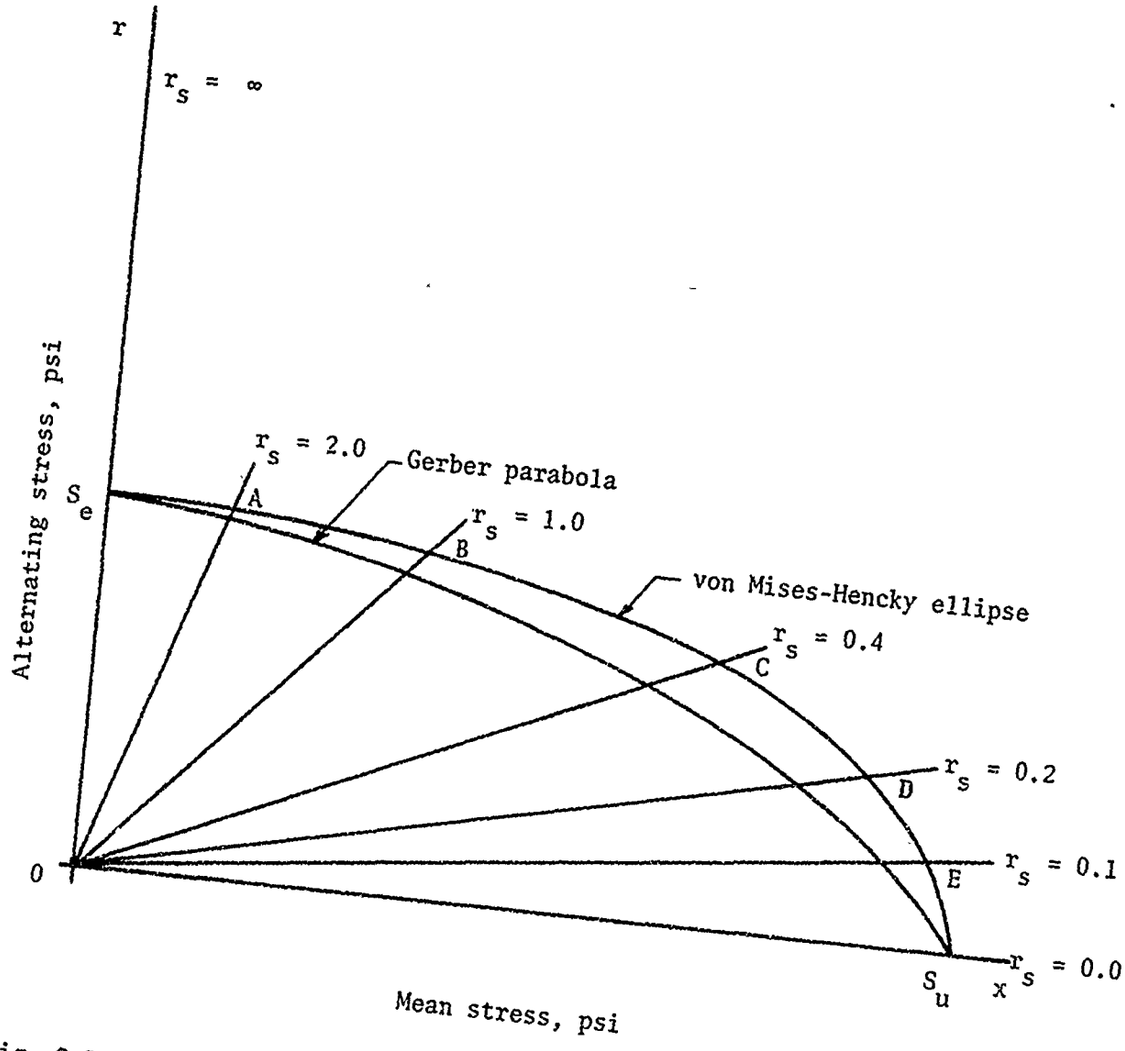

Fig. 2.3-2 Goodman diagram (empirical) showing the estimates of the mean of the stress vector, S_v, at different stress ratios, r_s.

and solving for S_m and substituting $r_s = \frac{S_a}{S_m}$ gives

$$S_m = \frac{S_e - S_u}{\left(S_u^2 - r_s^2 + S_e^2\right)^{1/2}} . \qquad (2.3\text{-}6)$$

Eq. (2.3-6) yields an estimate of S_m in terms of known quantities.

Now stress vector S_v may be calculated from

$$S_v = (S_a^2 + S_m^2)^{1/2} , \qquad (2.3\text{-}7)$$

where

$$S_a = \frac{\text{Alternating load}}{\text{Cross sectional area of specimen}} = \frac{P_a}{A} ,$$

and

$$S_m = \frac{\text{Mean load}}{\text{Cross sectional area of specimen}} = \frac{P_m}{A} .$$

Substitution of $r_s = \frac{S_a}{S_m}$ in Eq. (2.3-7) yields

$$S_v = S_m (r_s^2 + 1)^{1/2} . \qquad (2.3\text{-}8)$$

Thus the value of S_m found from Eq. (2.3-6) and applied to Eq. (2.3-8) provides an estimate of the mean of S_v, at a specified stress ratio. Points on the von Mises-Hencky ellipse calculated by this method[1] and used as initial values of S_v for staircase tests at various stress ratios are shown in Fig. 2.3.-2.

The estimates of S_m and S_v must be translated into axial mean and alternating loads for testing on the Axial Fatigue Research Machine. After Eq. (2.3-6) is used to obtain an estimate of S_m, the required mean load is determined from

$$P_m = S_m \cdot A . \qquad (2.3\text{-}9)$$

Footnote:

1. The PDP-8 program to calculate points on the Gerber parabola and the von Mises-Hencky ellipse is listed in Appendix F.

The corresponding alternating load is then calculated from

$$P_a = r_s \cdot P_m \,. \tag{2.3-10}$$

The mean load indicator of the Axial Fatigue Machine is scaled in one pound increments; therefore, the estimated values of S_m, and consequently of S_v, are adjusted to the nearest pound of force. The revised stress values, S_v and S_m, are calculated by reverse application of Eqs. (2.3-9) and (2.3-8).

Staircase testing requires steps of equal increments of stress. For this program an acceptable range of increments of S_v is 1,000 to 1,500 psi. Similar to revising the initial stress level, a method is required to adjust the initially selected stress increment to one which corresponds to an increment in multiples of pounds of mean load. The methodology used for calculating the starting stress level, S_v, and the stress increment, I_v is given below:

(1) Determine an estimate of S_m from the static ultimate strength of the specimen, Eqs. (2.3-1) and (2.3-6) and the desired stress ratio.

(2) Calculate an initial value of S_v from Eq. (2.3-7).

(3) Find the required mean load, P_m, from Eq. (2.3-9).

(4) Round P_m to the nearest pound and revise the estimated value of S_m.

(5) Calculate the corresponding values of S_v and S_a for the desired stress ratio.

(6) Select a tentative value for the stress increment, I_s.

(7) Calculate the comparable increment in mean stress from Eq. (2.3-8) rearranged in the form

$$I_m = I_s / (r_s^{\,2} + 1)^{1/2}. \tag{2.3-11}$$

(8) Find the required increment in mean load, I_{P_m}, from an adaptation of Eq. (2.3-9) as

$$I_{p_m} = I_m \cdot A. \qquad (2.3\text{-}12)$$

(9) Round the calculated value of I_{p_m} to the nearest pound, and apply Eqs. (2.3-11) and (2.3-12) in reverse order to determine the reversed stress increment.

(10) Calculate the required mean and alternating loads for each level of S_v anticipated for the test from the above equations. Each stress level of the test is determined from the preceding stress level (depending upon whether the specimen successfully completed 2×10^6 cycles or failed prior to that time) by the equation

$$S_v = S_v' \pm I_s . \qquad (2.3\text{-}13)$$

A PDP-8 computer program has been developed to calculate the initial stress level and subsequent stress levels, and the required mean and alternating loads. A copy of the program for the initial test point is listed in Appendix G, and for subsequent points in Appendices H and I.

2.3.1.3 PLOTTING AND REDUCTION OF STAIRCASE DATA

The data obtained from staircase testing are recorded and reduced using the methods discussed for the Wiedemann machines in Section 3.2.3.

2.3.2 RESEARCH PROGRAM AND DATA

During this reporting period AISI 1018 steel specimens were tested to get the strength distributions in terms of the mean and the standard deviation of S_v at different stress ratios. Table 2.3-2 summarizes the test program and points out the sections of this report where the raw data and the reduced data can be obtained.

Table 2.3-2 Axial Fatigue Machine test program for AISI 1018 steel specimens and references for the raw and the reduced data for groups of 35 specimens.

Group No.	Stress Ratio	Diameter of test section inches	Raw Data	Reduced Data Table No.	Reduced Data Figure No.
161	∞	0.075	8.3-5	9.3-3	9.3-3
160	2.0	0.075	8.3-4	9.3-2	9.3-2
159	1.0	0.075	8.3-3	9.3-1	9.3-1
158	0.4	0.070	Testing	incomplete	
157	0.2	0.070	Testing	incomplete	
156	0.0	0.250	8.3-1	Not applicable	

3.0 DATA REDUCTION AND RESULTS

Data generated by the experimental research discussed in Chapter 2 were reduced and analyzed to determine the dynamic strength characteristics of specimens of different AISI steels and geometry. Cycles-to-failure tests conducted at specified stress levels were analyzed to determine which distribution model provided the best fit to the data and to estimate the parameters of the distributions being evaluated. Stress-to-failure test data were reduced to determine the distribution parameters of endurance strength for the normal distribution.

3.1 CYCLES-TO-FAILURE DATA

The cycles-to-failure data presented in Section II were reduced with the aid of two CDC-6400 computer programs, program CYTOFR and program WEIBULL. The primary functions of the programs are to calculate distribution parameters from the data and to perform goodness-of-fit tests to provide indicators of the best distribution model.

3.1.1 PROGRAM CYTOFR

Program CYTOFR was discussed and the FORTRAN program statements were presented in the Fourth ONR Report (4 , pp. 163-174). During the past year a number of changes have been made to improve its effectiveness. The current program is listed in Appendix C. Program CYTOFR determines parameter estimates of the following distributions:

Normal:

$$f_N(T) = \frac{1}{\sigma\sqrt{2\pi}} e^{-\frac{1}{2}\left(\frac{T-\overline{T}}{\sigma}\right)^2} \qquad (3.1\text{-}1)$$

having the parameters

$\overline{T}$ = mean of cycles to failure

σ = standard deviation of cycles to failure

T = cycles to failure

Lognormal:

$$f_{LN}(T) = \frac{1}{T'_{\hat{\sigma}} \sqrt{2\pi}} e^{-\frac{1}{2}\left(\frac{T - \overline{T}'}{\sigma}\right)^2}, \qquad (3.1\text{-}2)$$

$\overline{T}'$ = mean of $\log_e T$

σ' = standard deviation of $\log_e T$

T = cycles-to-failure.

Program CYTOFR performs additional calculations and makes goodness-of-fit tests as follows:

1. Coefficient of Skewness, α_3.
2. Coefficient of Kurtosis, α_4.
3. Chi-Squared Goodness-of-Fit test.
4. Kolmogorov-Smirnov Goodness-of-Fit test.

The calculation of the distribution parameters are accomplished within the computer program by incorporation of the following equations:

The data mean, $\overline{T}$, is calculated from

$$\overline{T} = \frac{\sum_{i=1}^{n} T_i}{n}, \qquad (3.1\text{-}3)$$

where T_i, $i = 1, 2, ---, n$ are the values for n data points.

The unbiased estimate of the distribution variance, σ^2, is calculated from

$$\sigma^2 = \frac{\sum_{i=1}^{n} (T_i - \overline{T})^2}{n-1}. \qquad (3.1\text{-}4)$$

The coefficients of skewness and kurtosis, as discussed by Hahn and Shapiro, are summarized by the moments of the distribution about the mean connected to dimensionless coefficients for simplicity of use [8 , pp. 45-49]. The coefficient of skewness, α_3, uses the relationship between the second moment which measures dispersion and the third moment which measures skewness to obtain a standardized measure of skewness of the distribution relative to its degree of spread. If the distribution is normal $\alpha_3 = 0$.

The quantitive measure is found from the equation

$$\alpha_3 = \frac{M_3}{(M_2)^{3/2}} , \qquad (3.1\text{-}5)$$

where

$$M_3 = \sum_{i=1}^{n} \frac{(x_i - \overline{x})^3}{n} , \qquad (3.1\text{-}6)$$

and

$$M_2 = \sum_{i=1}^{n} \frac{(x_i - \overline{x})^2}{n} . \qquad (3.1\text{-}7)$$

Similarly the coefficient of kurtosis, α_4, uses the relationship between the second moment and the third moment of the distribution about the mean to obtain a standardized measure of peakedness of the distribution relative to its degree of spread. The quantitative value of α_4, which is equal to 3.0 for an exact normal distribution, is obtained from the equation

$$\alpha_4 = \frac{M_4}{(M_2)^2} , \qquad (3.1\text{-}8)$$

where

$$M_4 = \sum_{i=1}^{n} \frac{(x_i - \overline{x})^4}{n} \qquad (3.1\text{-}9)$$

and

M_2 is as given in (3.1-7).

The Chi-Squared goodness-of-fit test is the comparison of actual observations of grouped,ordered data with the expected number of observations calculated using the parameter estimates and the appropriate distribution equation. The methodology for application of this test is contained in the Third Technical Report [3 , pp. 256-267].

The Kolmogorov-Smirnov goodness-of-fit test is the comparison of the cumulative probability density graph of the data distribution calculated from the estimated parameters with the relative cumulative graph of each ordered data point. Discussions of the application of the K-S test to normal and lognormal distributions are presented in the Fourth Technical Report [4, pp. 51-58].

The normal and lognormal distributions and their applications to design-by-reliability methodology for dynamic mechanical components are discussed in the First ONR Report [1, pp. 44-52].

3.1.2 PROGRAM WEIBULL

Program WEIBULL has extended the data reduction techniques by the computerized calculation of Weibull distribution parameters from the data, and the application of the X^2 and K-S goodness-of-fit tests indicated above. The Weibull distribution is described by the function

$$f_N(T) = \frac{\beta}{\eta} \left(\frac{T - \gamma}{\eta}\right)^{\beta-1} e^{-\left(\frac{T - \gamma}{\eta}\right)^{\beta}}, \qquad (3.1\text{-}10)$$

where

β = shape parameter,

η = scale parameter,

γ = location parameter.

Consideration of the Weibull distribution as an appropriate model for the distribution of fatigue data was introduced and discussed in the Fourth Technical Report [4, pp. 63-84]. Development of the analysis capability was limited to manual techniques until program WEIBULL was completed.

The basic FORTRAN computer program to solve for estimates of Weibull parameters and cycle life for specified levels of reliability was provided by Mr. Thomas C. Stansberry, Delco Radio Division, General Motors Corporation. His program was adapted to The University of Arizona CDC-6400 computer and updated to include subroutines for the

Chi-Squared and Kolmogorov-Smirnov goodness-of-fit tests. A copy of the program FORTRAN statements is contained in Appendix D.

The first data card contains the sample size and the minimum life increment for use in linearizing the x-y relationship. Subsequent data cards (one for each specimen) contain the failure information. The first operation performed by the computer is to establish an ordered array of the failures and median ranks similar to standard tables [4, p. 67]. However, the computer calculates the median ranks so that manual use of tables for each data sample is unnecessary.

The next operation is the calculation of $y_i = \ln \ln \left[\frac{1}{1 - F(t_i)}\right]$ and $x_i = \ln(t_i - \gamma_k)$. Where $i = 1, 2, ---, n$ and γ_k = minimum life increment $(1, 2, ---, k)$ such that $\gamma_k < t_i$. As the array of y_i and x_i is computed the method of least squares is used to determine the degree of linearity. This operation is iterated with γ_k being increased in increments until the best fit straight line is obtained. At that time the computer records the estimates of β, γ, and η. It then calculates the one percent life, ten percent life, and median life with the associated 90 percent confidence intervals.

Upon completion of the calculations, the program calls the K-S test and Chi-Squared test subroutines in turn to provide a measure of the fit of the Weibull distribution with the estimated parameters to the data. The K-S subroutine "DTEST" applies the Kolmogorov-Smirnov goodness-of-fit test and prints differences, D, for each failure time in ascending order. Analysis of the K-S test is done by comparing the D value, largest in absolute value, with the critical value from an ordinary table of K-S D values.

The Chi-Squared test subroutine began with the application of the Chi-Squared test using a number of cells determined by Struges' rule, $K = 1.0 + 3.3 \log_{10} n$. However, analysis of the results showed that the expected and observed frequency of occurrences were too small in the tails of the distribution invalidating the test. The first modification to the subroutine involved combining cells at the tails until the observed value was at least five. This action, while being commonly recognized as being valid, resulted in a second problem.

The Weibull is known to be an extreme value, skewed distribution. Therefore, there is a small percentage of area contained in the long right side tail. The use of Sturges' rule for data with a sample size of 35 results in six cells of equal width. Consequently, when the data in adjacent end cells are combined to provide either observed or expected frequencies equal to or greater than 5, the number of filled cells may be reduced to as few as four. Since the distribution being tested is the three-parameter Weibull, the degrees of freedom (k-r-1) requires that the number of cells, k, be at least five in order to have one degree of freedom. This Chi-Squared test was applied to ten samples of cycles to failure data. It was found that six of the ten tests resulted in only four filled cells which provided zero degrees of freedom, and the Chi-Squared test was considered invalid. Thus, it appears that sample sizes should be increased if the standard Chi-Squared goodness-of-fit test is to be used.

Another modification of the subroutine was made and tested to see if the sample size problem could be circumvented. This modification involved the use of variable cell widths. The technique described by Hahn and Shapiro [4 , pp. 302-308] called for the calculation of cell widths to provide equal values for the expected number of observations. It was proposed that variable cell widths providing for equal numbers of actual observations would be equally valid as long as the expected frequency was not significantly less than 5. A modification to the subroutine was made dividing the range of the data so that each cell contains exactly 5 failures. For our sample size of 35 this provides 7 cells.

This subroutine was run for the same 10 sets of data, and the following observations were made: The expected frequency for the seventh cell was always less than 5.0, which according to accepted practices invalidated the test. It was observed, however, that as long as the expected frequency was equal to or greater than 2.0, the Chi-Squared value did not blow up. This observation was confirmed by a Monte Carlo simulation of 1,000 runs from which it was concluded that Chi-Squared errors resulting from expected frequencies between 2.0 and 5.0 are insignificant.

A final modification was made to the subroutine using variable cell widths and combining adjoining end cells to insure that the expected number of observations per cell equals or exceeds 5. When the same cycles to failure data was rerun to apply this Chi-Squared test subroutine, all tests resulted in six usable cells thus providing two degrees of freedom.

The operation and accuracy of the computer program were verified by using the same input data used by Lochner (9) in his solution using Weibull paper. Identical estimates were obtained for each parameter to the degree of accuracy obtainable from paper plots. The computer program provided parameter estimates of 5 decimals and used these decimals in subsequent calculations. Accuracy of the D-test subroutine for the Kolmogorov-Smirnov goodness-of-fit test and the Chi-Squared goodness-of-fit test were confirmed by manual (desk calculator) computation of a number of data points. After validation of the program was completed, it was used to reduce the current data.

3.1.3 SUBROUTINE GRAPH

The data reduction programs CYTOFR and WEIBULL have been extended to include the subroutine GRAPH. This subroutine performs the computations which enable the Calcomp plotter to draw a histrogram of the data and to overscribe a curve of the distribution. The distribution parameters are those calculated by the basic program, and the histogram cell width and number of observations are determined by the Chi-Squared test. A comparison of the distribution curve with the corresponding histogram provides a visual measure of whether the normal, lognormal or Weibull distribution is the best model for the data. Copies of subroutine GRAPH are included in the program statements for CYTOFR and WEIBULL in Appendicies C and D.

3.2 WIRE RESEARCH MACHINES

3.2.1 TENSILE DISTRIBUTIONAL PROPERTIES

The results of the static strength data on wires given in Section II are summarized in Table 3.2-1. The static strength data was reduced with the aid of the CDC-6400 program CYTOFR. The normal distribution was used to determine the mean and standard deviation parameters for the ultimate strength, breaking strength, and percent elongation.

3.2.2 CYCLES-TO-FAILURE DISTRIBUTIONAL PROPERTIES

The reduced results of the cycles-to-failure data on wires given in Section II are presented in Tables 3.2-2, 3.2-3, 3.2-4 and 3.2-5, and Figures 3.2-1, 3.2-2, 3.2-3 and 3.2-4, for AISI 1018, 1038, 4130 and 4340 steels.

The Chi-Squared and Kolmogorov-Smirnov goodness-of-fit tests were used to determine the best-fit distribution. Results of the K-S and the Chi-Squared tests are listed in Table 3.2-6, for both wires and rods. The results show that at the 0.05 level of significance, the K-S test, does not reject the Weibull distribution in 22 tests. The Chi-Squared test rejects the Weibull distribution in 7 out of the 22 tests.

The conclusions drawn from the above results are:

1. Based on the K-S test, the Chi-Squared test, the coefficient of skewness, and the coefficient of kurtosis values, the lognormal distribution is considered generally acceptable for cycles-to-failure data.

2. Based solely on the K-S test the Weibull distribution can be assumed to fit cycles-to-failure data and provides an alternate distribution to the log normal (base e) for analyzing cycles-to-failure data.

3. Based on the final Chi-Squared test results, 7 rejections out of 22 tests, the Weibull distribution cannot be considered generally acceptable for cycles-to-failure data consisting of only 35 data points. Therefore, care must be excerised in its application.

Table 3.2-1 The University of Arizona Experimentally Determined Distributional Static Strength Data for Wire.

Group No.	Mat'l AISI Steel	Composition	Diameter	Ultimate Strength Kpsi Mean*	Std.Dev.**	C.V.***	Breaking Strength Kpsi Mean	Std.Dev.	C.V.	Percent Elongation Mean	Std.Dev.	C.V.****	Sample Size
134	4130	C=.29 Si=.23 Mn-.52 Ni=.24 P=.033 Cr=1.0 S=.011 Mo=.21	.040	87	13	.15	78	18	.23	11.6	2.3	.20	35
141	1038	C=.36 Si=.19 Mn=.74 P=.016 S=.02	.040	77	19	.25	64	16	.25	21.1	1.9	.09	35
148	1018	C=.17 Mn=.27 P=.017 S=.026	.040	63	14	.22	49	20	.40	12.6	1.9	.15	35
155	4340	C=.4 Si=.3 Mn=.74 Ni=17.4 P=.01 Cr=.81 S=.011 Mo=.25	.040	106	12	.11	93	21	.22	9.5	.94	.10	35

* Rounded to nearest 1 Kpsi

** Rounded to nearest 0.1 Kpsi

*** Coefficient of variation $= \frac{\sigma_S}{\overline{S}}$

**** Coefficient of variation $= \frac{\sigma_{EL}}{\overline{EL}}$

EL = % elongation

Table 3.2-2 The University of Arizona Experimentally Determined Cycles-to-Failure Parameters for AISI 4340 SteelWire Under Pure Reversed Bending Fatigue Testing Conditions for Design use.

Group No.	Geometry in.	Alternating Stress Level psi	Normal Cycles		Log - Normal $\log_{10}$ cycles		Weibull***		
			Mean*	Std. Dev.**	Mean	Std. Dev.	Beta	Gamma	Eta
150	D = 0.040	73,500	395,000	158,500	12.807	0.410	2.230	69,600	367,757
151	D = 0.040	78,100	292,000	169,600	12.465	0.467	1.123	123,200	175,550
152	D = 0.040	80,100	249,000	130,800	12.309	0.478	0.559	79,899	429,255
153	D = 0.040	84,700	157,000	58,500	11.896	0.388	2.081	39,100	112,594
154	D = 0.040	90,000	150,000	72,200	11.822	0.423	1.231	66,100	90,019

* Rounded to nearest 1,000 cycles
** Rounded to nearest 100 cycles
*** Beta = shape parameter or slope
Gamma = minimum life (cycles)
Eta = scale parameter (cycles)

Table 3.2-3 The University of Arizona Experimentally Determined Cycles-to-Failure Parameters for AISI 4130 Steel Wire Under Pure Reversed Bending Fatigue Testing Conditions for Design use.

Group No	Geometry in.	Alternating Stress Level psi	Normal Cycles		Log - Normal $\log_{10}$ cycles		Weibull***		
			Mean*	Std. Dev.**	Mean	Std. Dev.	Beta	Gamma	Eta
129	D = 0.040	67,700	761,000	392,100	13.408	0.541	1.725	99,000	751,225
130	D = 0.040	70,000	482,000	254,100	12,962	0.502	1.638	101,899	429,637
131	D = 0.040	72,500	277,000	152,200	12.393	0.533	1.134	90,099	201,480
132	D = 0.040	74,700	152,000	59,200	11.876	0.351	1.642	65,399	96, 714
133	D = 0.040	77,800	141,000	64,000	11.761	0.445	1.670	39,100	114,833

* Rounded to nearest 1,000 cycles
** Rounded to nearest 100 cycles
*** Beta = shape parameter or slope
Gamma = minimum life (cycles)
Eta = scale parameter (cycles)

Table 3.2-4 The University of Arizona Experimentally Determined Cycles-to-Failure Parameters for AISI 1038 Steel Wire Under Pure Reversed Bending Fatigue Testing Conditions for Design use.

Group No.	Geometry in.	Alternating Stress Level psi	Normal Cycles		Log - Normal $\log_{10}$ cycles		Weibull***		
			Mean*	Std. Dev.**	Mean	Std. Dev.	Beta	Gamma	Eta
136	D = 0.040	64,500	608,000	352,100	13.168	0.561	1.509	113,600	549,475
137	D = 0.040	67,200	358,000	186,000	12.663	0.510	1.674	70,099	259,921
138	D = 0.040	69,200	236,000	144,200	12.248	0.473	1.328	83,399	163,986
139	D = 0.040	72,300	177,000	77,800	11.994	0.416	1.204	80,100	104,054

* Rounded to nearest 1,000 cycles
** Rounded to nearest 100 cycles
*** Beta = shape parameter or slope
Gamma = minimum life (cycles)
Eta = scale parameter (cycles)

Table 3.2-5 The University of Arizona Experimentally Determined Cycles-to-Failure Parameters for AISI 1018 Steel Wire Under Pure Reversed Bending Fatigue Testing Conditions for Design use.

Group No.	Geometry in.	Alternating Stress Level psi	Normal Cycles		Log - Normal $\log_{10}$ cycles		Weibull***		
			Mean*	Std. Dev.**	Mean	Std. Dev.	Beta	Gamma	Eta
143	D = 0.040	57,200	682,000	427,000	13.246	0.631	1.415	98,999	645,345
144	D = 0.040	60,000	560,000	251,000	13.151	0.409	1.303	238,999	353,483
145	D = 0.040	62,800	322,000	150,000	12.579	0.455	1.111	135,499	199,268

* Rounded to nearest 1,000 cycles
** Rounded to nearest 100 cycles
*** Beta = shape parameter or slope
Gamma = minimum life (cycles)
Eta = scale parameter (cycles)

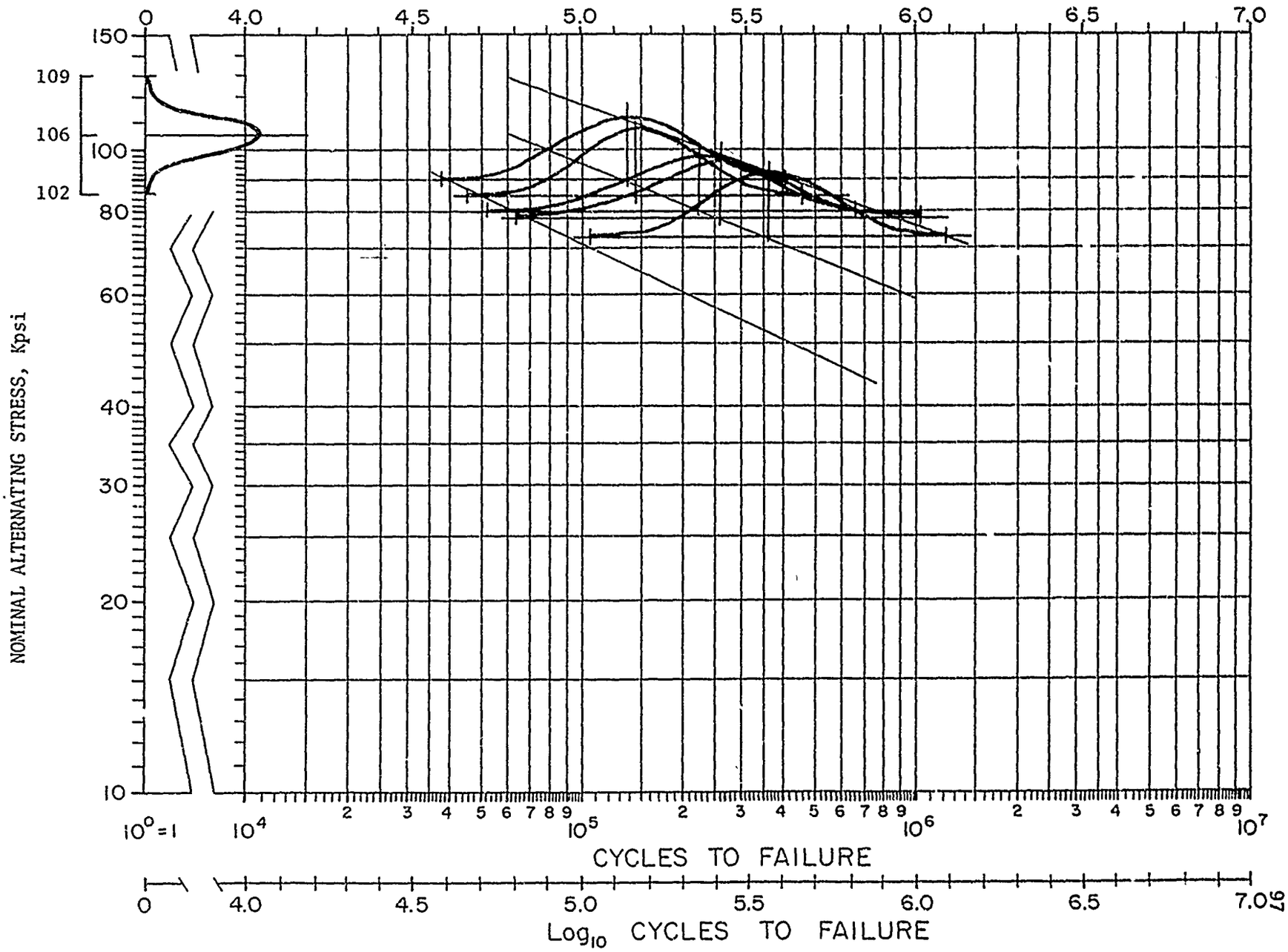

Fig. 3.2-1 Statistical S-N Surface for 35 specimen; D = 0.040 in., AISI 4340 steel wire for results summarized in Tables 3.2-1 and 3.2-2.

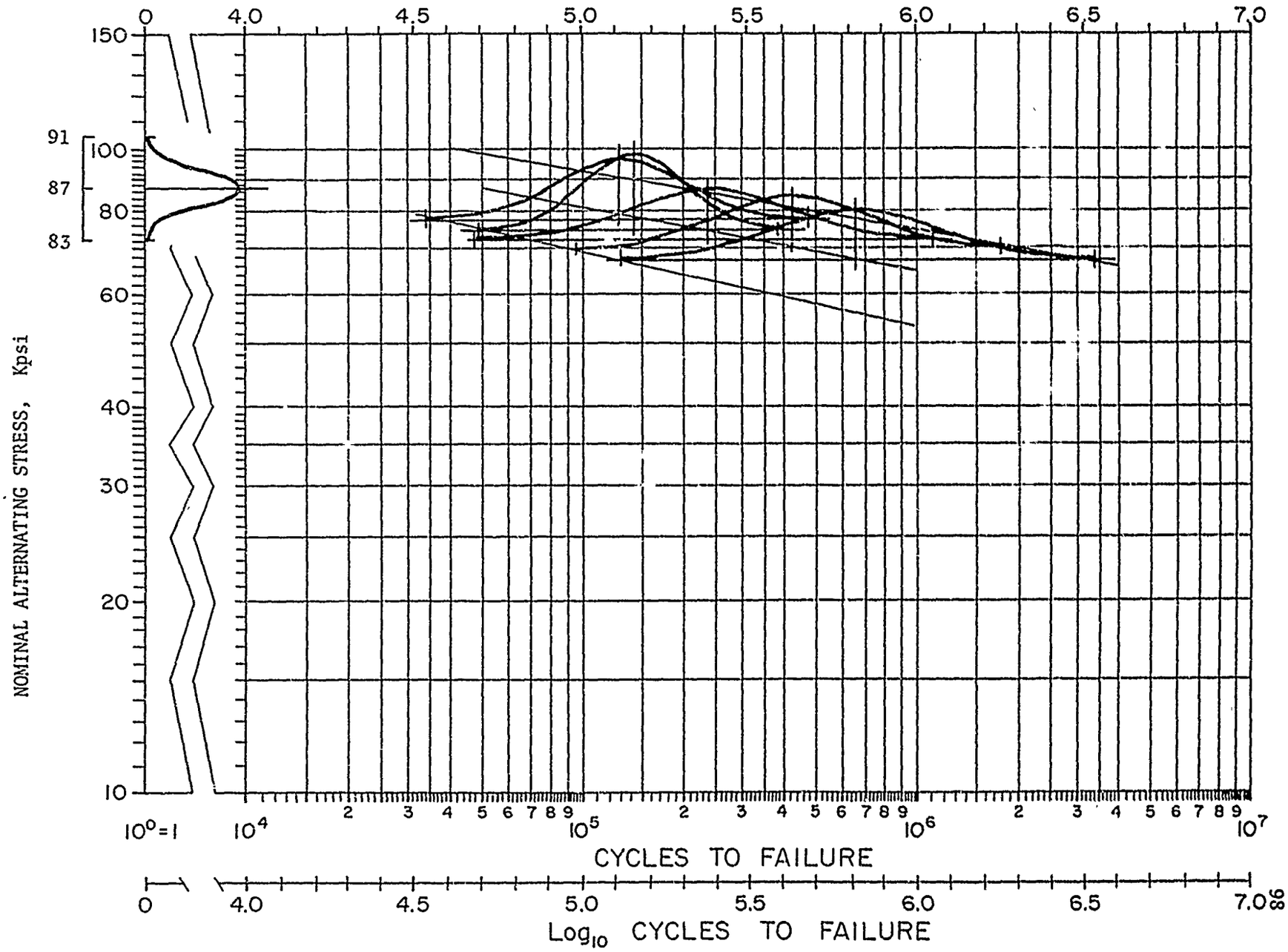

Fig. 3.2-2 Statistical S-N surface for 35 specimens; D = 0.040 in., AISI 4130 steel wire for results summarized in Tables 3.2-1 and 3.2-3.

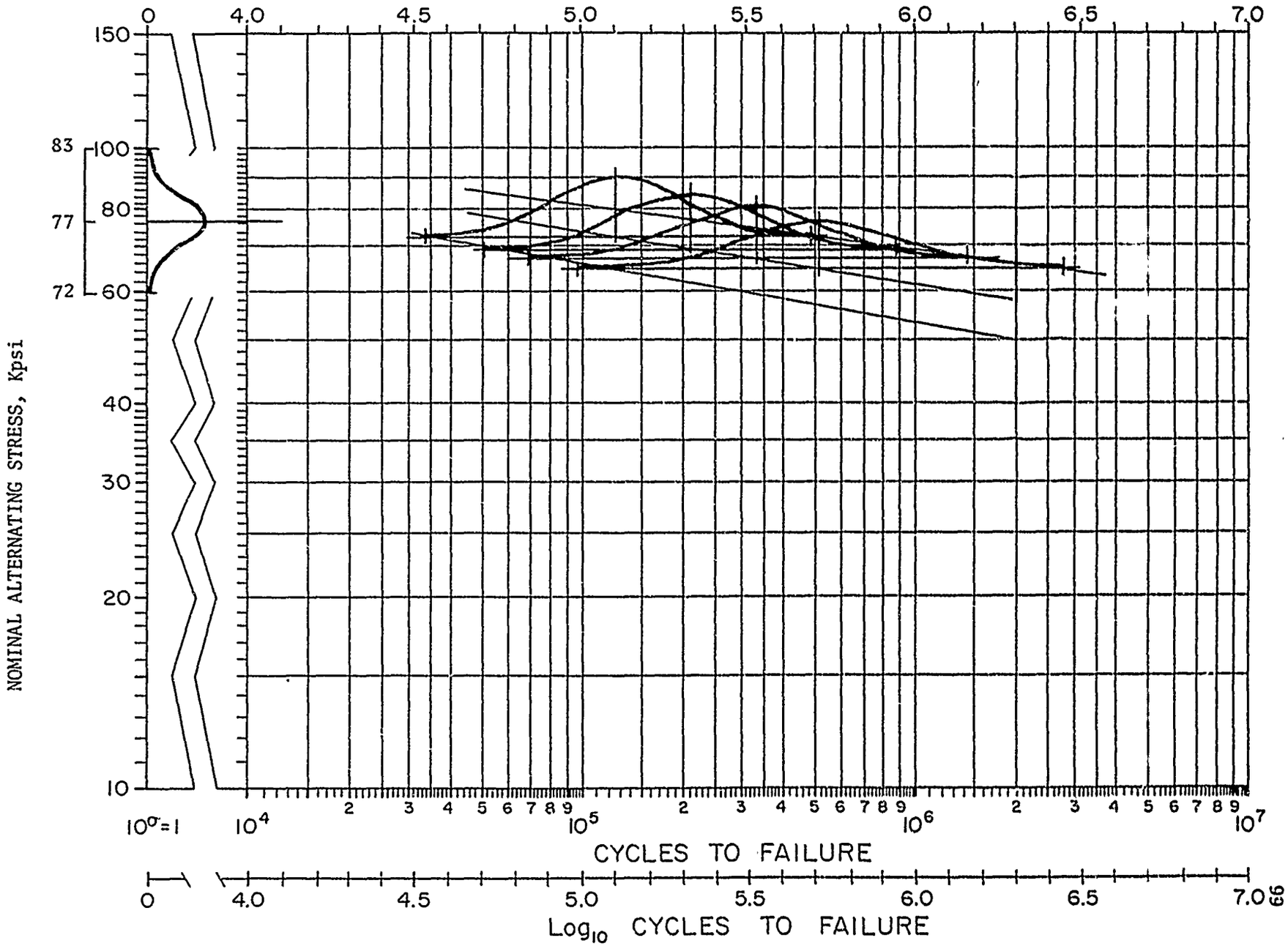

Fig. 3.2-3 Statistical S-N Surface for 35 specimen; D = 0.040 in., AISI 1038 steel wire for results summarized in Tables 3.2-1 and 3.2-4.

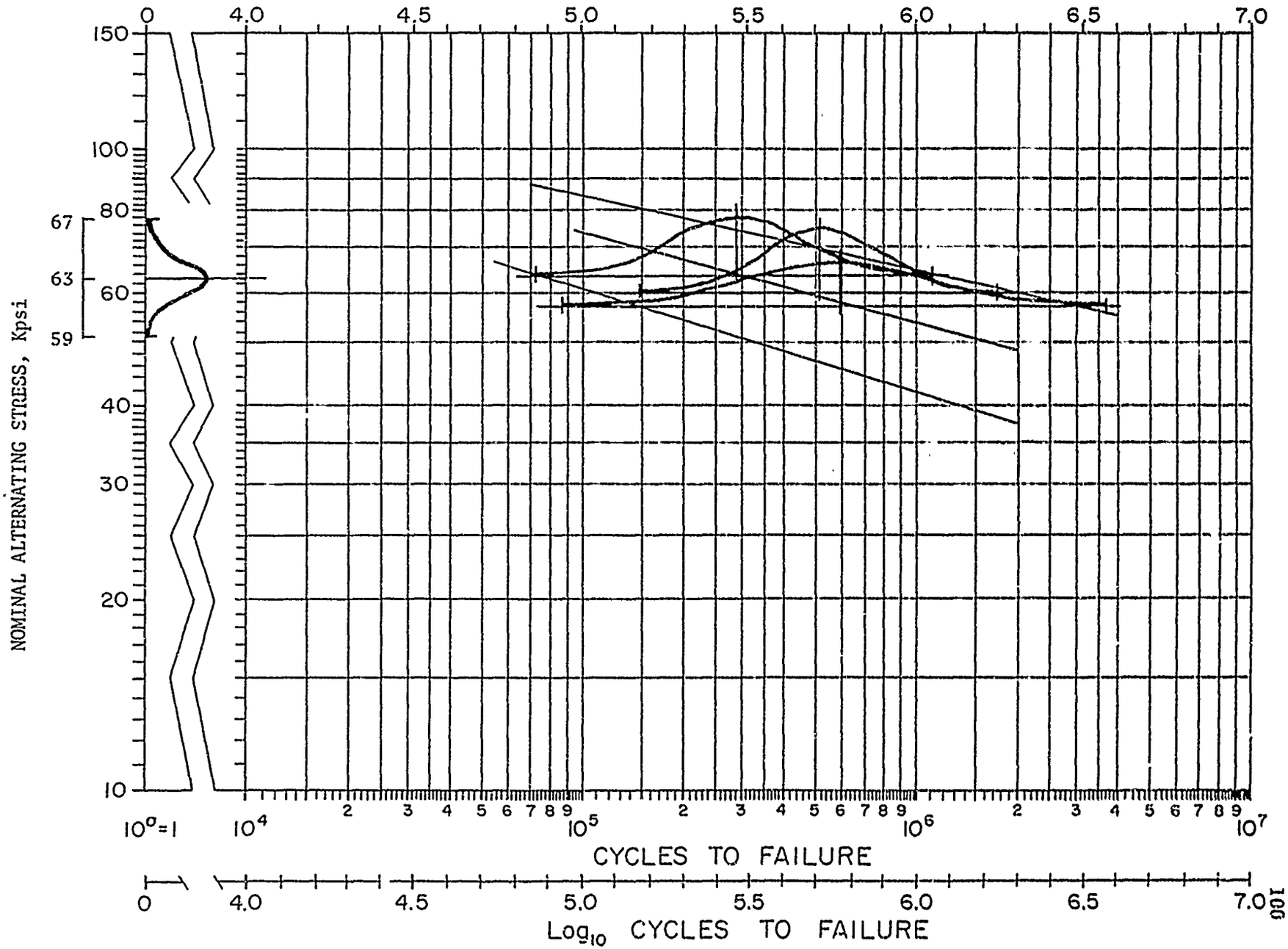

Fig. 3.2-4 Statistical S-N Surface for 35 Specimen; D = 0.040 in., AISI 1018 steel wire for results summarized in Tables 3.2-1 and 3.2-5.

Table 3.2-6 K-S and Chi-Squared test results for Weibull distribution.

Material AISI Steel	Stress Level psi	Maximum D Value (K-S)	dof	Chi-Squared Value
Wire D = 0.040 Stress Ratio = ∞				
4130	67,700	0.078	2	2.127
4130	70,000	0.124	2	8.102
4130	72,500	0.066	2	3.674
4130	74,700	0.114	2	4.097
4130	77,800	0.112	3	3.390
1038	64,500	0.102	2	3.708
1038	67,200	0.141	2	6.307
1038	69,200	0.167	3	4.245
1038	72,300	0.097	3	3.863
1018	57,200	0.114	2	3.724
1018	60,000	0.107	2	4.116
1018	62,800	0.064	1	2.546
4340	73,500	0.134	3	3.075
4340	78,100	0.106	3	4.993
4340	80,100	0.328	3	69.373
4340	84,700	0.059	3	1.227
4340	90,000	0.102	2	7.581
Rod r = 0.125 D = 0.375	d = 0.0937 Stress Ratio = ∞			
4130	75,000	.106	3	4.389
4130	85,000	.107	2	8.507
4130	95,000	.120	2	1.950
Rod r = 0.250 D = 0.375	d = 0.0937 Stress Ratio = ∞			
4130	70,000	.114	2	6.484
4130	80,000	.090	1	4.731
4130	90,000	.085	1	0.751

Critical Value at .05 Level of Significance:

K-S D Value 0.224.

Chi-Squared, 1 dof 3.841.

Chi-Squared, 2 dof 5.991.

Chi-Squared, 2 dof 7.815.

3.2.3 STAIRCASE TEST AND DISTRIBUTIONAL PROPERTIES

The staircase fatigue tests of 0.040 in. dia. wire for steels of AISI 4130, 4340, 1038 and 1018 are being run and shall be reported in ONR VI with completed S-N diagrams.

Knowing that the objective of staircase fatigue testing is to determine the mean and the standard deviation of the stress to failure for various metals with various geometries, a standard procedure for obtaining this information was established and appears next.

HOW MANY SPECIMENS TO RUN?

In determining the number of test specimens to use one must account for the (1) cost, (2) time and (3) the sufficiency of the sample size to draw significant conclusions from the results.

Since, staircase testing is concentrated near the mean fatigue strength the number of specimens tested may be less than for the "Probit" method [10, p. 12], which gives results for a wider range of stress values. In general it is recommended that at least 30 specimens be tested [10, p.13]. Thirty specimens also correspond to the minimum number of specimens needed for determining 95 percent confidence intervals for a population standard deviation, σ. For the data collected through staircase testing to be meaningful it is recommended that at least 35 specimens be tested.

HOW TO SELECT THE NUMBER OF CYCLES A SPECIMEN SHOULD RUN.

The number of cycles to run is determined by the cycles of life for which the stress-to-failure distribution is needed. For the endurance stress-to-failure (strength) distribution it must be insured that the specimen life chosen is beyond the knee of the S-N diagram. It has been found that normally the knee of the S-N curve will occur between 10^6 and 10^7 cycles for steel specimens. It is recommended here that the specimens be tested for 3×10^6 cycles or to failure whichever occurs first. Once the specimen has reached 3×10^6 cycles without failure the testing of that particular specimen should be terminated, and a fresh specimen be tested at one stress increment higher.

HOW TO DETERMINE THE INITIAL STRESS LEVEL FOR UNGROOVED SPECIMENS.

When initiating a staircase fatigue test it is desirable to begin the test at or near the mean endurance strength of the material under investigation. It has been determined experimentally that a good estimate for the beginning stress level of a staircase test is 0.54 of the material's ultimate strength. Therefore, when initiating a fatigue staircase test of ungrooved specimens the following initial stress level is recommended:

$$S_{st} = 0.54\ S_{Ultimate}\ . \qquad (3.2\text{-}1)$$

HOW TO DETERMINE THE INITIAL STRESS LEVEL FOR GROOVED SPECIMENS.

When fatigue testing grooved steel specimens the fatigue stress concentration due to the presence of the groove must be taken into account. To do this a factor, K_f, known as the fatigue stress concentration factor must be taken into account. A summary of estimated fatigue stress concentration factors is given in Chapter 2.2.1. Once the K_f value for the groove configuration has been determined the following relationship is recommended for the starting stress of a staircase test involving grooved specimens:

$$S_{st} = \frac{0.54\ S_{Ultimate}}{K_f}\ . \qquad (3.2\text{-}2)$$

HOW TO DETERMINE STRESS STEPS.

When conducting the staircase endurance tests on the modified Wiedemann and the unmodified Wiedemann research machines it is suggested that stress increments of 2,000 psi be used. The reason for this is that stress levels of less than 2,000 psi are extremely difficult to obtain due to the fact that only about 0.05 pounds of pan weight is required to change the stress level by 1,000 psi. Therefore, it is recommended that stress increments of 2,000 psi be used.

For the wire fatigue research machines the stress increment is determined from the calibration curve by selecting the change in stress level corresponding to 0.5° change in bend angle. While this procedure results in different stress increments for different test groups, it provides

for greater consistency in setting the bend angle carriage. The calibration curve is quite linear over the endurance range; therefore, use of a 0.5 degree change in bend angle results in linear stress increments.

HOW TO DETERMINE THE STRESS LEVEL TO USE FOR THE SECOND AND SUBSEQUENT SPECIMENS.

If the first test specimen fails before 3×10^6 cycles then a second test specimen should be tested at a stress level 2,000 psi below the first stress level. If the first test specimen survives to 3×10^6 cycles the second specimen should be tested at a stress level 2,000 psi higher than the first stress level, as shown in Fig. 3.2-5 . This procedure should be followed for all subsequent specimens tested.

WHEN TO TERMINATE A STAIRCASE TEST AND WHICH DATA TO USE.

In staircase testing the first few specimens are not included in the test if no change of mode (from failure to success or vice versa) occurs. The test is considered to have started with the specimen prior to the one where the first change of mode occurs. Only about half of the test results are used in computing the mean and standard deviation of the strength distribution. Either the successes or the failures are used, whichever are the fewer. Therefore, 33 specimens should be tested after the first mode change occurs. Thus, the staircase test may be terminated when 33 specimens have been tested after the initial mode change has occurred for a total of 35 good specimens.

HOW TO PLOT THE STAIRCASE DATA.

Standard forms have been developed for plotting staircase test data. On the ordinate of the form should appear the nominal stress level in Kpsi, and on the abscissa the number of specimens tested. To plot the data a legend of black dots and white dots are used. A black dot signifies that the test specimen failed prior to 3×10^6 cycles and a white dot signifies that the specimen survived to 3×10^6 cycles. All data should then be plotted accordingly, as shown in Fig. 3.2-5. .

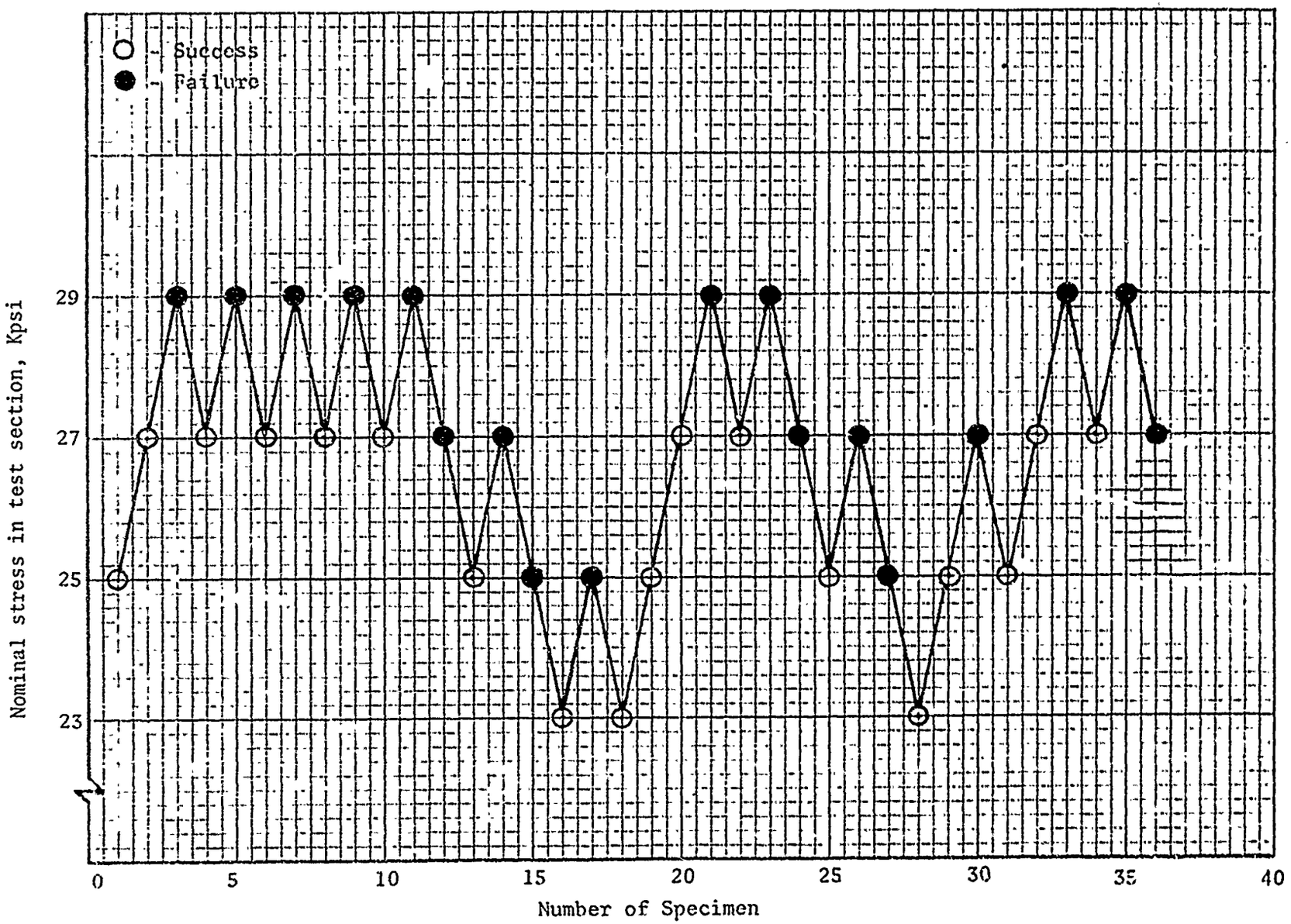

Fig. 3.2-5 Staircase test results obtained with the Wiedemann machine for AISI 1038 steel, d = 0.2700 in., r = 0.062 in., and 3 x 10^6 cycles of life (Group No. 163).

HOW TO CALCULATE THE STRESS-TO-FAILURE DISTRIBUTION'S MEAN AND STANTARD DEVIATION ASSUMING A NORMAL DISTRIBUTION.

The equations given here assume that the strength distribution is normal. Some distributions can be made normal by simple transforms, such as the lognormal. If the data can be assumed normal or transformed to normal, the statistical analysis of the data is as follows [11 , p. 114]:

The estimate for the mean strength is given by

$$\overline{X} = X_o + d\,[A/N \pm 1/2], \qquad (3.2\text{-}3)$$

where $\overline{X}$ = the estimate of mean strength, psi.

X_o = the lowest stress level used, psi.
(If the fewer events are the successes then the lowest stress level used is the lowest level of the staircase plot. In Fig. 3.2-5 this level is the 23,000 psi level. If the fewer events are the failures then the lowest stress level used is the lowest level in the staircase plot where failures have occurred. In Fig. 3.2-5 this level is the 25,000 psi level.

d = the stress increment, psi.
(Normally use 2,000 psi.)

N = total number of successes or failures whichever are the fewer in number.

The quantity, A, in Eq.(3.2-3) is defined as

$$A = \sum_{i=o}^{H} i n_i . \qquad (3.2\text{-}4)$$

In Eq.(3.2-4) "i" is the numerical order number of each stress level with the lowest stress level used in the calculations having i = o, the next stress level having i = 1, etc., and n_i is the number of failures or successes, whichever has been chosen as the basis for the calculations, occurring at each of the "i" stress levels. For an example of the calculations see Table 3.2-7 . H is the order number of the highest stress level used.

Table 3.2-7 Reduced Data for Group 163, AISI 1038 Steel. Wiedemann Fatigue Machine.

Staircase method at 3×10^6 cycles

Number of Useful Specimens: 35

Specimen geometry: D = 0.375 in.
d = 0.2700 in.
r = 0.062 in.

Alternating Stress psi	i	n_i Successes	in_i	i^2n_i
27,000	2	9	18	36
25,000	1	5	5	5
23,000	0	3	0	0
		N = 17	A = 23	B = 41

d = stress increment = 2,000 psi

X_o = lowest stress level = 23,000 psi

$\overline{X}$ = mean (estimate)

$\overline{X} = X_o + d\ A/N + 1/2 = 23{,}000 + 2{,}000 \left[\frac{23}{17} + \frac{1}{2}\right]$

$\overline{X}$ = 26,706 psi

s = standard deviation (estimate)

$s = 1.620\ d\ (NB-A^2)/N^2 + 0.029 = 1.620(2{,}000) \left[\frac{(17 \times 41 - 23^2)}{17^2} + 0.029\right]$

s = 1,976 psi

In Eq. (3.2-3) the positive (+) sign before the one-half (1/2) is used if the less frequent events are the successes, and the negative (-) sign if the failures are the less frequent.

The estimate of the standard deviation of the strength distribution is given by

$$S = 1.620\ d\ [(NB - A^2)/N^2 + 0.029], \qquad (3.2\text{-}5)$$

where S = standard deviation estimate, psi.

The dimensionless quantity B is defined as follows:

$$B = \sum_{i=o}^{H} i^2\ n_i. \qquad (3.2\text{-}6)$$

For an example of how to apply Eqs. (3.2-5) and (3.2-6) see Table 3.2-7 and Fig. 3.2-5.

See Appendix E for a PDP-8 Focal computer program to calculate $\bar{x}$ and S for the staircase test.

RECOMMENDATIONS

1. It is recommended that at least 35 specimens be tested when conducting staircase tests.

2. It is recommended that 3×10^6 cycles be used as the cut-off point when conducting staircase endurance tests.

3. When determining the starting stress level for ungrooved specimens use the following relationship:

$$S_{st} = 0.54\ S_{Ultimate}. \qquad (3.2\text{-}1)$$

4. When determing the starting stress level for grooved specimens use the following relationship:

$$S_{st} = \frac{0.54\ S_{Ultimate}}{K_f}. \qquad (3.2\text{-}2)$$

5. Stress increments of 2,000 psi are recommended when conducting staircase tests.

6. It is recommended that a staircase test not be terminated until 33 specimens have been tested after the first mode change has occurred, for a total of 35 useful specimens.

7. If when reducing the data the failures are being used the lowest stress level should be excluded from the calculations.

8. If when reducing the data the successes are being used the highest stress level should be excluded from the calculations.

9. When reducing the data the basis of the calculations should be the <u>less frequent event</u>; i.e., if there are fewer failures than successes then the failures should be used, if there are fewer successes than failures then the successes should be used.

10. It is recommended that the following relationship be used to calculate the mean of the strength distribution:

$$\overline{X} = X_o + d\ (A/N \pm 1/2)\ . \qquad (3.2\text{-}3)$$

11. It is recommended that the following relationship be used to calculate the standard deviation of the strength distribution:

$$S = 1.620\ d\ [(NB - A^2)\ /\ N^2 + 0.029]\ . \qquad (3.2\text{-}5)$$

3.3 WIEDEMANN RESEARCH MACHINES

3.3.1 TENSILE DISTRIBUTIONAL PROPERTIES

Table 3.3-1 presents the experimental data generated to determine the distributional static strength data for ungrooved steel rod under the ONR Contract. Listed in the table are the type of material tested, the geometry, the composition, sample size, yield strength, ultimate strength, breaking strength, percent elongation and their parameters.

3.3.2 CYCLES-TO-FAILURE DISTRIBUTIONAL PROPERTIES

Figures 3.3-1 and 3.3-2 present two S-N diagrams generated for AISI 4130 grooved steel rod in reversed bending for r = 0.250" and r = 0.125", respectively. The experimental data for these figures are given in Tables 3.3-2 and 3.3-3, respectively. Listed in each table are the type of material tested, the geometry, and the normal and lognormal distribution parameters of the cycles-to-failure data at various alternating stress levels. These tables provide a quick means for obtaining the mean and standard deviation of the cycles-to-failure distribution at various alternating stress levels. The S-N diagrams appearing in Figs. 3.3-1 and 3.3-2 contain the mean line of the cycles-to-failure distributions and the $\pm 3\sigma$ envelopes using the lognormal distribution as the one best representing the cycles-to-failure data at various stress levels.

3.3.3 STAIRCASE TEST AND DISTRIBUTIONAL PROPERTIES

Table 3.3-4 presents the experimental data generated to determine the distributional parameters for staircase testing of AISI 1038 steel rod under pure reversed bending. Listed in the table are the group number, geometry, number of useful specimens, and the mean and standard deviation of the endurance strength distribution for 3×10^6 cycles of life.

Table 3.3-1 The University of Arizona experimentally determined distributional static strength data for ungrooved steel rod.

	AISI 4130 Steel		AISI 4340 Steel	AISI 1038 Steel
Composition	.305C .53Mn .012P .011Su .22Mo .275I .98Cr .15Ni .16Cu		.385C .72Mn .009P .011Su .28Si .78Cr .175Ni .26Mo	.39C .80Mn .018Su .013P
Diameter in.	.250		.270	.250
Yield Strength Kpsi	Mean*	87		
	Std.Dev.**	2.0		
	C. V.***	.023		
Ultimate Strength Kpsi	Mean	106	116	69
	Std.Dev.	2.3	1.3	1.3
	C. V.	.020	.011	.019
Breaking Strength Kpsi	Mean	152		158
	Std.Dev.	4.9		6.4
	C. V.	.032		.040
Percent Elongation	Mean	8.5		20.9
	Std.Dev.	0.9		2.3
	C.V.****	0.10		0.11
Sample Size	35		35	35
Source	4, pp. 471,473,475		2. p. 205	4, p. 488

* Rounded to nearest 1 Kpsi

** Rounded to nearest 0.1 Kpsi

*** Coefficient of variation $= \dfrac{\sigma_S}{\overline{S}}$

**** Coefficient of variation $= \dfrac{\sigma_{EL}}{\overline{EL}}$

EL = % Elongation

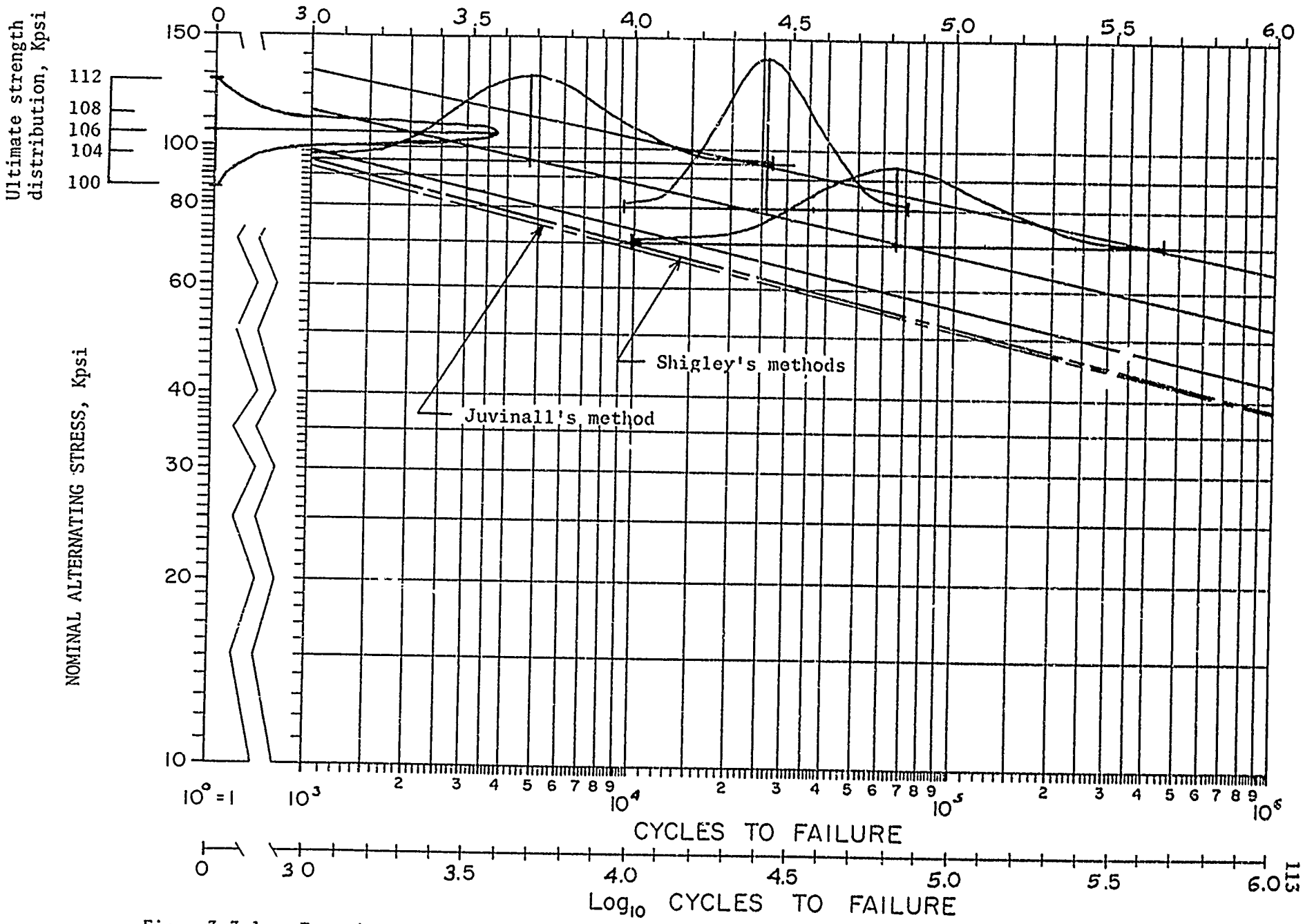

Fig. 3.3-1 Experimentally determined S-N diagram using ONR research results for AISI 4130 steel rod in reversed bending, D = 0.0375, d = 0.0937", and r = 0.250".

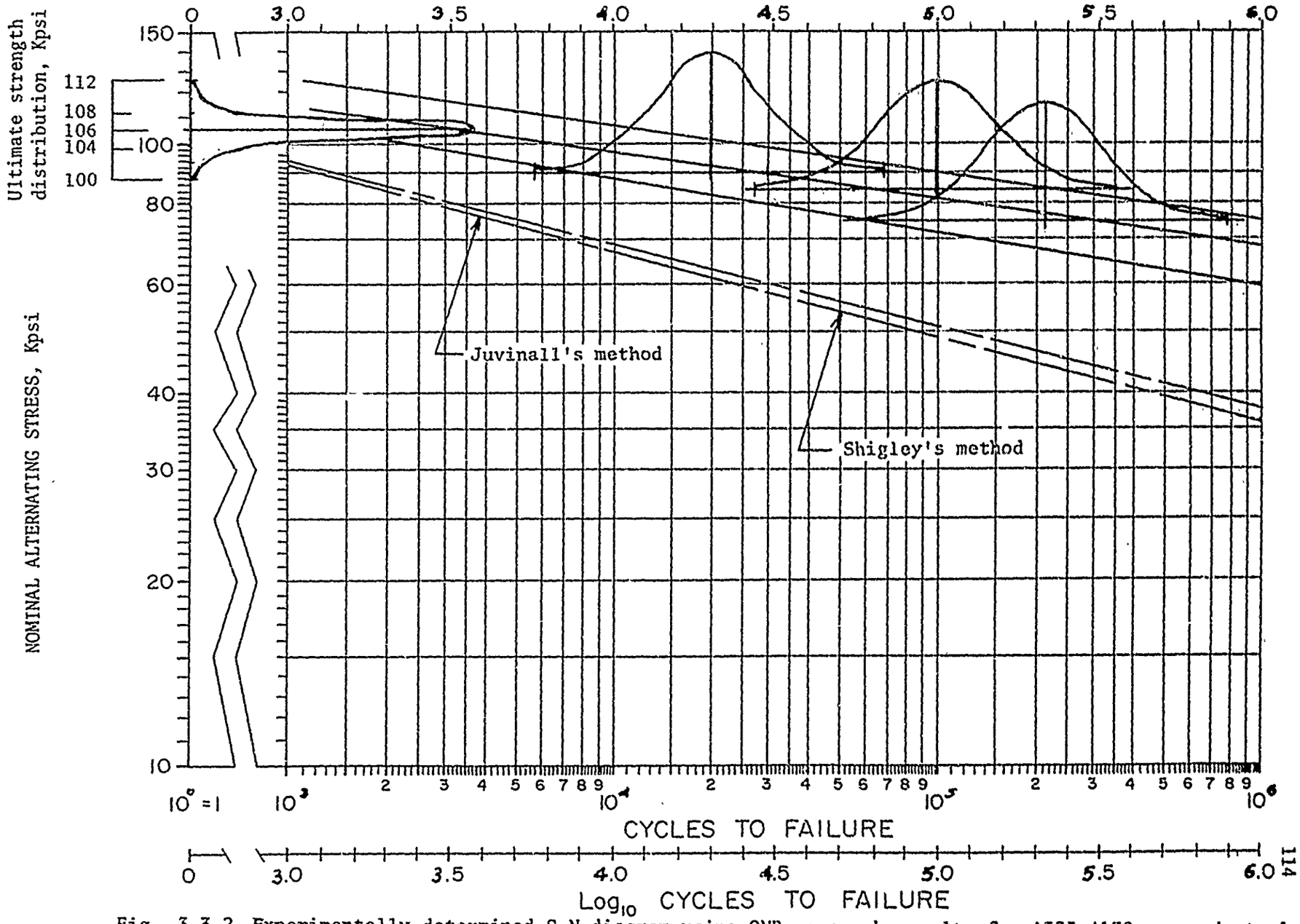

Fig. 3.3-2 Experimentally determined S-N diagram using ONR research results for AISI 4130 grooved steel rod in reversed bending, D = 0.375", d = 0.0937" and r = 0.125".

Table 3.3-2 The University of Arizona Experimentally Determined Cycles-to-Failure Parameters for AISI 4130 Steel Rod Under Pure Reversed Bending Fatigue Testing Conditions for Design use.

Group No.	Geometry in.	Alternating Stress Level psi	Normal Cycles		Log - Normal $\log_{10}$ cycles		Weibull***		
			Mean*	Std. Dev.**	Mean	Std. Dev.	Beta	Gamma	Eta
1	r = 0.250 d = 0.0937 D = 0.375	65,000	161,000	99,700	5.21	0.247			
2	r = 0.250 d = 0.0937 D = 0.375	70,000	65,000	71,600	4.81	0.277			
3	r = 0.250 d = 0.0937 D = 0.375	75,000	40,000	23,700	4.60	0.238			
4	r = 0.250 d = 0.0937 D = 0.375	80,000	26,000	10,600	4.41	0.150			
5	r = 0.250 d = 0.0937 D = 0.375	85,000	14,000	7,900	4.14	0.230			
6	r = 0.250 d = 0.0937 D = 0.375	90,000	8,000	4,600	3.93	0.227			
7	r = 0.250 d = 0.0937 D = 0.375	95,000	5,000	4,500	3.68	0.254			

* Rounded to nearest 1,000 cycles
** Rounded to nearest 100 cycles
*** Beta = shape parameter or slope
Gamma = minimum life (cycles)
Eta = scale parameter (cycles)

Table 3.3-3 The University of Arizona Experimentally Determined Cycles-to-Failure Parameters for AISI 4130 Steel Rod Under Pure Reversed Bending Fatigue Testing Conditions for Design use.

Group No.	Geometry in.	Alternating Stress Level psi	Normal Cycles		Log - Normal $\log_{10}$ cycles		Weibull***		
			Mean*	Std. Dev.**	Mean	Std. Dev.	Beta	Gamma	Eta
1	r = 0.125 d = 0.0937 D = 0.375	70,000	700,000	418,000	5.83	0.240			
2	r = 0.125 d = 0.0937 D = 0.375	75,000	208,000	118,200	5.32	0.188			
3	r = 0.125 d = 0.0937 D = 0.375	80,000	124,000	90,000	5.10	0.198			
4	r = 0.125 d = 0.0937 D = 0.375	85,000	95,000	62,200	4.98	0.206			
5	r = 0.125 d = 0.0937 D = 0.375	90,000	20,000	10,800	4.29	0.185			
6	r = 0.125 d = 0.0937 D = 0.375	95,000	14,000	5,800	4.16	0.173			
7	r = 0.125 d = 0.0937 D = 0.375	100,000	6,200	800	3.79	0.165			

* Rounded to nearest 1,000 cycles
** Rounded to nearest 100 cycles
*** Beta = shape parameter or slope
Gamma = minimum life (cycles)
Eta = scale parameter (cycles)

Table 3.3-4 The University of Arizona experimentally determined staircase parameters for AISI 1038 Steel rod under pure reversed bending, fatigue testing conditions for 3×10^6 cycles of life.

Group No.	Geometry in.	Number of Useful Specimens	Stress (psi) Mean*	Stress (psi) Std. Dev.*
162	r = .031 d = .2700 D = .375	33	23,800	400
163	r = .062 d = .2700 D = .375	36	26,700	2,000
164	r = .125 d = .2700 D = .375	37	30,444	1,500
165	r = .250 d = .2700 D = .375	35	32,200	1,200
166	r = 1.87 d = .2700 D = .375	36	37,100	2,100

* Rounded off to nearest 100 psi.

3.3.4 METHODOLOGY FOR CONSTRUCTING S-N DIAGRAMS EMPIRICALLY FROM STATIC ULTIMATE AND ENDURANCE STRENGTH DATA FOR GROOVED AND UNGROOVED SPECIMENS.

One of the objectives of fatigue research is to obtain expressions to estimate the life of a machine part, manufactured from a given material and subjected to cyclic loading.

The fatigue strength of a material may be defined as the maximum stress that can be applied repeatedly to the material without causing failure in less than a certain finite number of cycles. The endurance strength is the maximum stress that can be applied repeatedly to a material for a large number of cycles (beyond the knee of the S-N diagram or for 10^6 cycles or more for steels) without causing failure. The relationship between the magnitude of repeatedly applied stress and the number of cycles to failure is conventionally presented in the graphical form known as the S-N diagram [12,pp. 1-2].

Empirical results have shown that fatigue life is an exponential function of the maximum level of repeated stress. Other empirical relations developed for strain-cycle fatigue show that cyclic life is also related to the applied strain range exponentially. Therefore, S-N diagrams are usually presented in semi-log or log-log form [12,p.2]; however, the log-log form is the most prefered.

As the fatigue properties of a material are determined by a variety of factors, the shape of the S-N curve varies according to the conditions represented. Factors influencing the shape of the S-N curve are the type of loading, temperature, operating environment, surface finish, stress concentration and size effects. In this discussion machine parts subjected to fully-reversed bending stresses are investigated.

TYPE OF DESIGN DATA NEEDED FOR CONSTRUCTING THE S-N DIAGRAM

There are a number of suggested methods for constructing S-N diagrams, the most accurate being that based on experimental results. However, this is also the most costly and time consuming. The ultimate goal here is to develop a method for empirically constructing acceptable S-N diagrams from minimum and easily obtainable data, thereby saving both time and money.

The experimentally determined S-N diagram is based upon much testing. The static ultimate tensile strength for both grooved and ungrooved specimens must be established, as well as the endurance strength. Then at intermediate stress levels between the static ultimate and the endurance strength, the cycles-to-failure or stress-to-failure distributions must be generated. This requires over 200 specimens and extensive testing time. Therefore, it is highly desirable to establish empirical relationships to give good estimates of the S-N diagrams based on a minimun amount of data.

Most available empirical methods for constructing the S-N diagram use the ungrooved static ultimate tensile strength and make certain modifications to estimate the endurance strength. This requires the determination of the static ultimate tensile strength and certain modifications to estimate the endurance strength. This requires the determination of the static ultimate tensile strength of ungrooved specimens only, and modifying factors. However, there is one major pitfall involved in this. Preliminary test data generated by ONR research, indicates that the static ultimate tensile strength of grooved specimens is substantially greater than the static ultimate tensile strength of ungrooved specimens. Thus using ultimate strength data of ungrooved specimens to construct an S-N diagram for grooved specimens tends to yield very conservative results at the low-cycle end of of the S-N diagram. A full test plan for investigating the effects of using grooved ultimate tensile strength in constructing S-N diagrams is now being planned.

EMPIRICAL PROCEDURE FOR CONSTRUCTING S-N DIAGRAMS FOR UNGROOVED SPECIMENS

The method for constructing the S-N diagram for ungrooved specimens is considerably simpler than for grooved specimens. Shigley [6, pp. 160-191] and Juvinall [7, pp. 210-224] recommend identical methods. In the absence of specific endurance strength data they both recommend that the endurance strength be estimated as [6, p.162], [7, p. 211]

$$S_e = 0.5\, S_u, \qquad (3.3\text{-}1)$$

where

S_e = estimated endurance strength, psi.

S_u = ungrooved static ultimate tensile strength, psi.

To estimate the stress level at 10^3 cycles on the S-N diagrams both Shigley [6, p. 163] and Juvinall [7, p. 211] recommend the following rule of thumb:

$$S_{10^3 \text{ cycles}} = 0.9 \; S_u, \tag{3.3-2}$$

where

$S_{10^3 \text{ cycles}}$ = alternating stress at 10^3 cycles, psi.

PUBLISHED METHODOLOGIES FOR CONSTRUCTING S-N DIAGRAMS FOR GROOVED SPECIMENS

One published method for constructing S-N diagrams is that recommended by Shigley [6, pp. 161-199]. Shigley states the following [6, pp. 161-162]:

> "Great numbers of rotating beam tests have shown that the endurance limit varies from 40 to 60 percent of the ultimate tensile strength for steels with an ultimate strength up to 200,000 psi. It has become a more or less standard practice, when the results of tests are not available, to estimate the endurance limit for steels as
>
> $$S_e' = 0.5 \; S_u \quad \text{for } S_u \leq 200{,}000 \text{ psi},$$
>
> and
>
> $$S_e' = 100{,}000 \text{ psi for } S_u > 200{,}000 \text{ psi}." \tag{3.3-3}$$

Shigley then suggests modification of Eq. (3.3-1) to consider the effects of surface finish, size and stress concentration [6, p. 166]. The modified relationship is

$$S_e = k_a \, k_b \, k_e \, (0.5 \; S_u), \tag{3.3-4}$$

where

S_e = corrected endurance limit, psi

k_a = surface factor

k_b = size factor

k_e = modifying factor for stress concentration (This is not the same as the stress concentration factor, K_t).

Shigley discusses the effects of surface finish on fatigue life and presents Fig. 3.3-3 for obtaining the surface factor, k_a, for steels when the tensile strength and the surface finish are specified. The surface factor for wrought and cast aluminum, magnesium and other non-ferrous materials may be taken as unity, because the endurance limits listed by the manufacturers of these materials usually include the effect of surface finish [6, pp. 166-167].

It is clear, however, that the surface finish, at least for steel parts, has a significant effect on the endurance limit. Fig. 3.3-3 shows that the endurance limits for hot-rolled and as-forged parts improve very little with increase in tensile strength. It also shows that, when fatigue loading is an important design factor, there is little to be gained, even with a ground finish, by selecting steels having tensile strengths greater than 200,000 psi [6, p. 166].

The standard rotating beam test gives the endurance limit for a specimen of 0.30 in. in diameter at the test section. When specimens of larger diameter are tested subjected to completely reversed stress in bending or torsion, it is found that the endurance strength is 10 to 15 percent lower for specimens up to 2 in. in diameter [6, p. 168]. Therefore, Shigley suggests a size factor, k_b, of 0.85 for specimens with a diameter greater than 0.30 in. subjected to reversed bending or torsional stresses. No reduction was found for completely reversed axial loading; consequently $k_b = 1.0$ for axial loads [6, p. 168]. Shigley then suggests that for machine elements larger than 2 in. in diameter, adjustments somewhat larger than 10 percent be made to the endurance strength but specific values are not given.

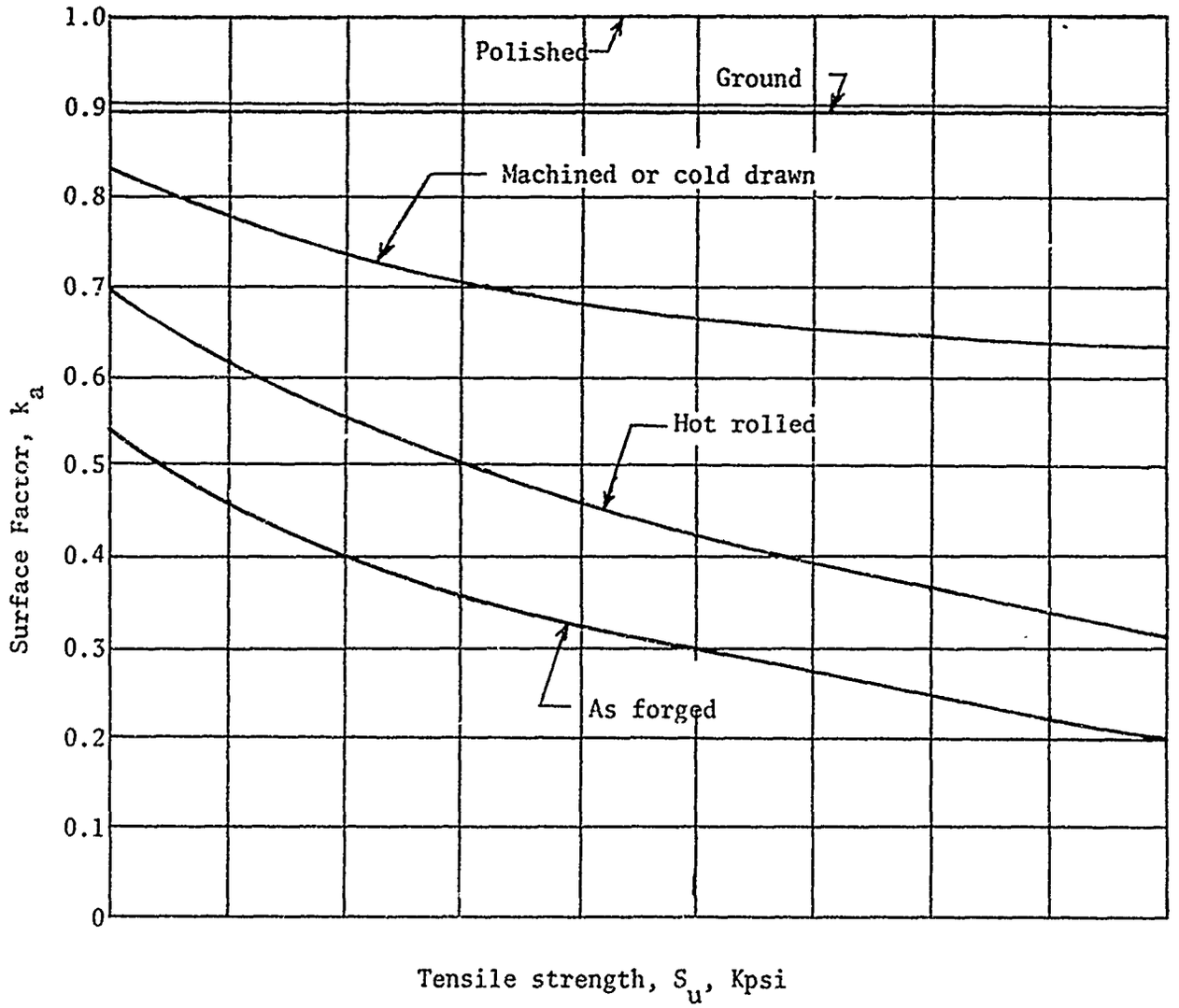

Fig. 3.3-3 Modifying factors for surface finish for steels [6 , Fig. 5.26 , p. 167].

As a fatigue failure almost always originates at a discontinuity the effect of stress concentration should be brought in. Usually the crack begins at a groove, a notch, a shoulder or at the edge of a hole, but it may also start at a tool mark, a scratch or even at an inspection mark. In the investigation of fatigue failures it is found that some materials are much more sensitive to notches than others. This means that the stresses for insensitive materials need not be increased by the full amount of the geometric stress concentration factor, K_t. For this reason it is useful to define a fatigue stress-concentration factor, K_f, as follows [6, p. 170]:

$$K_f = \frac{\text{Endurance limit of ungrooved specimes}}{\text{Endurance limit of grooved specimens}} . \qquad (3.3\text{-}5)$$

Shigley then denotes k_e as a fatigue-strength reduction factor and defines this modifying factor for fatigue stress-concentration as

$$k_e = \frac{1}{K_f} . \qquad (3.3\text{-}6)$$

In order to account for the various sensitivities of materials to notches a factor, q, known as notch sensitivity is introduced as

$$q = \frac{K_f - 1}{K_t - 1} , \qquad (3.3\text{-}7)$$

where q is between zero and unity. Equation (3.3-7) shows that if $q = 0$, $K_f = 1$ and the material has no sensitivity to notches at all. On the other hand, if $q = 1$, then $K_f = K_t$ and the material has full notch sensitivity. In analysis for design work one first determines K_t from the geometry of the part. Then, the material having been specified, q can be found. Equation (3.3-7) also provides a means for estimating K_f without generating test data. Solving Eq. (3.3-7) for K_f yields

$$K_f = 1 + q\,(K_t - 1) . \qquad (3.3\text{-}8)$$

Charts prepared by Peterson [5, pp. 9-10] give notch sensitivity values for steels in reversed bending which have been used widely. Thus, after locating the notch sensitivity value and the theoretical stress concentration value from other charts given by Peterson [5, pp. 47-50] for the machine part under investigation, Eq.(3.3-8) can be used to obtain the K_f value.

Shigley suggests that whenever there is any doubt concerning the proper notch sensitivity value to use, one can always make $K_f = K_t$ and err on the safe side. Shigley also suggests that when the groove radius is quite large K_t is not far from unity and the error of assuming K_f equal to K_t will be quite small [6, p. 172].

USE OF SHIGLEY'S METHOD TO CONSTRUCT AN S-N DIAGRAM FOR ONR GROOVED TEST SPECIMENS

Shigley's method for constructing an S-N diagram will be applied to parts like the test specimen used in this research. The results will then be compared with the S-N diagram obtained by the use of the experimental data generated during this research with specimens of AISI 4130 steel rod subjected to fully reversed bending and having an outside diameter of $D = 0.375$ in., a diameter at the base of the groove of $d = 0.0937$ in., and a groove radius of $r = 0.250$ in. The ungrooved ultimate tensile strength, S_u, was found experimentally to have a mean value of 106,000 psi. The groove in the specimen was machined and then polished to approximately 4μ-in. per in. The polishing technique involved the use of medium grit emery paper and then a fine grit lapping compound.

Using Shigley's approximation for S_e' as given by Eq. (3.3-3)

$$S_e' = 0.5\ (106{,}000),$$

or

$$S_e' = 53{,}000 \text{ psi.}$$

The modifying factors are:

$k_b = 0.85$ [6, p. 168],

$k_a = 0.89$ [6, p. 167],

and

$$k_e = \frac{1}{K_f} = \frac{1}{1 + q(K_t - 1)}, \qquad (3.3\text{-}9)$$

where q values are obtained from Peterson's notch sensitivity charts [5, p. 9]. For this case q = 0.893 [5, p.9, Fig. 8] . Entering with $\frac{d}{D} = 0.250$ and $\frac{r}{D} = 0.667$ into Peterson's charts yields $K_t = 1.06$ [5, p.49, Fig. 40]. Substitution of these values into Eq. (3.3-9) yields

$$k_e = \frac{1}{1 + (0.893)(1.06-1)},$$

or

$$k_e = 0.948 .$$

Finally, substitution of all values into Eq. (3.3-4) gives

$$S_e = (0.948)(0.89)(0.85)(53,000),$$

or

$$S_e = 38,110 \text{ psi}.$$

Thus we have a modified estimate of the endurance strength mean which is plotted on the S-N diagram at 10^6 cycles.

Shigley then suggests that the 10^3 cycles point on the S-N diagram be estimated as 0.9 S_u [6, p. 162], or

$$S_{10^3 \text{ cycles}} = 0.9\, S_u . \qquad (3.3\text{-}10)$$

Substitution of 106,000 psi, the static ultimate tensile strength, into Eq. (3.3-10) gives

$$S_{10^3 \text{ cycles}} = 0.9(106,000) ,$$

or

$$S_{10^3 \text{ cycles}} = 95,400 \text{ psi.}$$

Thus the estimated S-N diagram can now be constructed for the specimen involved, using Shigley's recommendations, as shown in Fig. 3.3-3.

COMPARISON OF SHIGLEY'S EMPIRICAL METHOD WITH EXPERIMENTAL RESULTS

Upon comparing Fig.3.3-4 (S-N diagram constructed using Shigley's methods) with Fig. 3.3-1 , which was constructed using exclusively experimental data generated during this research, it is found that Shigley's method gives very conservative results. The mean value at 10^3 cycles by Shigley's method is 95.4 Kpsi, whereas in Fig. 3.3-1 the value is 112 Kpsi. It also gives conservative results for the endurance strength at 10^6 cycles. With Shigley's method the endurance strength is 38.1 Kpsi while the ONR experimental results give a value of 54 Kpsi. As can be seen, Shigley's method is more conservative toward the endurance end of the S-N diagram and the entire curve generated by Shigley's method falls outside the -3σ limit at both ends of the experimentally determined S-N diagram. Although Shigley's method is very easy to apply, as it requires the knowledge of the static ultimate strength only, it should be employed when data such as is being generated by this research is not available. Even then being so far on the conservative side has its penalties in the form of cost and weight, and it ignores the distributional, statistical nature of the fatigue phenomenon.

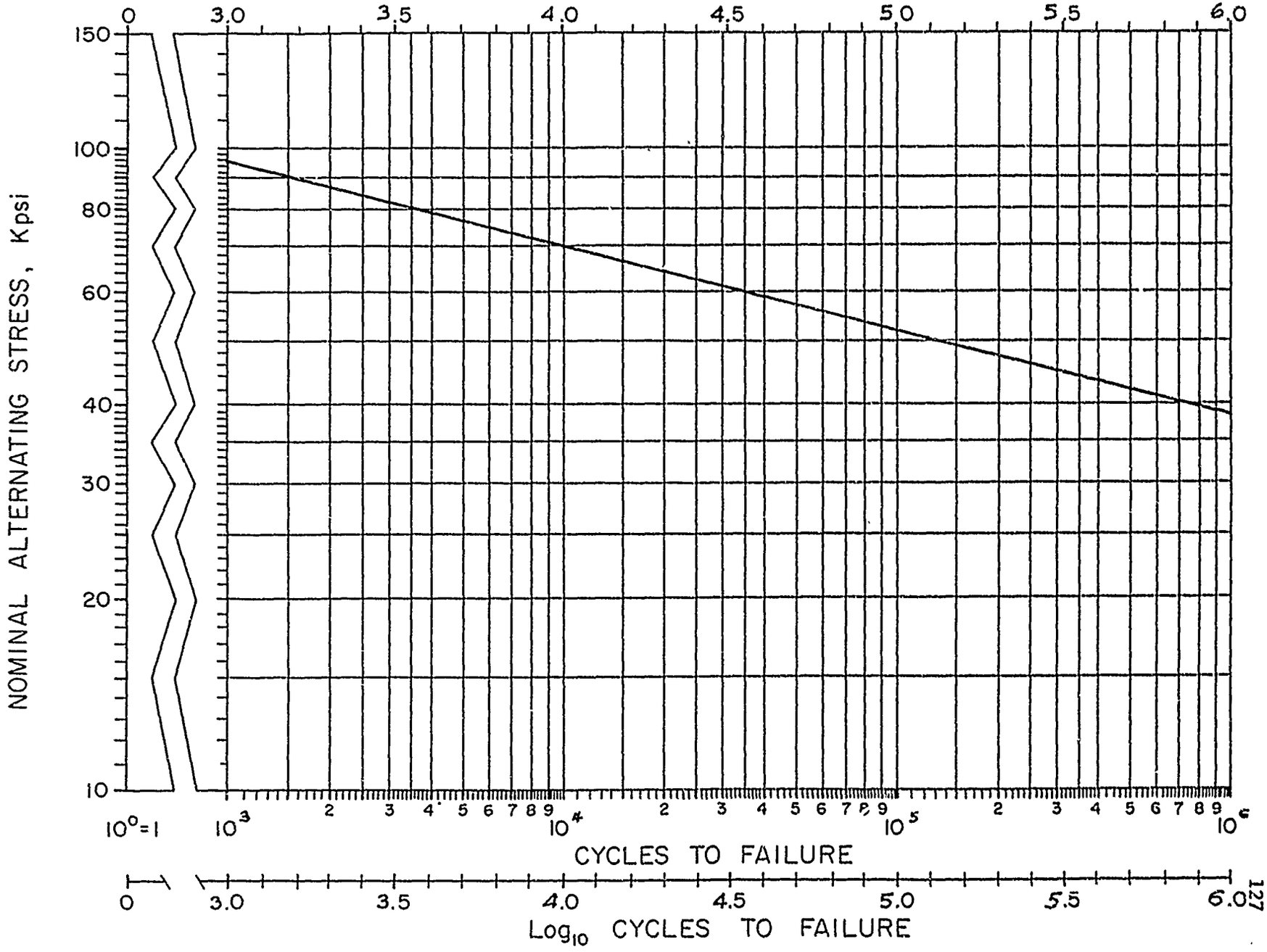

Fig. 3.3-4 S-N diagram plotted for AISI 4130 steel rod D = 0.375", d = 0.0937" and r = 0.250", using Shigley's recommendations.

JUVINALLS' METHOD FOR CONSTRUCTING S-N DIAGRAMS FOR GROOVED SPECIMENS IN BENDING

The S-N diagram discussed by Juvinall [7, pp. 210-262] is constructed in basically the same manner as Shigley's [6 . pp. 160-191]. Both methods base the entire procedure on the use of the ungrooved static ultimate tensile strength and both are identical for ungrooved specimens. However, Juvinall's method of constructing the S-N diagram for grooved specimens differs from Shigley's in the use of strength reduction modifiers.

In considering the development of the S-N diagram for grooved specimens Juvinall offers a more detailed account of notch-sensitivity and stress concentration [7, pp. 237-262]. However, his modifications for estimating the notched endurance strength differs only slightly from Shigley's. In the absence of specific data Juvinall recommends that the grooved endurance strength be estimated from

$$S_e = \frac{0.5\, S_u\, k_e\, k_b\, k_a}{K_f} , \qquad (3.3\text{-}11)$$

where

S_u = static tensile ultimate strength

k_e = load constant

k_b = size factor or diameter factor

k_a = surface finish factor

K_f = fatigue stress concentration factor.

Juvinall then offers the following modification to Eq. (3.3-8), the relationship for calculating K_f from q and K_t:

$$K_f = 1 + (K_t - 1)\, q\, k_a, \qquad (3.3\text{-}12)$$

and explains [7, pp. 256-257]:

> "A conservative procedure which is often followed in estimating the endurance limit of notched parts with various surface finishes is to (1) multiply the basic endurance limit (0.5 S_u) by the surface finish factor k_a and (2) divide by the fatigue stress-concentration factor K_f as determined from Eq. (3.3-8). The surface factor should of course, pertain to the finish at the stressraiser, as this is the point where a fatigue fracture would presumably originate. For parts having values of k_a appreciably less than 1, the above procedure probably errs somewhat on the conservative side. The reason is that surface irregularities reduce the additional damage which can be caused by a notch in much the same way as internal irregularities do. Equation (3.3-8) reflects the influence of internal irregularities in reducing the severity of the notch. A modified version of this equation is suggested which uses the factor k_a to compensate for the influence of surface irregularities", in the form of Eq. (3.3-12).

In discussing the load factor, k_e, [7, pp. 226-231] Juvinall suggests that in reversed bending the loading really has no effect upon the modified endurance strength, thereby recommending that k_e be equal to unity for machine parts in purely reversed bending. Juvinall then suggests the following thumb rules for determing the effect of loading [7, p. 231]:

Reversed or rotating bending:

$$k_e = 1.0.$$

Reversed axial loads:

k_e = 0.9 with no bending.

k_e = 0.6 to 0.85 with indeterminate bending.

Reversed torsion:

k_e = 0.58 for ductile materials.

k_e = 0.80 for cast iron.

Juvinall is in close agreement with Shigley in estimating the effect of the size factor, k_b. He provides the following procedure for estimating k_b [7, p. 236]:

k_b = 1.0 for $d \leq 0.4$ in., and for either bending or torsion. (3.3-13)

k_b = 0.9 for 0.4 in. $\leq d \leq$ 2 in. and for either bending or torsion. (3.3-14)

k_b = 1.0 for axial loading. (3.3-15)

For estimating the stress level to be plotted at 10^3 cycles, Juvinall introduces a modified fatigue stress-concentration factor, K_f' [7, pp. 260-262]. Juvinall explains:

> "Thus far we have noticed that the influence of stress raisers on strength at infinite life (or a very large number of cycles) is represented by K_f and that the effect of stress raisers on static strength is commonly neglected with ductile materials. Our understanding of the material behavior for these two limiting cases leads us to expect that the influence of a stress raiser would increase in some continuous manner over the intermediate or finite-life range. This is indeed the case. Stress concentration factors for finite life are designated by K_f', where $1 \leq K_f' \leq K_f$."

Juvinall presents a curve to estimate the values of K_f' [7, Fig. 13.26, p. 260] in the form of Fig.3.3-5, once K_f and S_u have been established. Juvinall suggests the following relationship for estimating the stress level at 10^3 cycles:

$$S_{10^3 \text{ cycles}} = \frac{0.9\, S_u}{K_f'} \quad . \qquad (3.3\text{-}16)$$

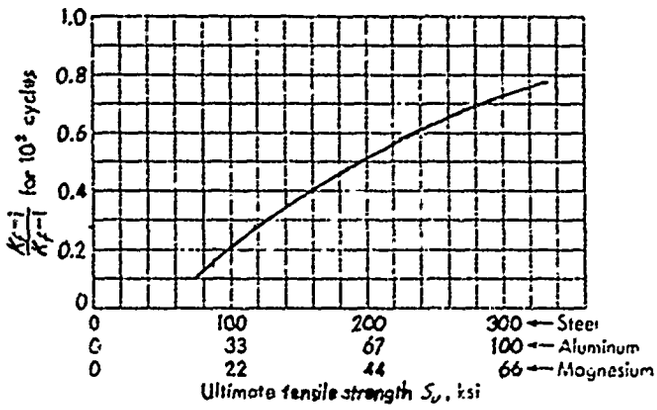

Fig. 3.3-5 Severity of K_f' at 10^3 cycles [7, Fig. 13.26 , p. 260].

Having determined the necessary parameters for using Juvinalls' recommendations the S-N diagram may now be plotted for the same specimen. Using Juvinalls' development for estimating the grooved endurance strength at 10^6 cycles, or Eq.(3.3-11), we have

$$S_e = \frac{0.5\, S_u\, k_e\, k_b\, k_a,}{K_f}$$

where

$$S_u = 106{,}000 \text{ psi},$$

$$k_e = 1 \quad [7, \quad p.\ 231],$$

$$k_b = 1 \quad [7, \quad p.\ 238],$$

and

$$k_a = 0.75 \quad [7, \quad p.\ 234].$$

Employing $q = 0.89$ and $K_t = 1.06$, Eq. (3.3-12)

gives

$$K_f = 1 + (1.06 - 1)(0.89)(0.75),$$

or

$$K_f = 1.04.$$

The calculation of S_e may be completed by substituting K_f into Eq.(3.3-11) or

$$S_e = \frac{(0.50)(106{,}000)(1)(1)(0.75)}{1.04},$$

and

$$S_e = 38.2 \text{ Kpsi}.$$

This is the stress level at the 10^6 cycle point on the S-N diagram.

Now the stress level at the 10^3 cycle point must be calculated using Eq. (3.3-16). Knowing S_u and K_f, K_f' is found to be 1.009 from Fig. 3.3-5. Substituting all values into Eq. (3.3-16) yields the 10^3 cycles stress level as

$$S_{10^3 \text{ cycles}} = \frac{(0.9)(106,000)}{1.009},$$

or

$$S_{10^3 \text{ cycles}} = 94.6 \text{ Kpsi}.$$

The S-N diagram can now be plotted, as shown in Fig. 3.3-6. The corresponding experimentally determined S-N diagram for this specimen is superimposed in Fig. 3.3-6. The same procedure was used for the same specimen but for a groove radius of r = 0.125 in. The results are superimposed in Fig. 3.3-6.

COMPARISON OF JUVINALL'S EMPIRICAL METHOD WITH EXPERIMENTALLY DETERMINED RESULTS

Upon comparing in Fig. 3.3-6 the S-N diagram constructed using Juvinall's method with that constructed using experimental data exclusively, it is found that, like Shigley's method, Juvinall's method gives very conservative results. This, however, is not surprising considering the close proximity of the two methods. The mean value at 10^3 cycles by Juvinall's method is 94.6 Kpsi, whereas the mean value line on the experimentally determined S-N diagram crosses the ordinate for 10^3 cycels at 112 Kpsi. Also like Shigley's method, Juvinall's method gives conservative results at the endurance end of the spectrum. At 10^6 cycles Juvinall's value is 38.2 Kpsi while the experimental endurance value is 54 Kpsi. This it would seem that Juvinall's method becomes more conservative toward the endurance end of the S-N diagram. However, when there is a lack of data, or time to run experimental tests, either Juvinall's or Shigley's method can be used and all errors would be on the "safe side".

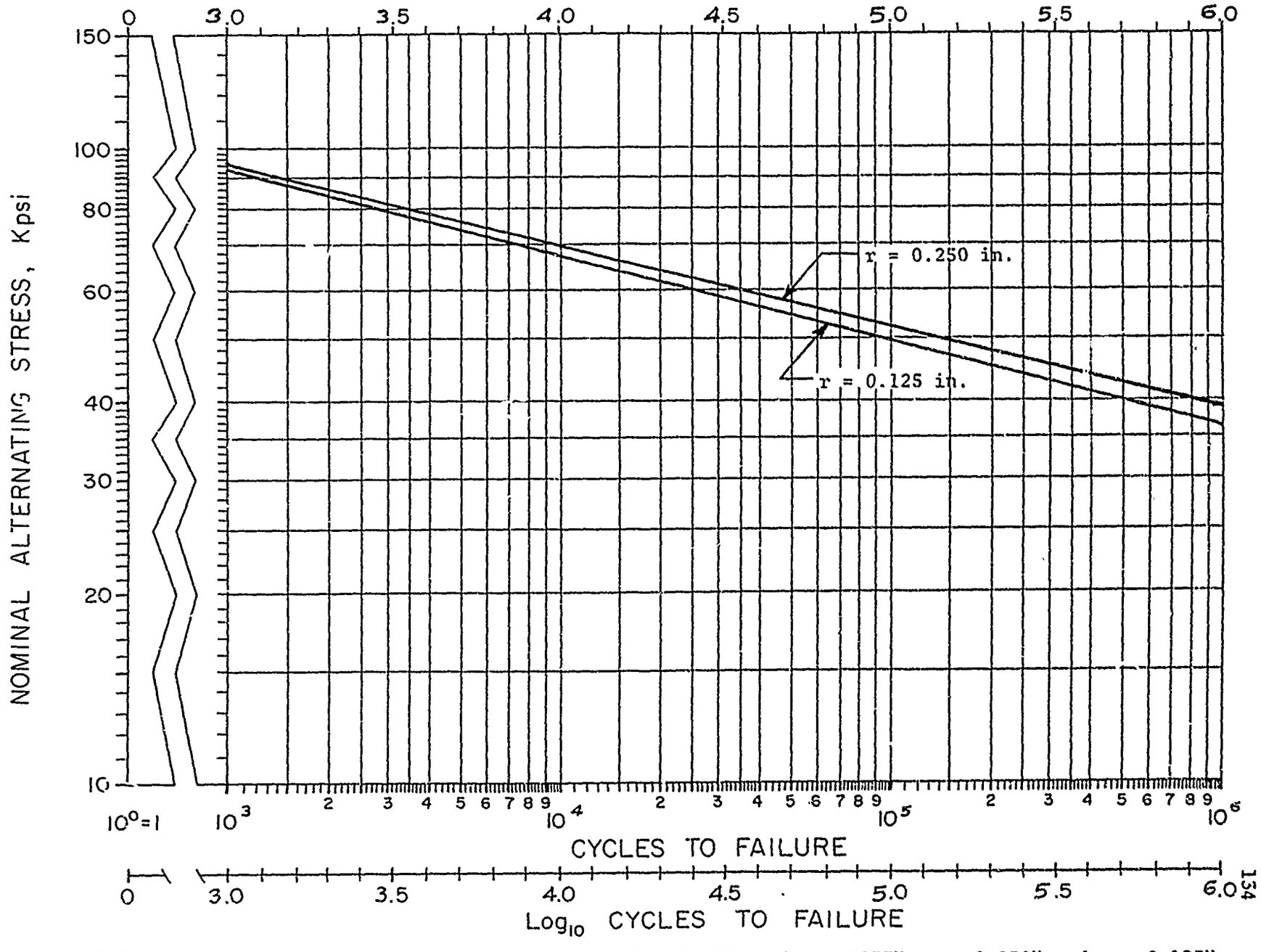

Fig. 3.3-6 S-N diagram for AISI 4130 steel rod, D = 0.375", d = 0.0937", r = 0.250" and r = 0.125" using Juvinall's recommendations.

ALTERNATIVE METHODS FOR CONSTRUCTING S-N DIAGRAMS FOR GROOVED AND UNGROOVED SPECIMENS

Yokobori [13, pp. 195-336], Madayag [14, pp. 110-113] and Osgood [15, p. 371] all attempt to develop equations to express the S-N curve in a functional form for both ungrooved and grooved specimens. The equations developed by all three authors depend upon empirically determined constants. Yokobori gives the following equations representing attempts to express the S-N curve in a functional form [13, p. 195]:

$$S = AN^{-\gamma}, \tag{3.3-17}$$

$$S = a - b \log N, \tag{3.3-18}$$

$$\log (S - S_e) = c - d \log N, \tag{3.3-19}$$

$$\log (S - S_e) = e - f \log (N + g). \tag{3.3-20}$$

Equations (3.3-17) and (3.3-18) apply only for stresses greater than the endurance limit, while Eqs. (3.3.19) and (3.3-20) include the endurance limit, S_e. Due to the wide scatter in N for a given stress level, attempts to determine values for the constants in Eqs. (3.3-17) through (3.3-20) have not been very reliable and should be carried out on a statistical basis [13, p. 196]. It should be pointed out that Eqs. (3.3-17) through (3.3-20) can be used for both grooved and ungrooved parts as the constants would change for grooved specimens.

Madayag [14, pp. 110-113] also gives equations that attempt to express the S-N curve in mathematical form. The first equation is that proposed by Weibull [14, p.113] and is of the form

$$(S - S_e)(N + B)^a = b, \tag{3.3-21}$$

where S_e is the endurance limit and a, b and B are constants. Valluri [14, p. 113] proposed the following equation for determining N:

$$N = \frac{2 \log_e(\sigma_u/\sigma) \log_e[(\sigma - \sigma_i)/K]}{c\,[(\sigma - \sigma_i)/E]^2\,[(\sigma - \sigma')/\sigma_i]^2}, \tag{3.3-22}$$

where

σ = maximum cyclic stress,

σ' = minimum cyclic stress,

σ_u = ultimate tensile strength,

σ_i = internal stress,

K, c = material constants,

E = Young's modulus.

Osgood also develops a relationship for the S-N curve [15, p. 371]. For ungrooved steel bars in rotating-bending, S_e, the endurance strength, was derived as,

$$S_e = (1.0139)^{1/n}(K)^{0.911}, \tag{3.3-23}$$

and for grooved bars,

$$S_e = (1.0108)^{1/n}(K)^{0.828}, \tag{3.3-24}$$

where n is the slope of the true stress-strain curve and K is the stress-intensity factor.

All of the equations given above depend upon empirically determined constants. Whether or not realistic values for these constants can be determined, it is obvious that the methods presented by Shigley and Juvinall are much more convenient for the designer in estimating the fatigue strength of a given material. These methods only depend on knowing the tensile strength of a given material which is easily obtained, and on applying the various thumb rules and modifying factors, to come up with the complete S-N diagram.

3.3.5 NOTCH SENSITIVITY

3.3.5.1 ASPECTS OF NOTCH SENSITIVITY IN FATIGUE

In discussing fatigue strength and the construction of S-N diagrams in Section 3.3.4 the influence of the various stress raisers such as surface finish, size effects and stress concentration was presented. Although all stress raisers should be accounted for in a good engineering design the most significant and most difficult to predict is that due to stress concentration.

Stress concentration in a machine part may be influenced by a variety of factors such as internal cracks or irregularities caused by machining. However, the most common cause of stress concentration is that due to unavoidable changes in the cross-sectional area of the machine part, such as a hole, groove, or keyway. In order to account for the decrease in strength due to the presence of a groove, etc., a factor known as the fatigue stress concentration factor, K_f, was defined in Section 2.2.-1 by Eq. (2.2-12),

$$K_f = \frac{S_{\text{nominal for ungrooved specimens}}}{S_{\text{nominal for grooved specimens}}} . \qquad (2.2\text{-}12)$$

However, in the investigation of fatigue failure it has been found that some materials are more sensitive to notches, or grooves, than others; this means that the stresses for insensitive materials are not increased by the full theoretical amount of the geometric stress concentration factor, K_t. In order to define the sensitivity of

different materials to the presence of a groove an index, q, known as notch sensitivity was defined in Section 2.2.-1 by Eq. (2.2-27),

$$q = \frac{K_f - 1}{K_t - 1} \quad . \tag{2.2-27}$$

Since K_t values are readily available the notch sensitivity index was defined primarily to give designers a method to calculate K_f without extensive experimental testing. A material fully notch sensitive would have a q of 1 and a material completely insensitive to notches would have a q of 0. However, since q in addition to material properties is also affected by the sharpness of the groove, the depth of the groove, etc. very little reliable notch sensitivity data has been generated to date elsewhere. The problem is basically the same as that for finding K_f; i.e. extensive testing is required to determine q. Although q normally assumes values between zero and 1, in some instances values of q greater than one have been calculated. The cause of this may be traced to the problem of maintaining complete control over the variability involved in fatigue testing. Published data by NASA researchers illustrating this problem is depicted in Fig. 3.3-7.

TABLE 3.3-5 VALUES OF FATIGUE-NOTCH FACTOR AND FATIGUE-NOTCH SENSITIVITY*

Specimen diameter, in.	Notch radius, r, in.	K_t	Fatigue notch factor, K_f, at 10^7 cycles**		Fatigue-notch-sensitivity q, at 10^7 cycles**	
			Mean	Extreme	Mean	Extreme
1/8	0.010	2.0	1.5	1.2 1.9	0.5	0.2 .9
1/4	.020	2.0	2.1	1.8 2.5	1.1	.8 1.5
1/2	.040	2.0	2.1	1.8 2.4	1.1	.8 1.4
1	.080	2.0	1.7	1.4 2.0	.7	1.4 1.0
$1\frac{3}{4}$	.140	2.0	1.6	1.4 1.8	.6	.4 .8
$1\frac{3}{4}$	.001	19.2	1.8	1.6 2.1	.04	.03 .06

* Data is for 75S-T6 aluminum alloy.

** The mean and extreme values were calculated from values listed in Hyler, [et.al. 16, p. 25, Table 12].

K_f = unnotched fatigue strength/notched fatigue strength; $q = (K_f - 1) / (K_t - 1)$.

Table 3.3-6 - Rotating Beams With Circumferential Grooves [17, p. 16, Table 1].

Type of steel	Maximum diameter, in.	Minimum diameter, in.	Shape of notch	Root radius, in.	K_T	Ultimate tensile strength, ksi	Endurance limit (notched) ksi	Endurance limit (unnotched), ksi	K_F	A* in.	K_N	K_N/K_F	Reference
AISI 1020	0.145	0.125	Semicircle	0.010	2.00	62.0	21.2	33.0	1.55	0.010	1.50	0.97	3
AISI 1020	.290	.250	Semicircle	.020	2.00	62.0	20.2	32.0	1.59	.010	1.59	1.00	3
AISI 1020	.580	.500	Semicircle	.040	2.00	62.0	17.1	28.0	1.63	.010	1.67	1.02	3
AISI 1020	1.160	1.000	Semicircle	.080	2.00	62.0	17.0	28.0	1.64	.010	1.74	1.06	3
AISI 1020	2.175	1.875	Semicircle	.150	2.00	62.0	17.7	29.0	1.64	.010	1.74	1.06	3
AISI 1035	.145	.125	Semicircle	.010	2.00	87.6	26.0	40.0	1.54	.0054	1.59	1.03	3
AISI 1035	.290	.250	Semicircle	.020	2.00	87.6	24.7	40.0	1.62	.0054	1.66	1.02	3
AISI 1035	.580	.500	Semicircle	.040	2.00	87.6	20.0	34.6	1.73	.0054	1.73	1.00	3
AISI 1035	1.160	1.000	Semicircle	.080	2.00	87.6	19.8	35.0	1.77	.0054	1.79	1.01	3
AISI 1035	2.175	1.875	Semicircle	.150	2.00	87.6	19.8	35.0	1.77	.0054	1.84	1.04	3
AISI 4130**	.145	.125	Semicircle	.010	2.00	141.8	45.0	70.0	1.93	.0015	1.72	.89	3
AISI 4130**	.290	.250	Semicircle	.020	2.00	141.8	37.0	69.5	1.88	.0015	1.78	.95	3
AISI 4130**	.580	.500	Semicircle	.040	2.00	141.8	35.8	65.0	1.82	.0015	1.84	1.01	3
AISI 4130**	1.160	1.000	Semicircle	.080	2.00	141.8	35.0	63.7	1.82	.0015	1.88	1.03	3
AISI 4130**	2.030	1.750	Semicircle	.140	2.00	141.8	34.9	63.5	1.82	.0015	1.90	1.04	3
AISI 4340	.145	.125	Semicircle	.010	2.00	163.8	51.7	82.5	1.60	.00084	1.78	1.11	4
AISI 4340	.290	.250	Semicircle	.020	2.00	163.8	48.0	81.0	1.69	.00084	1.83	1.08	4
AISI 4340	.580	.500	Semicircle	.040	2.00	163.8	48.0	78.0	1.62	.00084	1.87	1.15	4
AISI 4340	1.160	1.000	Semicircle	.080	2.00	163.8	46.0	74.0	1.61	.00084	1.90	1.18	4
AISI 4340	2.030	1.750	Semicircle	.140	2.00	163.8	42.0	74.0	1.76	.00084	1.93	1.10	4
AISI 1045	.375	.300	60°V	.010	2.90	104.7	26.0	61.5	2.37	.0036	1.99	.84	5
AISI 1045	.375	.300	60°V	.010	2.90	119.9	27.0	67.0	2.48	.0026	2.07	.83	5
AISI 3140	.375	.300	60°V	.010	2.90	108.2	28.0	65.5	2.34	.0034	2.00	.86	5
AISI 3140	.375	.300	60°V	.010	2.90	109.0	22.0	62.5	2.84	.0032	2.07	.73	5
AISI 2340	.375	.300	60°V	.010	2.90	115.7	30.0	71.0	2.37	.0028	2.05	.86	5
AISI 2340	.375	.300	60°V	.010	2.90	122.1	22.0	68.0	3.09	.0024	2.09	.68	5
AISI 2340	.375	.300	60°V	.010	2.90	118.9	21.0	67.0	3.19	.0026	2.06	.65	5
AISI 2340	.375	.300	60°V	.010	2.90	130.1	26.5	75.0	2.83	.0020	2.12	.75	5
AISI 2340	.375	.300	60°V	.010	2.90	134.2	26.5	79.5	3.00	.0018	2.13	.71	5
AISI 1020	.250	.125	Semicircle	.0625	1.26	59.9	23.0	29.0	1.26	.012	1.18	.94	6
AISI 1020	.200	.160	Semicircle	.0200	1.74	59.9	20.5	29.0	1.41	.012	1.42	1.01	6
AISI 1020	.500	.250	U	.0625	1.47	59.9	21.25	29.0	1.36	.012	1.33	.98	6

* A is Neuber's material constant based on grain size.
** These materials have been heat treated.

Table 3.3-6 - Rotating Beams With Circumferential Grooves (Cont'd).

Type of steel	Maximum diameter, in.	Minimum diameter, in.	Shape of notch	Root radius, in.	K_T	Ultimate tensile strength, ksi	Endurance limit (notched) ksi	Endurance limit (unnotched), ksi	K_F	A* in.	K_N	K_N/K_F	Reference
AISI 1020	.625	.500	Semicircle	.0625	1.74	59.9	19.5	28.0	1.44	.012	1.52	1.05	6
AISI 1020	.540	.500	Semicircle	.0200	2.38	59.9	16.5	28.0	1.70	.012	1.78	1.04	6
AISI 1020	1.040	1.000	Semicircle	.0200	2.60	59.9	15.5	28.0	1.81	.012	1.90	1.05	6
AISI 1020	1.250	1.000	Semicircle	.125	1.74	59.9	18.0	28.0	1.55	.012	1.57	1.01	6
AISI 1020	2.040	2.000	Semicircle	.020	2.80	59.9	15.0	28.0	1.87	.012	2.01	1.07	6
AISI 1020	2.500	2.000	Semicircle	.250	1.74	59.9	17.5	28.0	1.60	.012	1.61	1.01	6
AISI 1035	.290	.250	Semicircle	.020	2.00	77.6	39.0	23.5	1.66	.0069	1.63	.98	6
AISI 2345	.250	.125	Semicircle	.0625	1.26	125.5	56.5	70.25	1.24	.0023	1.22	.98	6
AISI 2345	.200	.160	Semicircle	.020	1.75	125.5	44.5	70.75	1.59	.0023	1.56	.98	6

Table 3.3-6 - Rotating Beams With Circumferential Grooves (Cont'd) *

Type of steel	Maximum diameter, in.	Minimum diameter, in.	Shape of notch (a)	Root radius in.	K_T	Ultimate tensile strength, ksi (a)	limit (notched), ksi	Endurance limit (unnotched), ksi	K_F	A* in.	K_N	K_N/K_F	Reference
AISI 2345	0.500	0.250	U	0.0625	1.46	125.5	50.0	66.75	1.34	0.0023	1.39	1.04	6
AISI 2345	.425	.300	Semicircle	.0625	1.54	125.5	48.25	70.0	1.45	.0023	1.45	1.00	6
AISI 2345	.340	.300	Semicircle	.020	2.10	125.5	37.0	70.0	1.89	.0023	1.82	.96	6
AISI 2345	.375	.300	Semicircle	.0375	1.75	125.5	43.5	70.0	1.61	.0023	1.60	.99	6
AISI 2345	.540	.500	Semicircle	.020	2.38	125.5	33.55	66.5	1.99	.0023	2.03	1.02	6
AISI 2345	.625	.500	Semicircle	.0625	1.75	125.5	44.5	66.5	1.59	.0023	1.63	1.03	6
AISI 2345	1.000	.875	Semicircle	.0625	2.06	125.5	35.0	64.0	1.83	.0023	1.89	1.03	6
AISI 2345	1.750	1.500	U	.0625	2.54	125.5	29.5	66.5	2.24	.0023	2.29	1.02	6
AISI 1020	1.875	1.750	Semicircle	.0625	2.42	59.9	15.25	28.0	1.83	.012	1.99	1.09	7
AISI 1020	1.750	1.500	U	.0625	2.54	59.9	14.75	28.0	1.90	.012	2.07	1.09	7
AISI 1020	1.000	.875	Semicircle	.0625	2.07	59.9	17.0	28.0	1.65	.012	1.74	1.05	7
AISI 1020	.875	.625	U	.0625	1.92	59.9	18.0	28.0	1.55	.012	1.64	1.06	7
AISI 1020	.375	.300	Semicircle	.0375	1.76	59.9	19.5	28.0	1.44	.012	1.49	1.03	7
AISI 1020	.340	.300	Semicircle	.020	2.10	59.9	18.0	28.0	1.55	.012	1.62	1.05	7
AISI 1020	.425	.300	Semicircle	.0625	1.51	59.9	20.75	28.0	1.35	.012	1.36	1.01	7
AISI 2345	2.187	1.750	Semicircle	.2187	1.76	125.5	39.0	66.5	1.70	.0023	1.69	.995	7
AISI 2345	1.790	1.750	Semicircle	.020	2.80	125.5	28.5	66.5	2.33	.0023	2.34	1.005	7
AISI 2345	1.500	1.375	Semicircle	.0625	2.30	125.5	31.0	66.5	2.14	.0023	2.09	1.02	7
AISI 2345	1.250	1.000	Semicircle	.125	1.76	125.5	38.5	64.0	1.66	.0023	1.66	1.00	7
AISI 2345	1.040	1.000	Semicircle	.020	2.65	125.5	29.0	64.0	2.21	.0023	2.23	1.01	7
AISI 2345	.875	.625	U	.0625	1.92	125.5	37.0	66.5	1.80	.0023	1.77	.98	7
AISI 4130	.480	.355	45°V	.010	3.20	120	23.5	54.5	2.32	.0027	2.30	.99	8
0.1 % C	.600	.584	(0°)	.002	4.50	(60)	----	----	1.07	.0112	2.04	1.91	9
0.1 % C	.300	.294	(0°)	.002	4.24	(60)	----	----	1.21	.0112	1.65	1.36	9
0.29 % C	.480	.404	(0°)	.010	3.13	(80)	----	----	2.62	.0065	2.18	.83	9
0.29 % C	.480	.328	(0°)	.015	2.73	(80)	----	----	2.50	.0065	2.04	.82	9
0.29 % C	.591	.405	(0°)	.063	1.65	(80)	----	----	1.53	.0065	1.49	.97	9
0.29 % C	.716	.404	(0°)	.125	1.37	(80)	----	----	1.31	.0065	1.30	.99	9
0.29 % C	.966	.404	(0°)	.250	1.20	(80)	----	----	1.22	.0065	1.17	.96	9
0.36 % C	.340	.316	(0°)	.006	3.04	(85)	----	----	1.75	.0058	2.03	1.16	9
0.42 % C	.600	.584	(0°)	.002	4.50	(90)	----	----	1.43	.0052	2.34	1.63	9
0.62 % C	.340	.316	(0°)	.006	3.04	(115)	----	----	1.78	.0029	2.21	1.24	9
Cr-Ni Annealed	.340	.316	(0°)	.006	3.04	(65)	----	----	1.95	.0097	1.90	.97	9
Cr-Ni Heat treated	.340	.316	(0)	.006	3.04	(100)	----	----	2.20	.0041	2.12	.96	9

Table 3.3-6 - Rotating Beams With Circumferential Grooves (Cont'd.).*

Type of steel	Maximum diameter, in.	Minimum diameter, in.	Shape of notch (a)	Root radius in.	K_T	Ultimate tensile strength, ksi (a)	Endurance limit (notched), ksi	Endurance limit (unnotched), ksi	K_F	A* in.	K_N	K_N/K_F	Reference
Cr-Ni Heat treated	.600	.584	(0°)	.002	4.5	(150)	----	----	2.00	.0012	2.97	1.48	9
Cast Steel	.300	.284	(0°)	.002	4.04	(60)	----	----	1.31	.0121	1.91	1.46	9

Table 3.3-7 Check Of Computed Strength-Reduction Factor (k') With Strength-Reduction Factor Determined Directly by Fatigue Tests [18, p. 517].

The Neuber constant ρ' is computed from the formula, $\rho' = 0.2\ (1 - S_y/S_u)^3 \times (1 - 0.05/d)$, in which S_y is the yield strength of the metal, S_u the tensile strength, and d is the diameter of the specimen.

(1) Metal	(2) Diameter of Specimen, d, in.	(3) Endurance Limit from Tests, S'_e, psi. Unnotched	(4) Endurance Limit from Tests, S'_e, psi. Notched	(5) Radius at Root of Notch, ρ, in.	(6) Depth of Notch, t, in.	(7) ρ' from Formula Above, in.	(8) "Theoretical" Stress-Concentration Factor,	(9) Strength-Reduction Factor k'	(10) Strength-Reduction Factor from Tests, (3) / (4)	(11) Deviation of (10) from (9), per cent
S.A.E. 1020 steel, as rolled (series II)	0.125	34 000	22 000	0.01	0.01	0.0133	2.00	1.47	1.54	-4.6
	0.250	32 000	20 000	0.02	0.02	0.0177	2.00	1.51	1.60	-5.6
	0.500	28 900	17 800	0.04	0.04	0.0200	2.00	1.59	1.62	-1.9
	1.000	28 200	17 200	0.08	0.08	0.0210	2.00	1.66	1.67	-0.6
	1.875	28 200	16 000	0.14	0.14	0.0216	2.06	1.76	1.76	0
S.A.E. 1020 steel, strain relieved (series I)	0.125	------	23 000	0.0625	0.0625	0.0087	1.26	1.26	----	----
	0.160	29 000	20 500	0.0200	0.0200	0.0100	1.74	1.43	1.41	+1.4
	0.250	29 000	21 250	0.0625	0.1250	0.0116	1.47	1.33	1.36	-2.2
	0.500	28 000	19 500	0.0625	0.0625	0.0131	1.74	1.51	1.44	+4.9
	0.500	28 000	16 500	0.0200	0.0200	0.0131	2.38	1.76	1.70	+3.5
	1.000	28 000	15 500	0.0200	0.0200	0.0138	2.60	1.87	1.81	+3.3
	1.000	28 000	18 000	0.125	0.125	0.0138	1.74	1.56	1.55	+0.6
	2.000	28 000[a]	15 000	0.0200	0.0200	0.0200	2.80	1.98	1.87	+5.9
	2.000	28 000[a]	17 500	0.2500	0.2500	0.1415	1.74	1.60	1.60	0
S.A.E. 1035 steel, as rolled (series II)	0.125	39 000	27 000	0.01	0.01	0.0117	2.00	1.47	1.44	+2.1
	0.250	39 000	25 000	0.02	0.02	0.0156	2.00	1.55	1.56	-0.6
	0.500	35 000	22 000	0.04	0.04	0.0175	2.00	1.60	1.59	+0.6
	1.000	34 400	19 300	0.08	0.08	0.0185	2.00	1.68	1.78	-5.6
	1.875	34 400	19 300	0.14	0.14	0.0189	2.06	1.78	1.78	0

Table 3.3-7 Check Of Computed Strength-Reduction Factor (k') With Strength-Reduction Factor Determined Directly by Fatigue Tests (Cont'd).

The Neuber constant ρ' is computed from the formula, $\rho' = 0.2\ (1 - S_y\ S_u)^3 \times (1 - 0.05/d)$, in which S_y is the yield strength of the metal, S_u the tensile strength, and d is the diameter of the specimen.

(1) Metal	(2) Diameter of Specimen, d, in.	(3) Endurance Limit from Tests, S'_e, psi. Unnotched	(4) Endurance Limit from Tests, S'_e, psi. Notched	(5) Radius at Root of Notch, ρ, in.	(6) Depth of Notch t, in.	(7) ρ' from Formula Above, in.	(8) "Theoretical" Stress-Concentration Factor, k_t from Fig. 2	(9) Strength-Reduction Factor from Fig. 3, k'	(10) Strength-Reduction-Factor from Tests, (3) / (4)	(11) Deviation of (10) from (9), per cent
S.A.E. 1035 steel, bright anneal (series II)[b]	0.250	39 000	23 500	0.02	0.02	0.0136	2.00	1.55	1.66	-7.1
S.A.E. 1035 steel, heat treated (series I)	0.125	70 250	56 500	0.0625	0.0625	0.00107	1.26	1.20	1.24	-3.2
	0.160	70 750	44 500	0.0200	0.0200	0.00123	1.75	1.60	1.59	+0.7
	0.250-	66 750	50 000	0.0625	0.1250	0.00143	1.46	1.43	1.34	+6.7
	0.300	70 000	48 250	0.0625	0.0625	0.00148	1.54	1.47	1.45	+1.4
	0.300	70 000	37 000	0.0200	0.0200	0.00148	2.10	1.87	1.89	-1.1
	0.300	70 000	43 500	0.0375	0.0375	0.00148	1.75	1.65	1.61	+2.5
	0.500	66 500	33 550	0.0200	0.0200	0.00160	2.38	2.07	1.99	+3.0
	0.500	66 500	44 500	0.0625	0.0625	0.00160	1.75	1.64	1.59	+3.1
	0.875	64 000	35 000	0.0625	0.0625	0.00169	2.06	1.92	1.83	+4.9
	1.500	66 500	29 500	0.0625	0.1250	0.00173	2.54	2.32	2.25	+3.1
S.A.E. X4130 steel (series II)	0.125	75 400	38 600	0.01	0.01	0.00072	2.00	1.79	1.95	-8.2
	0.250	69 800	37 300	0.02	0.02	0.00096	2.00	1.82	1.87	-2.7
	0.500	65 000	35 800	0.04	0.04	0.00108	2.00	1.86	1.82	+2.2
	1.000	63 600	34 600	0.08	0.08	0.00114	2.00	1.87	1.84	-1.6
	1.750	63 600	34 800	0.14	0.14	0.00116	2.06	1.91	1.83	+4.4

Mean deviation of predicted values of strength-reduction factor k' from test values (disregarding sign) = 2.92 per cent.
Maximum deviations = + 6.7 and - 8.2 per cent.
[a] Unnotched specimen 1.875 in. in diameter.
[b] These specimens were notched and polished after annealing.

Table 3.3-8 Stress concentration factor, K_t; fatigue notch factors, K_f; and notch sensitivity indices q for various alloys in rotating bending [15, p. 104, Table 3.3] .

Alloy	K_t	K_f	q
Aluminum 2024-0	1.6	1.0	0
Magnesium AZ80-A	1.6	1.1	0.16
Stainless steel, type 18-8	1.6	1.0	0
Structural steel (BHN = 120)	1.6	1.3	0.5
Hardened steel (BHN = 200)	1.6	1.6	1.0
Gray cast iron	1.6	1.0	0
Bronze forging	1.6	1.0	0
Aluminum 7075-T73	6.7	1.8	0.13
Titanium 6Al-4V	3.5	2.8	0.72

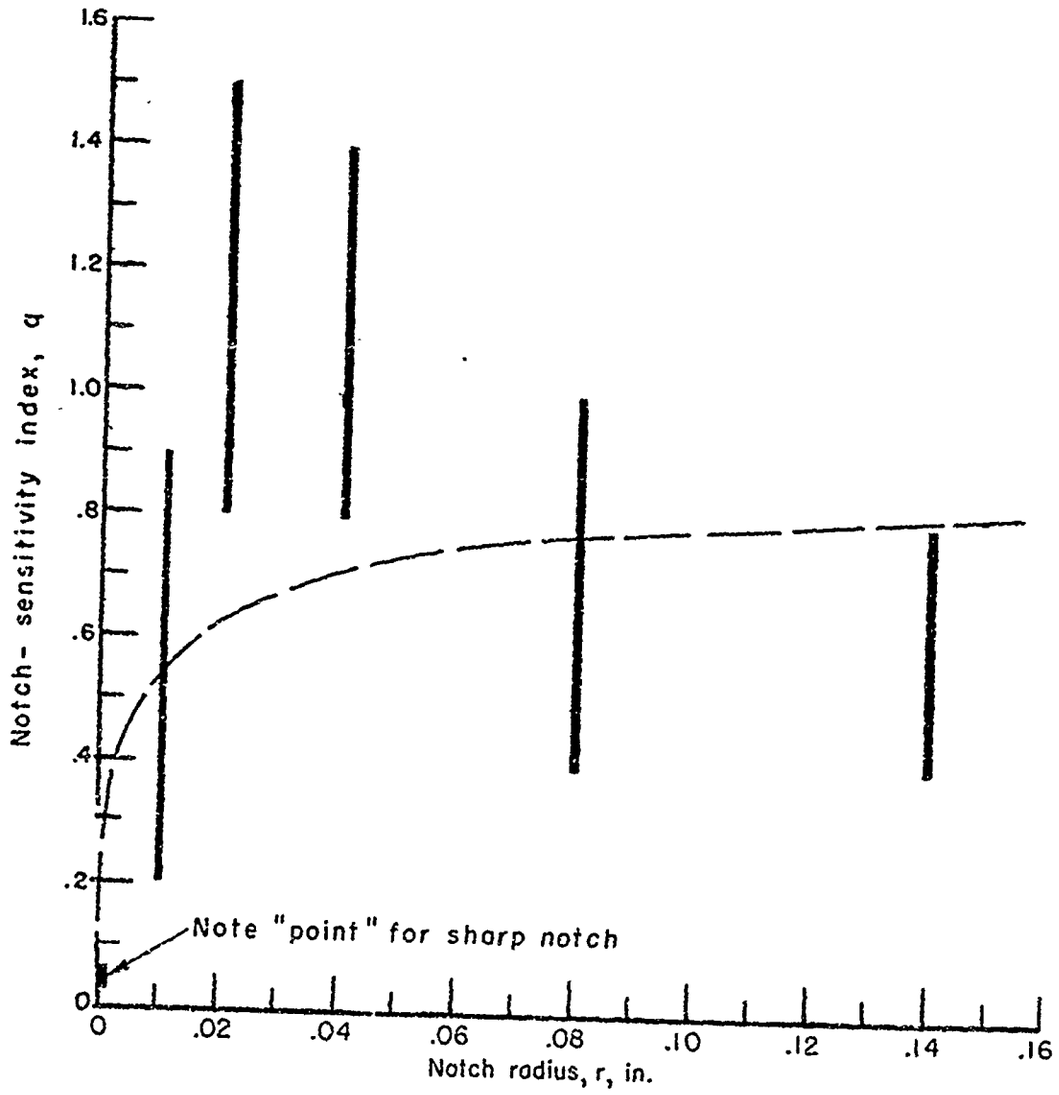

Fig. 3.3-7 Notch sensitivity versus notch radius. Vertical lines represent observed "points". Dashed line represents Neuber's theory [16, p. 47, Fig. 24].

The first detailed analysis of the influence of stress gradients and material micro-structure on the values of stress raisers was made by Neuber [19, p. 17]. Neuber undertook an extensive theoretical analysis of notch effects, and developed the Neuber's technical stress-concentration factor designed by K_n [19, p. 16]. The equation for K_n is given by

$$K_n = 1 + \frac{K_t - 1}{1 + \left(\frac{\pi}{\pi-\omega}\right)\sqrt{\frac{a}{r}}}, \tag{3.3-25}$$

where r is the notch radius in inches, ω is the notch flank angle in radians, K_t is the theoretical geometric stress concentration factor and "a" is an empirical constant which represents half the length of an equivalent grain of the material. Values of "a" are found by experiment, to be portional to grain size in a very general way, but are actually several times the actual size. Kuhn [17, p. 27, Fig. 3] has published curves giving values for various materials, which is reproduced in Fig. 3.3-8. This curve, however, is very general and there still is much discussion and research involved with Neuber's material constant.

A refinement of Neuber's original approach was developed by Peterson [5, pp. 10-16]. This refinement is convenient to use and has been widely accepted. Peterson bases his curves on the notch sensitivity factor, q, and Eq. 3.3-8.

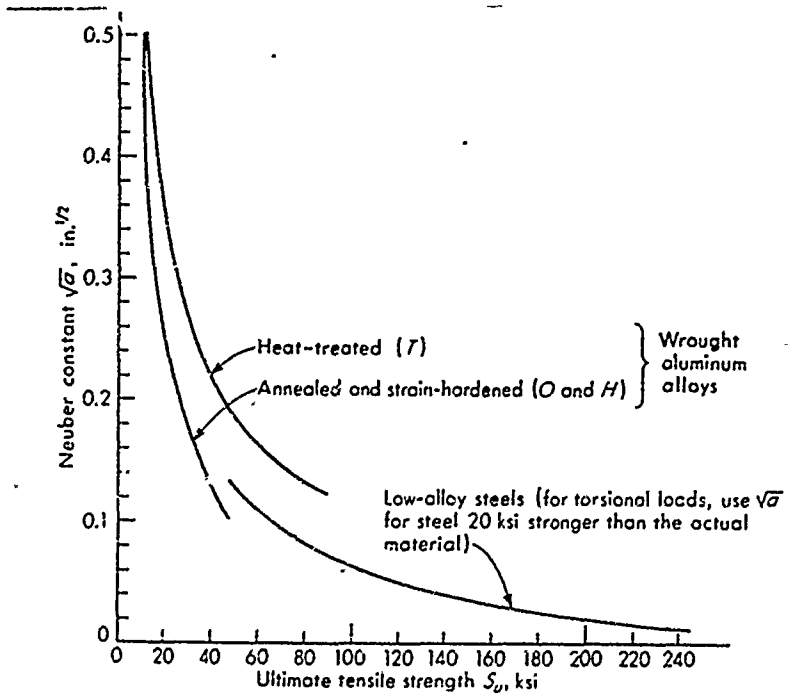

Fig. 3.3-8 Neuber grain size constants for steel and aluminum for use in Eq. (3.3-25), [7, p. 254, Fig. 13.20].

Using specimens with a zero flank angle he reduces Neuber's equation to

$$K_f = \frac{1 + K_t - 1}{1 + \sqrt{\frac{a}{r}}} \quad . \tag{3.3-26}$$

Substitution of Eq. (3.3-26) into Eq. (3.3-8) yields

$$q = \frac{1}{1 + \sqrt{\frac{a}{r}}} \quad . \tag{3.3-27}$$

Eq. (3.3-27) supplemented with values of "a" from Fig. 3.3-8 gives vaules of q for bending, axial and torsional loading. Such values are plotted in Fig. 3.3-9. Most of the notch sensitivity work undertaken in this research is based on Peterson's refinement of Neuber's theories. Figs. 3.3-10 and 3.3-11, also generated by Peterson, relate q to geometric configuration and are based on Neuber's work. The curves are completely theoretical and do not directly involve Neuber's material constant. The set of equations derived by Neuber for K_t and used by Peterson to plot his K_t curves given in Figs. 2.2-7, 2.2-8, 2.2-11, and 2.2-12 for circumferentially grooved, round rods in bending are given in Fig. 3.3-12.

It has been shown by many test that use of the full theoretical value of K_t in fatigue design will generally give results on the conservative side, but for materials of any reasonable degree of ductility plastic strain occurs in the notches and reduces the stress concentration effect to a value somewhat below that calculated from pure geometry. This, leads into another definition of notch sensitivity in terms of K_t and K_f. It has been found experimentally that there is a limiting small value of the notch radius below which there is no additional stress concentration effect. The ratio between the apparent increase in local stress in fatigue and the increase predicted by the elastic theory of stress concentration is another way of explaining the parameter, q [15, pp. 103-104].

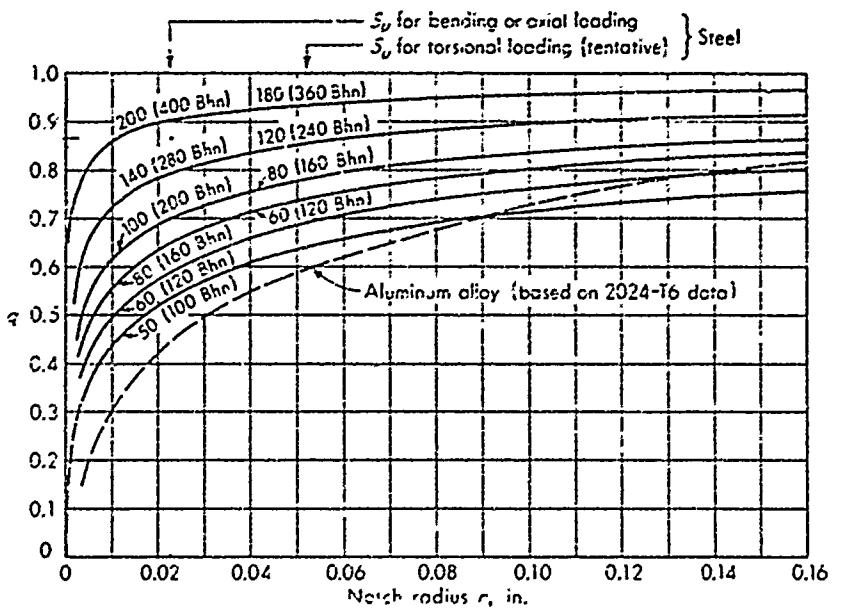

Fig. 3.3-9 Notch sensitivity values versus notch radius [7, p. 255, Fig. 13.21].

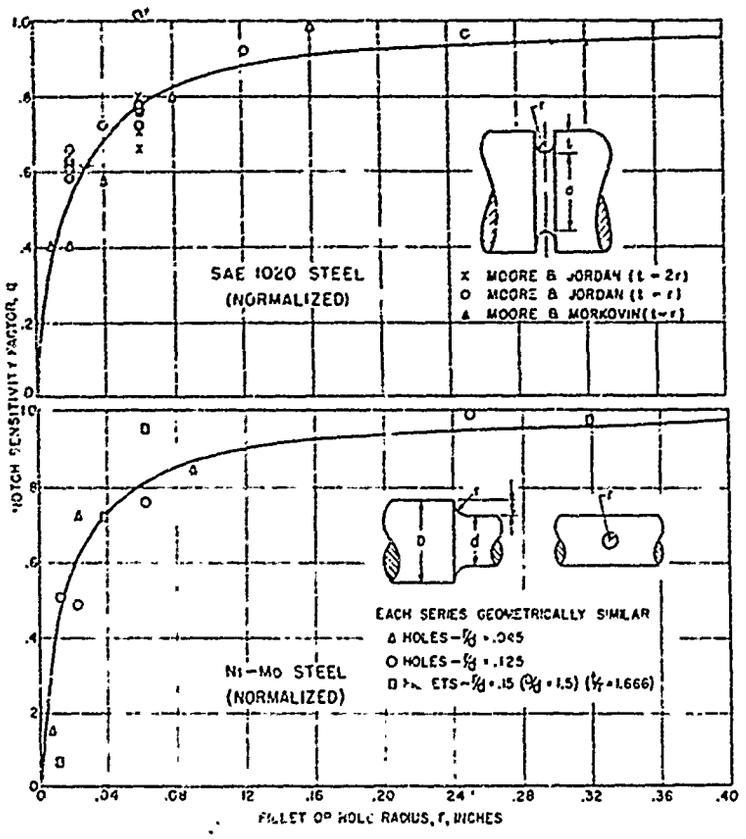

Fig. 3.3-10 Notch sensitivity values versus hole or fillet radius [5, p. 9, Fig. 8].

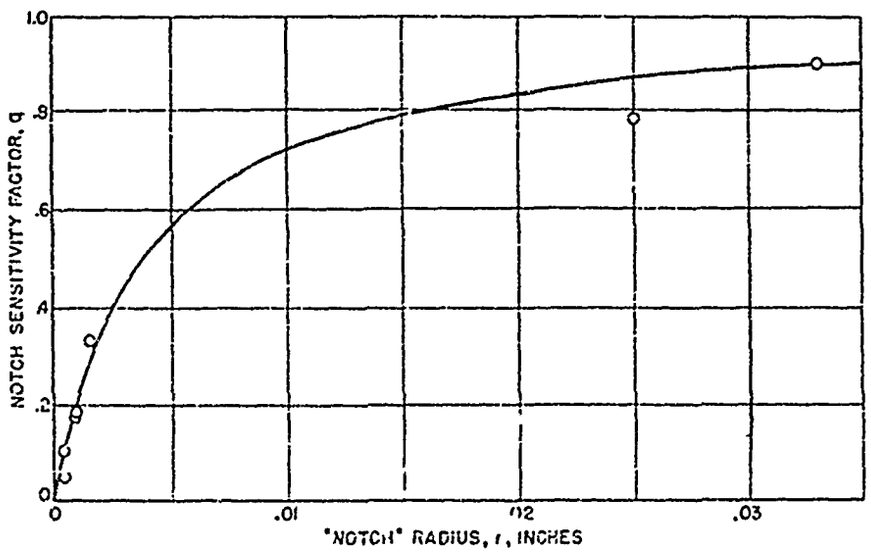

Fig. 3.3-11 Notch sensitivity of quenched and tempered alloy steel versus notch radius [5, p. 9, Fig. 9].

Circumferential Notched Round Bar in Bending

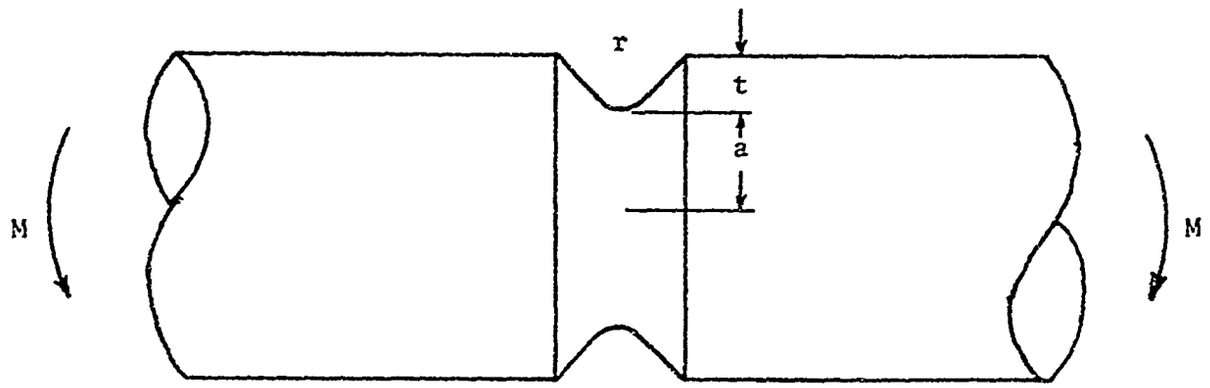

$$N = 3\left(\frac{a}{r} + 1\right) + \left(1 + \frac{4}{m}\right)\sqrt{\frac{a}{r} + 1} + \frac{1 + \frac{1}{m}}{1 + \sqrt{\frac{a}{r} + 1}}$$

$\frac{1}{m}$ = Poisson's ratio

$$K_{tk} = \frac{3}{4N}\left(\sqrt{\frac{a}{r} + 1} + 1\right)\left[3\frac{a}{r} - \left(1 - \frac{2}{m}\right)\sqrt{\frac{a}{r} + 1} + 4 + \frac{1}{m}\right]$$

$$K_{fk} = 1 + 2\sqrt{\frac{t}{r}}$$

$$K_t = 1 + \frac{(K_{tk} - 1)(K_{fk} - 1)}{\sqrt{(K_{tk} - 1)^2 + (K_{fk} - 1)^2}}$$

Fig. 3.3-12 Neuber's theoretical stress concentration factor relationships [Ref. 6, p. 66].

3.3.5.2 COMPARISON OF THEORETICAL AND ONR EXPERIMENTAL NOTCH SENSITIVITY RESULTS

Notch sensitivity is a highly sensitive parameter and varies significantly depending upon (1) the material, (2) the type and severity of the notch, and (3) the type and severity of loading [15, p. 104]. For this research fully reversed bending is the only loading considered. It has been observed, as in Table 3.3-8, that some alloys show a K_f equal to one indicating nc reduction in fatigue strength due a notch while in this research some configurations of AISI 1038 steel have a K_f value as high as 1.54, as given in Table 3.3-9, indicating a high reduction in strength due to the presence of the notch.

The results of this research for q and K_f are given in Table 3.3-9 and are plotted in Figs. 3.3-13 and 3.3-14 and confirm the accepted theory as illustrated in Figs. 3.3-15, 3.3-16, and 3.3-17.

However, it should be noted that K_f and q are highly sensitive parameters and great care must be taken in specimen preparation and testing.

Table 3.3-9 The University of Arizona Experimentally Determined Distributional Fatigue Notch Sensitivity Design Data for AISI 1038 Steel Rod in Fully Reversed Bending.

Notch Radius in.	Notch Diameter in.	Overall Diameter in.	Fatigue Strength Kpsi			Fatigue Stress Concentration Factor K_f			Theoretical Stress Concentration Factor K_t****			Notch Sensitivity q			Sample Size
			Mean*	Std.Dev.**	C.V.***	Mean	Std.Dev.	C.V.	Mean	Std.Dev.	C.V.	Mean	Std.Dev.	C.V.	
1.87	0.2700	0.375	37.118	2.141	.057	-	-	-							35
0.250	0.2700	0.375	32.244	1.192	.038	1.151	.0786	.068	1.16			0.943			35
0.125	0.2700	0.375	30.444	1.464	.050	1.225	.0931	.076	1.28			0.803			35
0.062	0.2700	0.375	26,706	1.976	.073	1.385	.1310	.094	1.52			0.770			35
0.031	0.2700	0.375	23.750	0.447	.167	1.563	.2680	.174	1.85			0.662			35

* Rounded to nearest 1 Kpsi

** Rounded to nearest 0.1 Kpsi

*** Coefficient of Variation = $\frac{\text{Std. Dev.}}{\text{Mean}}$

**** Taken from Paterson [5, p. 49, Fig. 40]

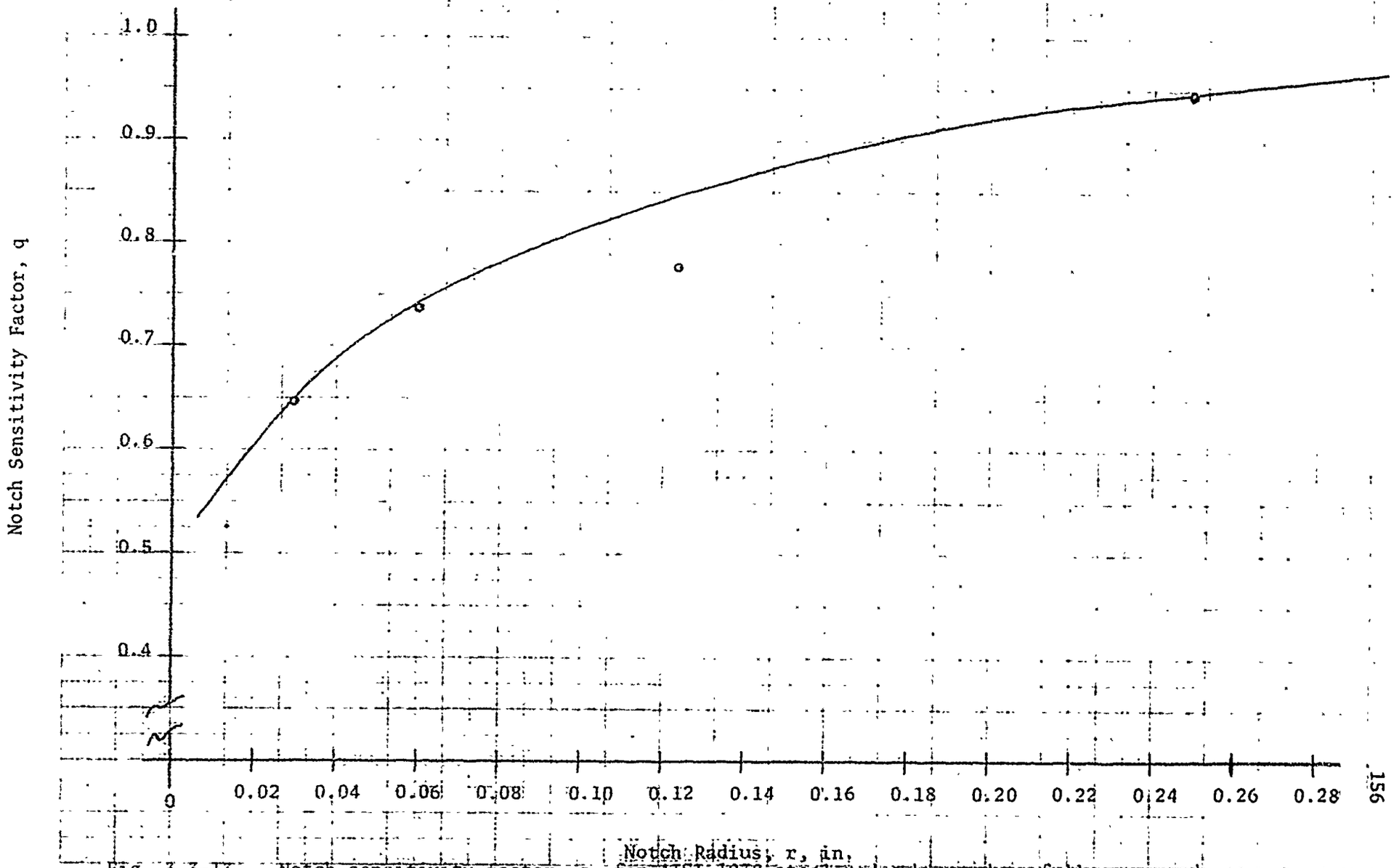

Fig. 3.3-13 Notch sensitivity factor, q, for AISI 1038 steel rod subjected to fully reversed bending (See Table 3.3-9).

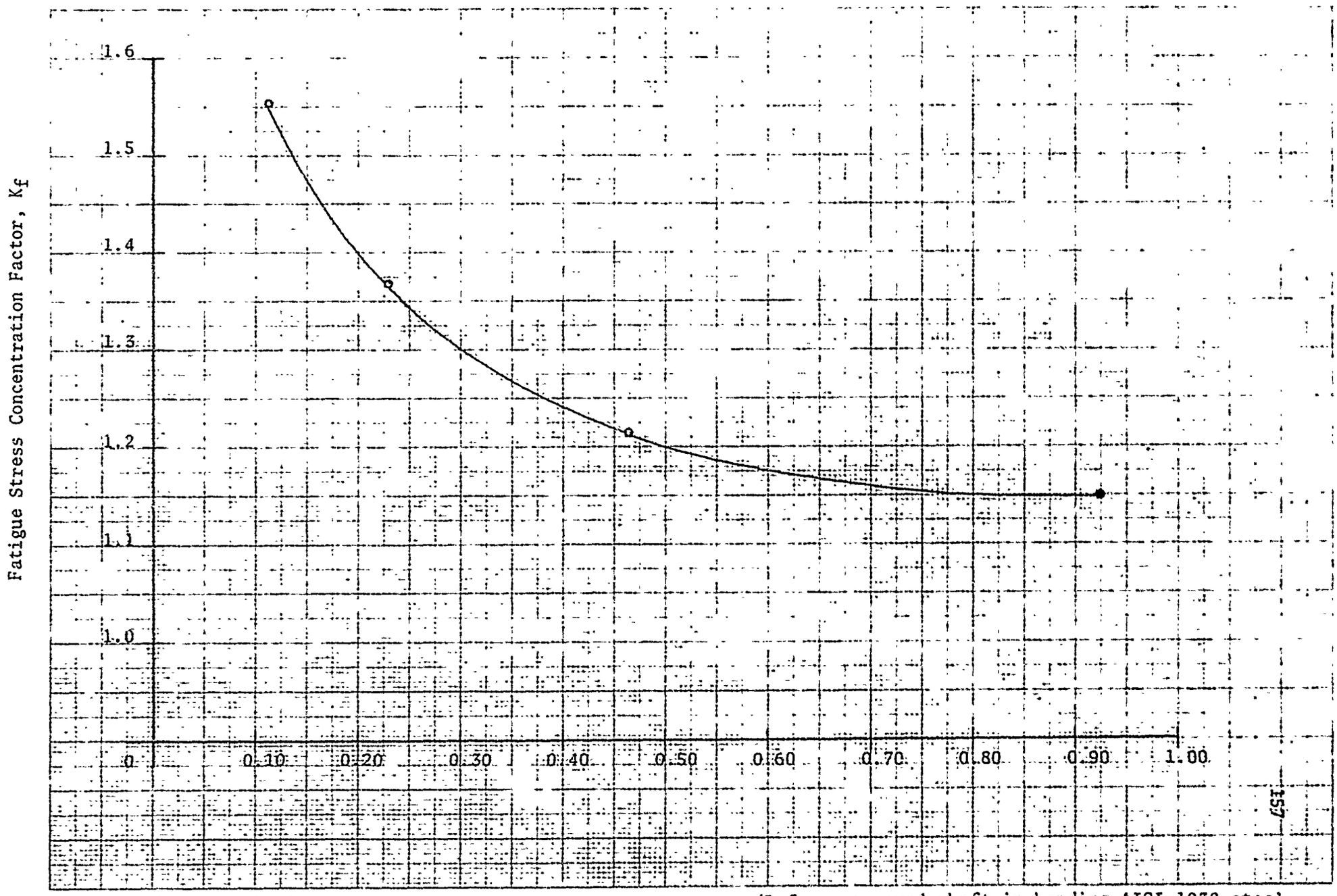

Fig. 3.3-14 Fatigue Stress Concentration Factor, K_f, vs. r/D for a grooved shaft in bending AISI 1038 steel rod, endurance at 3×10^6 cycles, rod diameter D = 0.375 in., base diameter. d = 0.2700 in. varied notch radii.

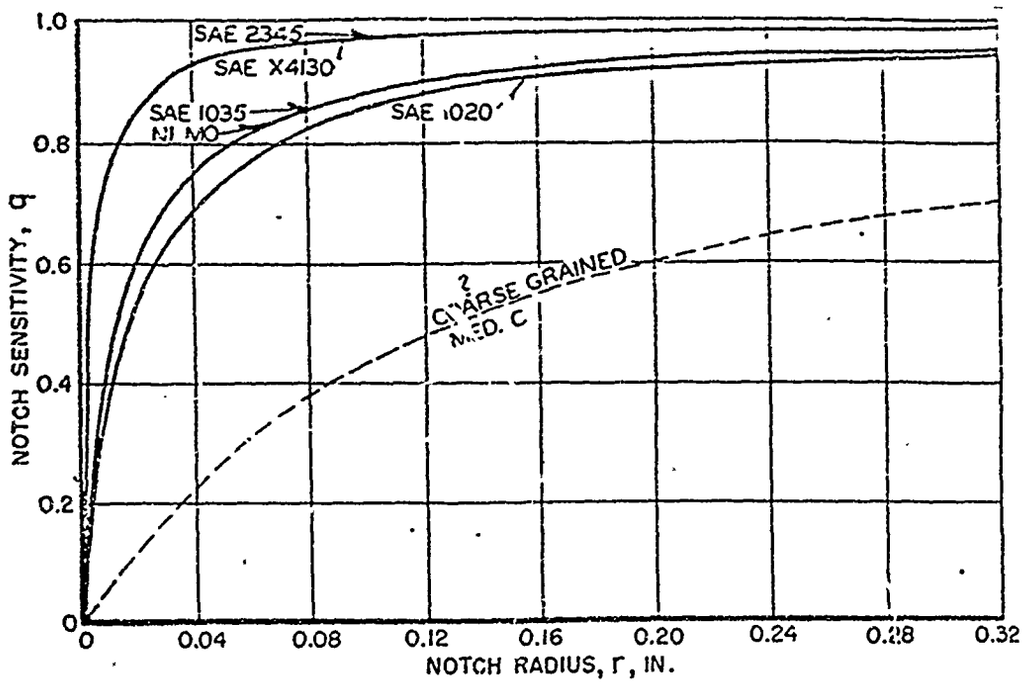

Fig. 3.3-15 Notch sensitivity versus notch radius
[18, p. 526, Fig. 4]

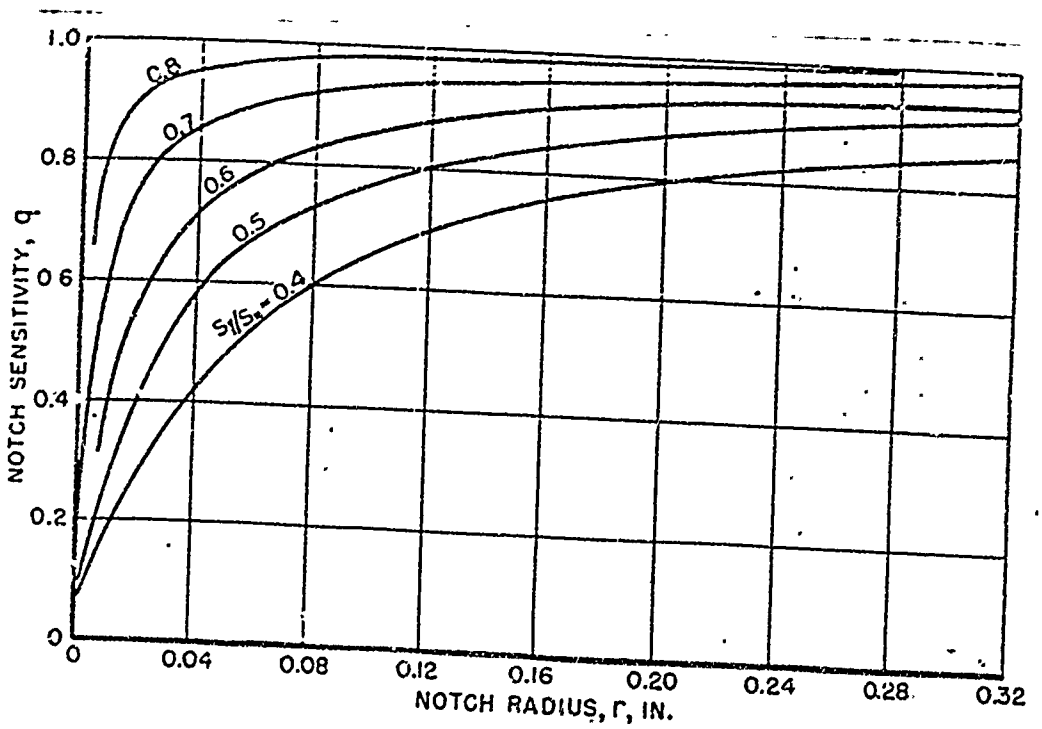

Fig. 3.3-16 Notch sensitivity values for normalized steels versus notch radius [18, p. 527, Fig. 6].

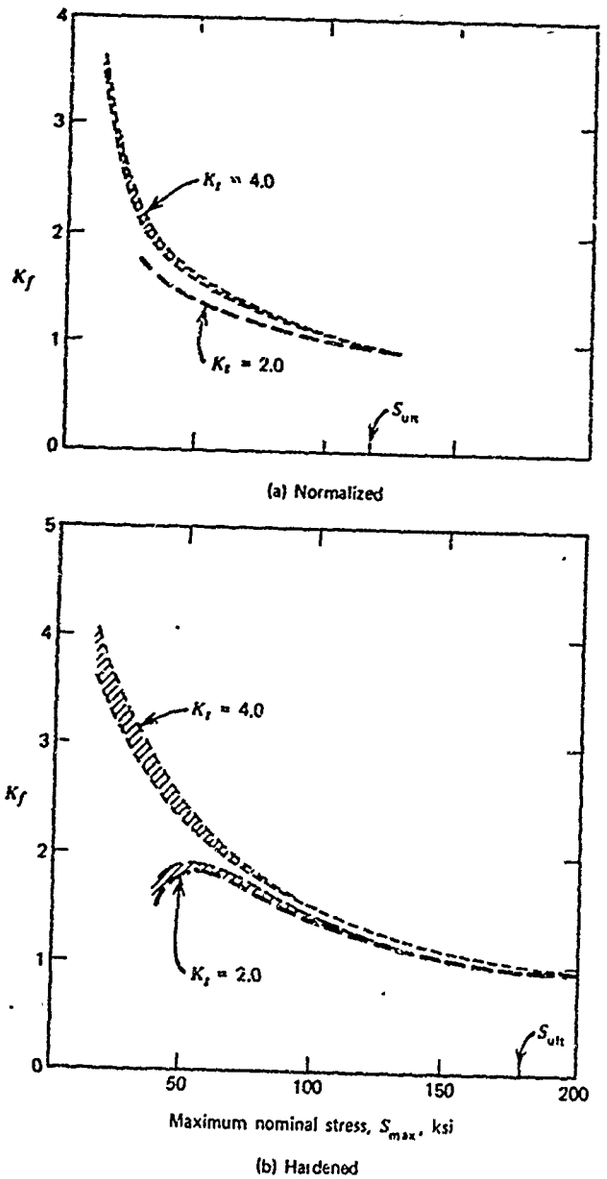

Fig. 3.3-17 Relations among K_f, K and S_{Max} for notched AISI 4130 steel [15, p. 416, Fig. 4.25]

The AISI 1018, AISI 4340 and AISI 4130 are under investigation now. Their notch sensivity and fatigue notch stress-concentration factors will be presented in the next report.

3.3.5.3 RESULTS DRAWN FROM NOTCH SENSITIVITY TESTING

The results of these notch sensitivity tests, summarized in Table 3.3-9, are based upon data presented in Section II of this report. The objective was to determine the effect of decreasing notch radius upon fatigue stress concentration factor, K_f, and notch sensitivity, q.

The response to notch configuration plotted in Figs. 3.3-13 and 3.3-14 indicates that a decrease in K_f from 1.540 to 1.155 and an increase in q from 0.636 to 0.968 results from an increase in the r/d ratio. Although the fatigue stress-concentration factor, K_f, increases as the r/d ratio decreases the notch sensitivity factor, q, decreases. This indicates that as r/d decreases the material becomes less notch sensitive although the strength of the specimen is decreased due to the presence of the notch.

The results presented in Table 3.3-9 and the curves plotted in Figs. 3.3-13 and 3.3-14 may be employed for the design of shafts of similar configurations in reversed bending.

3.4 AXIAL FATIGUE RESEARCH MACHINE

3.4.1 TENSILE DISTRIBUTIONAL PROPERTIES

Table 8.3-1 presents the experimental data generated to determine the distributional static ultimate, yield, and breaking strengths of AISI 1018 steel rod used in this research. Table 8.3-2 presents the hardness and percent elongation for the static test specimens.

3.4.2 DISTRIBUTIONAL GOODMAN DIAGRAMS FOR AISI 1018 STEEL

3.4.2.1 DETERMINATION OF THE STRENGTH PARAMETERS AT SPECIFIC STRESS RATIOS

Fatigue tests were conducted using AISI 1018 steel specimens to determine the endurance strength at 2.0×10^6 cycles of life. The specimens were subjected to alternating axial stresses superimposed onto mean tension stresses at alternating-to-mean stress ratios, r_s, of ∞, 2.0, 1.0, 0.4 and 0.2.

The staircase test procedure discussed in Section 3.2.3 was followed and the test results were reduced using the standardized data reduction procedure presented in that section. A PDP-8 computer program was developed and used to calculate the mean and standard deviation of the strength-to-failure (endurance) data and is presented in Appendix E.

Once the mean and standard deviation of the stress vector, S_V, is calculated; the mean and $\pm 3\ \sigma$ envelopes for each stress ratio can be located and a distributional Goodman diagram for specimens of a specific material and geometry may be constructed.

3.4.2.2 CONVERSION OF STAIRCASE TEST RESULTS INTO DISTRIBUTIONAL GOODMAN DIAGRAMS

Goodman diagrams are plotted with the mean stress located on the abscissa and the alternating stress on the ordinate. The results of the staircase test provides the mean and standard

deviation of the stress vector, S_v. Thereby allowing the stress vector distribution to be plotted directly; with the stress ratio, r_s, determining the angle, α, that the stress vector makes in relation to the abscissa, as shown in Fig. 3.4-1.

The curve drawn through the mean value, $\overline{S}_v$, of each stress vector distribution at the various stress ratios constitutes the mean of the Goodman diagram. Similarly, the curves connecting the $\overline{S}_v + 3\sigma$ and $\overline{S}_v - 3\sigma$ values provide the $\pm 3\sigma$ envelopes, hence the distributional Goodman diagram.

3.4.2.3 COMPARISON OF EXPERIMENTAL FATIGUE TEST RESULTS WITH ESTABLISHED FAILURE THEORIES

The Goodman diagram constructed from experimental results is compared with curves drawn theoretically using the Distortion Energy Theory and the Maximum Shear Stress Theory. The Goodman diagram constructed in accordance with the Distortion Energy Theory is described by the von Mises-Hencky ellipse and is defined by

$$\left(\frac{S_a}{S_e}\right)^2 + \left(\frac{S_m}{S_u}\right)^2 = 1 \quad . \tag{3.4-1}$$

The Goodman diagram constructed in accordance to the Maximum Shear Stress Theory is slightly more conservative than the von Mises-Hencky ellipse and is known as the Gerber parabola defined by

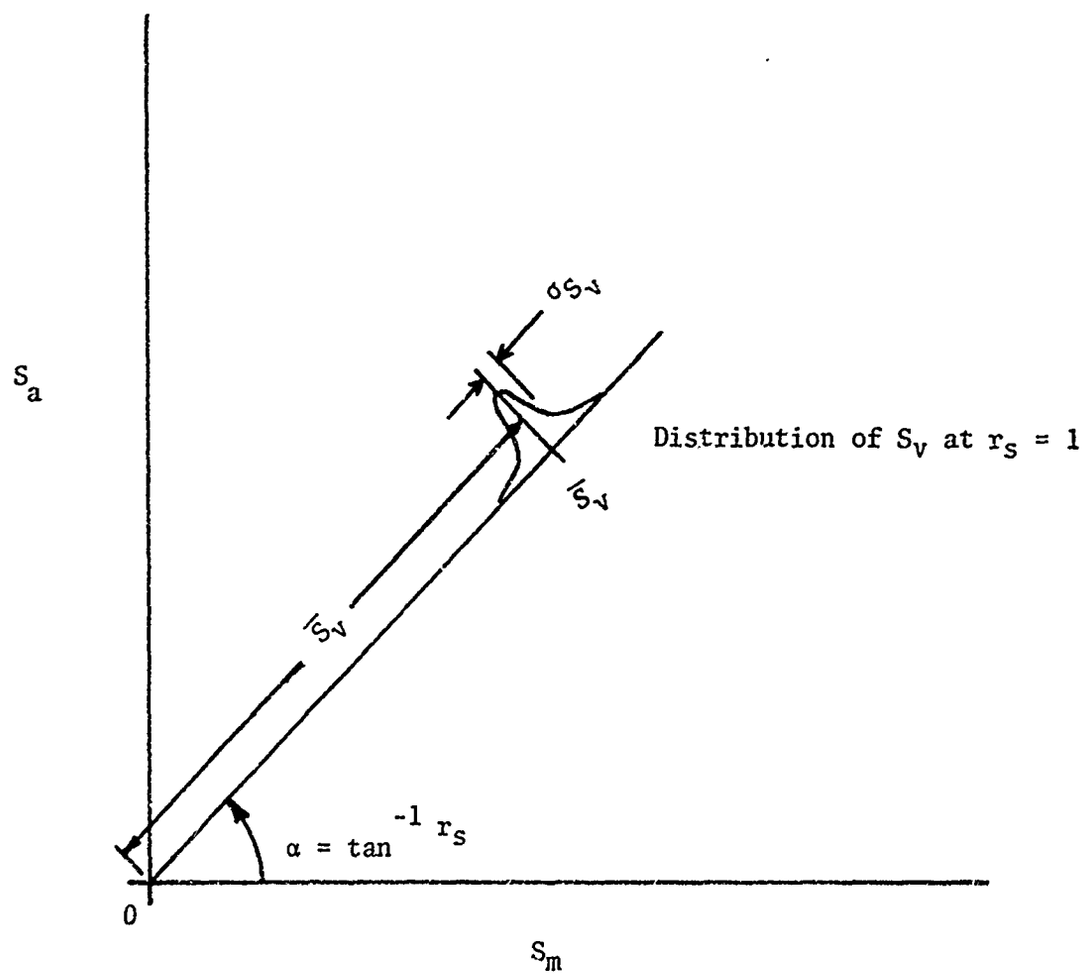

Fig. 3.4-1 Example of plot of a stress vector distribution for a stress ratio, $r_s = 1$.

$$\frac{S_a}{S_e} + \left(\frac{S_m}{S_u}\right)^2 = 1 \ . \tag{3.4-2}$$

The curves generated by using the established failure theories are plotted by calculating the stress vector, S_v, corresponding to each stress ratio and using the established endurance strength, S_e, and the static ultimate tensile strength, S_u, for the specified material. For a selected mean stress, S_m, and stress ratio, r_s, the stress vector can be computed from

$$S_v = S_m \ (1 + r_s)^{\frac{1}{2}} \ , \tag{3.4-3}$$

where S_m is calculated using Eq. (3.4-1) or Eq. (3.4-2) depending upon the failure theory selected.

Points on the von Mises-Hencky ellipse are computed by selecting several stress ratios and substituting the appropriate S_e and S_u values into the following equation:

$$S_{m_e} = \frac{S_u - S_e}{(S_e^2 + r_s^2 \ S_u^2)^{\frac{1}{2}}} \ . \tag{3.4-4}$$

The corresponding stress vector, S_v, value is calculated using Eq. (3.4-3) and substituting the value of S_m found from Eq. (3.4-4) into Eq. (3.4-3).

If the Gerber parabola is used to describe the Goodman diagram the following relationship is used to calculate S_m:

$$S_{m_p} = \frac{(r_s^2 S_u^4 + 4 S_u^2 \cdot S_e^2)^{1/2} - r_s \cdot S_u^2}{2 S_e} . \qquad (3.4\text{-}5)$$

Equation (3.4-3) is then used to calculate the stress vector, S_y, corresponding to the S_m value found by Eq. (3.4-5).

A PDP-8 computer program has been developed which identifies the points on the von Mises-Hencky ellipse and the Gerber parabola when S_e and S_u are known and values of r_s are specified. The program is presented in Appendix F .

The curves generated by the von Mises-Hencky ellipse, the Gerber parabola and the ONR experimental test results for AISI 1018 steel are shown in Fig. (3.4-2). It is apparent that neither the ellipse nor the parabola fit the experimental data, because the experimental data curve lies between these two.

3.4.2.4 METHODOLOGY FOR FINDING THE BEST-FIT CURVE THROUGH THE EXPERIMENTAL DATA POINTS

A comparison of Eq. (3.4-1), describing the von Mises-Hencky ellipse, and Eq. (3.4-2), describing the Gerber parabola, reveals that both theories can be expressed generally in the same form by

$$\left(\frac{S_a}{S_e}\right)^a + \left(\frac{S_m}{S_u}\right)^2 = 1 , \qquad (3.4\text{-}6)$$

where $a = 1$ for the parabola and $a = 2$ for the ellipse. Since the

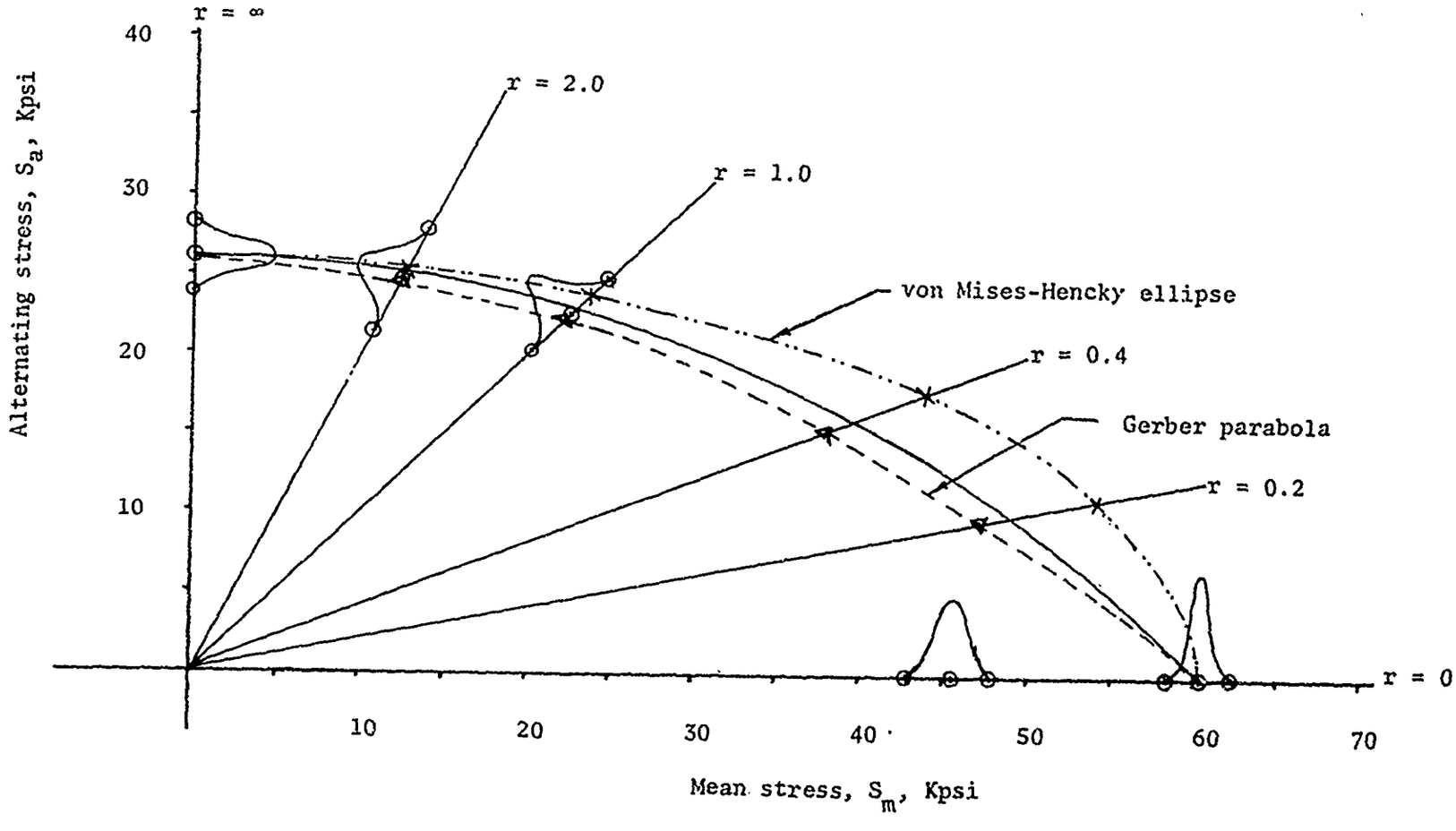

Fig. 3.4-2 Distributional Goodman strength diagram for 2.0×10^6 cycles of life with AISI 1018 steel ungrooved specimens.

experimental data for AISI 1018 steel lie between the ellipse and the parabola, there exists a value of the exponent, a, which will describe the experimental curve. Transformation of Eq. (3.4-6) into a linear relationship allows the use of the standard "least squares" method of curve fitting to solve for the value of the exponent, a.

Substitution of $y = \frac{S_a}{S_e}$ and $x = S_m/S_u$ into

Eq. (3.4-6) yields

$$y^a + x^2 = 1 ,$$

or

$$y^a = 1 - x^2 .$$

Taking the natural logarithm of both sides of the transformed Eq. (3.4-6) yields

$$a \ln y = \ln (1 - x^2) . \tag{3.4-7}$$

Further substitution of $Y = \ln y$ and $X = \ln (1 - x^2)$ into Eq. (3.4-7) gives

$$a Y = X ,$$

or

$$Y = \frac{1}{a} X . \tag{3.4-8}$$

Equation 3.4-8 is now the linear form of Eq. (3.4-6) and is in the

form of a straight line where the y - intercept is zero and the slope is $1/a$.

A CDC-6400 FORTRAN computer program has been developed which calculates the slope, $1/a$, from experimental data. Inputs to the program include the values of S_a and S_u for the material and values of S_v and r_s from the staircase testing program. Outputs of the program include the exponent, α, for Eq. (3.4-6) and the correlation coefficient for the fit of the line describing the data points. Additional outputs of the program include any specified number of S_v and r_s coordinates to provide for the plotting of the experimental curve.

Analysis of the program results to date have revealed two significant points:

1. The exponent calculated by the program is sensitive to the presence or absence of data in the stress ratio range of 0.2 to 0.4.
2. Inclusion of the end point where $Ys = 0$ resulting in $S_m = S_u$ cannot be included directly because it results in taking the natural logarithim of zero which is undefined. However, inclusion of the end point is needed to assure the proper curvature of the data line. This problem was circumvented by making use of the

extreme accuracy of the CDC-6400 computer and offsetting the end point, S_u, by 0.0001 psi and the stress ratio, r_s, by 0.0001.

The significance of the first point lies in the fact that the difference between the ellipse and the parabola is the maximum in the same range of stress ratios of 0.2 to 0.4. Consequently more fatigue tests must be conducted in this range of stress ratios to determine the correct exponent of Eq. (3.4-6). Figure 3.4-2 is, therefore, tentative. Fatigue tests for AISI 1018 steel are continuing in this stress ratio range. The results will be included in the next report.

The CDC-6400 program briefly described above is being expanded to include the calculation of data points for the distributional Goodman diagrams $\pm$ 3 σ envelopes. The final program will be included in the next report.

4.0 OVERALL CONCLUSIONS

4.1 WIRE FATIGUE RESEARCH MACHINE TESTS

1. Static tensile tests were successfully completed on 0.040 in. diameter wire specimens made of AISI 1018, 1038, 4130 and 4340 steel. The distributional strength parameters are given in Table 3.2-1.
2. The ultimate strength mean values for wires are in general agreement with conventional tabled values for the specified material.
3. The coefficients of variation vary inversely with the values of ultimate strength. The coefficient of variation values range from 11% for AISI 4340 steel to 25% for AISI 1038 steel, values somewhat higher than for steel rods of the same material.
4. Static strength distributions can be effectively represented by the normal distribution.
5. Cycles-to-failure tests were successfully completed on the wires of the same materials and diameters. Distributional parameters calculated for the normal, $\log_e$ normal, and Weibull distributions are listed in Tables 3.2-2 through 3.2-5.
6. Preparation of distributional S-N diagrams have not been completed because endurance testing is still in progress. Preliminary plots shown in Figs. 3.2-1 through 3.2-4 confirm that distributional means and envelopes can be

Preceding page blank

approximated by straight lines when the logarithms of cycles to failure are plotted vs the logarithm of stress.

7. The cycles-to-failure distributions have large variances with coefficients of variation values as high as 50% at the lower stress levels. This variability further emphasizes the importance of design by reliability techniques to replace conventional design based on estimates of deterministic values.

8. Based on the results of the K-S and Chi-Squared goodness-of-fit tests, the coefficients of skewness and kurtosis, and phenomenological considerations the lognormal distribution provides the best fit to the cycles-to-failure data. However, the normal distribution also appears to provide a useful fit.

9. The three-parameter Weibull distribution can be considered to provide an acceptable fit for cycles-to-failure data based on the K-S goodness-of-fit test results. As the Chi-Squared test is more discriminating for small sample sizes, its result show that the Weibull distribution should be used with care for sample sizes of 35 or fewer.

4.2 WIEDEMANN RESEARCH MACHINE TESTS

1. Static tensile test results on AISI 1038, 4130 and 4340 steel ungrooved rods of 0.25-in. nominal diameter are summarized in Table 3.3-1. The following conclusions may be drawn:

   a) Ultimate strength mean values are in general agreement with published properties.

   b) The coefficient of variation for the ultimate strength varies from 1% to 2% which attests to the homogeneity of the materials and the high precision in the tests.

   c) The percent elongation of the AISI 1038 steel specimens had a mean of 20.9% as compared with the mean of 8.5% for AISI 4130 steel specimens. These results are as expected since AISI 1038 steel is considerably softer than AISI 4130 steel.

   d) Because elongation is accompanied by a decrease in the cross-sectional area, the mean breaking strength of the AISI 1038 steel specimens, based on final diameters, is larger than for the AISI 4130 specimens. These results illustrate that caution must be excercised when using the breaking strength as a design criterion.

2. Cycles-to-failure test results for AISI 4130 steel rod specimens with 0.0250" and 0.125" groove radii are complied in Tables 3.3-3 and 3.3-3, respecitvely. The following conclusions may be drawn:

a) S-N diagrams plotted on log-log scales using normal cycles-to-failure distribution parameters confirmed that distributional S-N diagrams approximated by straight-line loci for the mean and $\pm 3\sigma$ envelopes are good representations of the data.

b) The variability of the cycles to failure increased as the stress levels decreased so that the distributional S-N diagram retained the straight line fit with widening $\pm 3\sigma$ envelopes as the stress levels decreased.

c) A comparison of the experimentally generated S-N diagrams with existing empirical methodologies showed that (1) the empirical methodologies are conservative and (2) the distributional information provided by the experimental diagrams allows for improvements in design accuracy.

3. Endurance tests on AISI 1038 steel rod specimens with various groove radii under reversed bending stresses were conducted using the staircase methodology. The following conclusions may be drawn from the results tabulated in Table 3.3-4.

a) Specimens having a groove radius of 1.87" which provides a stress concentration factor of approximately 1.0, have a mean endurance strength of 37,100 psi. As the groove radius is decreased to 0.031", the mean endurance strength decreases to 23,800 psi.

b) A plot of the endurance strength for different groove radii provided for an analysis of notch sensitivity. The values of notch sensitivity given in Table 3.3-9 agreed very closely with published results.

c) When conducting staircase endurance tests, it was found that to minimize invalid test points the initial stress level should be 0.54 times the ultimate strength (S_u) for groove radii of 1.87 or larger. For smaller groove radii the initial stress level should be 0.54 S_u/K_f.

4.3 AXIAL FATIGUE RESEARCH MACHINE TESTS

Endurance staircase testing was completed on AISI 1018 steel specimens at alternating to mean stress ratios of ∞, 2.0, and 1.0, and is in progress for stress ratios of 0.4 and 0.2. The following conclusions may be drawn from the results given in Table 2.3-1 and Figs. 9.3-1 thru 9.3-3.

1. At the stress ratio of ∞, the endurance strength was 0.434 S_u which is in general agreement with prior results obtained for AISI 1038, 4130, and 4340 steels. Thus 0.45 S_u provides a good starting stress level for staircase type endurance tests with mean and alternating axial loads.
2. While the experimental Goodman diagram more closely approximates the Gerber parabola than the ellipse, the correct curve is somewhere bewteen the two. A least square regression analysis is being developed to determine the best representation of the Goodman diagram data.

3. The largest difference between the Gerber parabola and the von Mises-Hencky ellipse occurs in the stress ratio range of 0.2 to 0.4; consequently more experimental data must be obtained within this range of stress ratios to assure a more accurate determination of the Goodman diagrams for their more effective use in design.

5.0 RECOMMENDATIONS

1. Experimental research in progress on AISI 1018, 1038, 4130, and 4340 steel specimens should be completed. Priority should be given to the following incomplete efforts:

   a. Development of distributional S-N diagrams for 0.040 diameter wire specimens of the above four steels.

   b. Development of the distributional Goodman diagram for AISI 1018 steel rods subjected to axial alternating and mean loads. Experimental fatigue data is needed for stress ratios of 0.4 and 0.2 to assure accurate determination of the curvature of the Goodman surface.

   c. Development of distributional S-N diagrams for AISI 4130 0.0937" diameter steel rods with groove radii of 0.031" and 0.062", subjected to reversed bending.

   d. Completion of endurance strength staircase testing of AISI 1038 and 4130 steel rods for notch sensitivity analysis.

2. Experimental data generated under this research effort has been reported in a series of technical reports. Distributional data tables should be developed and published which present experimentally validated data for use by designers and reliability engineers. The data tables should also include published data available from other sources.

3. Analysis of the data tables should be performed and generalized thumb rules for the use of the data should be developed. The thumb rules should not only provide assistance in the use of the data tables but should include rules for extending the data to other materials through appropriate relationships.

4. A combination of experimental research and theoretical study should be completed to determine the most accurate failure governing criteria for AISI 1018, 1038, 4130 and 4340 steels subjected to fatigue loading. The following are recommended:

   a) Determine functional relationships among the fatigue failure governing criteria, type of load, notch sensitivity, and size.

   b) Analyze singularly and jointly the distributions of notch sensitivity and size effects, and synthesize these distributions into failure governing stress and strength distributions.

   c) Determine the functional relationships by regression analysis between fatigue strength and the notch sensitivity factor, and fatigue strength and the size factor.

5. The effect on service life and reliability of rotating components of cumulative fatigue loads should be determined.

6. An error analysis should be performed to determine the quantitative effects on the calculated reliability resulting from the use of either the normal, the lognormal or the Weibull distributions to model fatigue cycles-to-failure distributions.

6.0 REFERENCES

1. "Interaction Among the Various Phenomena Involved in the Design of Dynamic and Rotary Machinery and Their Effects on Reliability", D. Kececioglu and E. B. Haugen, The University of Arizona, Tucson, Arizona, First Technical (Progress) Report submitted to the Office of Naval Research (ONR), Washington, D. C. on Contract N00014-67-A-0209-0002, 30 April 1968, 379 pp.

2. "Interaction Among the Various Phenomena Involved in the Design of Dynamic and Rotary Machinery and Their Effects on Reliability", D. Kececioglu and E. B. Haugen, The University of Arizona, Tucson, Arizona, Second Technical (Progress) Report submitted to the Office of Naval Research (ONR), Washington, D. C. on Contract N00014-67-A-0209-0002, 15 July 1969, 242 pp.

3. "Interaction Among the Various Phenomena Involved in the Design of Dynamic and Rotary Machinery and Their Effects on Reliability", D. Kececioglu and E. B. Haugen, The University of Arizona, Tucson, Arizona, Third Technical (Progress) Report submitted to the Office of Naval Research (ONR), Washington, D. C. on Contract N00014-67-A-0209-0002, 13 August 1970, 453 pp.

4. "Interaction Among the Various Phenomena Involved in the Design of Dynamic and Rotary Machinery and Their Effects on Reliability", D. Kececioglu and E. B. Haugen, The University of Arizona, Tucson, Arizona, Fourth Technical (Progress) Report submitted to the Office of Naval Research (ONR), Washington, D. C. on Contract N00014-67-A-0209-0002, 31 August 1971, 495 pp.

5. "Stress Concentration Design Factors", R. E. Peterson, John Wiley and Sons, Inc., New York, N. Y., 1953, 155 pp.

6. "Mechanical Engineering Design", Joseph E. Shigley, McGraw-Hill Book Co., Inc., New York, N. Y., 1963, 631 pp.

7. "Engineering Considerations of Stress, Strain and Strength", Robert C. Juvinall, McGraw-Hill Book Co., Inc., New York, N. Y., 1967, 580 pp.

8. "Statistical Models in Engineering", G. J. Hahn and S. S. Shapiro, John Wiley and Sons, Inc., New York, N. Y., 1968, 355 pp.

9. "When and How to Use the Weibull Distribution", Robert H. Lochner, Ninth Annual Reliability Engineering and Management Institute Lecture Notes, The University of Arizona, Tucson, Arizona, November 1971, 45 pp.

10. "A Guide for Fatigue Testing and the Statistical Analysis of Fatigue Data", American Society of Testing Materials (ASTM), ASTM Special Technical Publication No. 91-A, 1963, 83 pp.

Preceding page blank

11. "A Method for Obtaining and Analyzing Sensitivity Data", Dixon, W.J., and Mood, A. M., Journal of the American Statistical Association, Vol. 43, 1948, pp. 109-126.

12. "Methodology for Generating S-N and Goodman Diagrams from Static and Endurance Data for Grooved Components", W. Gunther, Master of Science Report submitted to the Faculty of the Aerospace and Mechanical Engineering Department, The University of Arizona, Tucson, Arizona, August 1971, 215 pp.

13. "The Strength, Fracture and Fatigue of Materials", T. Yokobori, translated by S. Matsuo and M. Inoue, P. Noordhoff Publishing Co., The Netherlands, 1964, 372 pp.

14. "Metal Fatigue: Theory and Design", A. F. Madayag, John Wiley and Sons, Inc., New York, N. Y., 1969, 425 pp.

15. "Fatigue Design", Carl C. Osgood, John Wiley and Sons, Inc., New York, N. Y., 1970, 523 pp.

16. "Experimental Investigation of Notch Size Effects on Rotating Beam Fatigue Behaviour of 75S-T6 Aluminum Alloy", W. Hyler, R. Lewis and H. Grover, NACA TN 3291, November 1954, 47 pp.

17. "An Engineering Method for Estimating Notch Size Effect in Fatigue Tests on Steel", P. Kuhn and H. F. Hardrath, NACA TN 2805, October 1952, 35 pp.

18. "Study of Size Effect and Notch Sensitivity in Fatigue Tests on Steel", H. F. Moore, Proc. ASTM, Vol. 45, 1945, pp. 507-531.

19. "Kerbspannungslehre", Heinz Neuber, Berlin, 1937 and 1958 (2nd. ed.) translated by The Navy Department, David Taylor Model Basin, Washington, D. C., November 1945, 225 pp.